DYNAMICS OF ACTIN FILAMENTS IN AN ACTIN-MYOSIN MOTILITY ASSAY

by

Olivia Saffer

Thesis presented in partial fulfilment of the requirements for the degree of Master of Science (Theoretical Physics) in the Faculty of Science at Stellenbosch University

Supervisor: Prof. K. K. Müller-Nedebock

Co-supervisor: Dr. J. N. Kriel

March 2023

Declaration

By submitting this thesis electronically, I declare that the entirety of the work contained therein is my own, original work, that I am the sole author thereof (save to the extent explicitly otherwise stated), that reproduction and publication thereof by Stellenbosch University will not infringe any third party rights and that I have not previously in its entirety or in part submitted it for obtaining any qualification.

Date: March 2023

Abstract

DYNAMICS OF ACTIN FILAMENTS IN AN ACTIN-MYOSIN MOTILITY ASSAY

Z. O. Saffer

Department of Physics,
University of Stellenbosch,
Private Bag X1, Matieland 7602, South Africa.

Thesis: MSc (Phys)

March 2023

Actin filaments form important parts of biological cells. Actin filaments frequently interact with myosin motors. In particular, actin filaments and myosin motors are responsible for muscle contraction in animal cells: the myosin motors attach to the actin filaments and contract, causing the filaments in the muscle to slide over each other.

One way to study muscle contraction is to use experiments known as actin-myosin motility assays. This is the system we strive to model and understand in this thesis. However, there is also a broader interest in these sort of systems, since the actin-myosin motility assay is an example of an active system.

After setting up our model mathematically, we begin by investigating the dynamics of a single actin filament in a motility assay by using a Langevin equation. From there, we move to including the effects of other filaments. This is achieved using hydrodynamic considerations.

In order to move to a fuller picture of the dynamics of multiple filaments in a dense system, we turn to the Martin-Siggia-Rose formalism and a systematic approximation scheme known as the Random Phase Approximation.

Throughout our exploration of this system, we look to derive experimentally-measurable correlation functions. While we do this, we also identify intrinsic length and time scales.

Uittreksel

DINAMIKA VAN AKTIENFILIMENTE IN 'N AKTIEN-MIOSIEN-MOTILITEITSESSAIËRING

("DYNAMICS OF ACTIN FILAMENTS IN AN ACTIN-MYOSIN MOTILITY ASSAY")

Z. O. Saffer

Fisika Departement,
Universiteit van Stellenbosch,
Privaatsak X1, Matieland 7602, Suid Afrika.

Tesis: MSc (Fis)

Maart 2023

Aktienfilamente vorm belangrike dele van biologiese selle. Aktienfilamente is gereeld met miosienmotors in wisselwerking. Aktienfilamente en miosienmotors is veral verantwoordelik vir spiersametrekking in dierselle: die miosienmotors heg aan die aktienfilamente en trek saam, en veroorsaak daardeur dat die filamente in die spier oor mekaar gly.

Een manier om spiersametrekking te bestudeer is deur middel van eksperimente bekend as aktien-miosien-motiliteitsessaiëring. n hierdie tesis streef ons na die modellering en verstaan van dié sisteem. Daar is egter ook wyer belangstelling in hierdie soort stelsels, aangesien die aktien-miosien-motiliteitsessaiëring 'n voorbeeld van 'n aktiewe stelsel is.

Ons stel eers ons model wiskundig op, en begin dan deur die dinamika van 'n enkele aktienfilament in 'n motiliteitsessaiëring te ondersoek deur gebruik te maak van 'n Langevin-vergelyking. Ons volg daarop deur die effekte van ander filamente in te sluit. Dit word bereik deur middel van hidrodinamiese oorwegessaiëringings.

Om aan te beweeg na 'n vollediger beeld van die dinamika van veelvuldige filamente in 'n digte sisteem, wend ons ons na die Martin-Siggia-Rose formalisme en 'n sistematiese benaderingskema bekend as die Lukrake-Fase Benadering ('Random Phase Approximation').

Tydens ons verkenning van hierdie stelsel probeer ons immer voortdurend om eksperimenteel-meetbare korrelasiefunksies af te lei. Terselfdertyd identifiseer ons ook intrinsieke lengte- en tydskale.

Acknowledgements

I would like to express my sincere gratitude to the Wilhelm Frank Trust for funding my masters.

Contents

List of Figures

Nomenclature

Variables

$\vec{\mathbf{R}}(s,t)$ Position vector to the point s on the filament at a time t

$\theta(s,t)$ Tangent angle of the filament body with respect to the x-axis at a point s and time t

$\phi(\mathfrak{s},t)$ Tangent angle of the filament head with respect to the x-axis at a point $\mathfrak{s}$ and time t

$\tilde{\phi}_1(t)$ First mode of the tangent angle ϕ

$\Phi_0(t)$ Zeroth mode of the tangent angle ϕ

From Section 4.2 onwards

$\vec{\mathbf{R}}_j(s,t)$ Position vector to the point s on the j^{th} filament at a time t

$\vec{\mathbf{r}}_j(t)$ Position vector from the head-body join to the tip of the j^{th} filament at a time t

$\phi_{1,j}(t)$ First mode of the tangent angle ϕ_j of the j^{th} filament at a time t

$\Phi_{0,j}(t)$ Zeroth mode of the tangent angle ϕ_j of the j^{th} filament at a time t

From Section 4.5 onwards

$\vec{\mathbf{R}}_j(t)$ Position vector from the origin to the head-body join of the j^{th} filament at a time t

Parameters and their corresponding dimensions

κ Bending rigidity of the polymer . . . . . $[\frac{\mathrm{ML}}{\mathrm{t}^2}]$

L Length of the filament body . . . . . $[L]$

ℓ Length of the filament head . . . . . $[L]$

v Constant *active* speed at which the filament moves . . . . . $[\frac{\mathrm{L}}{\mathrm{t}}]$

ς Drag coefficient for the drag force on the head . . . . . $[\frac{\mathrm{M}}{\mathrm{t}}]$

λ Strength of the stochastic force . . . . . $[\frac{\mathrm{M}^2\mathrm{L}^2}{\mathrm{t}^3}]$

$\xi = \frac{2\varsigma\ell}{\pi}$ Effective drag coefficient . . . . . $[\frac{\mathrm{ML}}{\mathrm{t}}]$

$k = \frac{\kappa\pi^3}{8\ell^2} + \frac{\varsigma v\pi}{2}$ Effective spring coefficient . . . . . $[\frac{\mathrm{ML}}{\mathrm{t}^2}]$

v_f Speed of the flow field . . . . . $[\frac{\mathrm{L}}{\mathrm{t}}]$

$a = \frac{k}{\xi}$ Introduced in Section 2.2 . . . . . $[\frac{1}{\mathrm{t}}]$

$b = \frac{\varsigma v_f v\pi}{2\xi\ell}$ Introduced in Section 3.1 . . . . . [$\frac{1}{\mathrm{t}^2}$]

$\alpha = \varsigma$ Renamed for convenience in Section 4.5 . . . . . [$\frac{\mathrm{M}}{\mathrm{t}}$]

$\beta = \frac{\varsigma\ell}{v} + \frac{k}{v^2}\frac{2\ell}{\pi}$ Introduced in Section 4.5 . . . . . [M]

Chapter 1

Background and introduction

1.1 Active systems

Active matter refers to collections where the individual constituents are inherently "active" in that they are able to utilise energy in the system to produce directed movement [1–5]. Active systems are thus non-equilibrium systems, although they may show steady-state behaviour [2–4; 6–10]. It is the non-equilibrium nature of active matter systems that gives rise to many interesting and challenging physics problems. Thus, active matter and active systems have generated a lot of interest in recent years and have been the subject of some review articles [1; 2].

An important point to take note of in active systems is that the individual components themselves are active and therefore produce motion. In non-active non-equilibrium systems that are studied, the force that drives the system out of equilibrium is external or only present at the boundaries of the system. In active systems, the source of energy is homogeneously distributed throughout the system and the energy is utilised on a *local* scale by each active particle. In systems where orientation of the components plays a role, the individual components typically determine their orientation based on their own anisotropy [1; 2].

Active systems display some remarkable properties. For example, they can show phase changes (see Redner *et al.* [9] for example), pattern formation (see Surrey *et al.* [11]) or large-scale order of an entirely different character to the individual components. This last behaviour is touched on in Section 1.1.1.

While there are several examples of synthetic active matter systems, such as those investigated in Deseigne *et al.* [12]; Palacci *et al.* [13], the active matter systems that are primarily under investigation are biological systems. The scale of these systems ranges from the macro- to nanoscopic.

Examples of biological systems under study include collections of moving bacteria [14–17]; parts of the cell nucleus such as DNA or chromatin [18–25]; parts of the cellular cytoskeleton such as actin-myosin networks or kinesin and microtubles [26–35]; and even flocks of animals [2; 4].

The complexity and sheer number of variables poses a challenge for physicists modelling such systems.

1.1.1 Collective motion

One particular phenomenon of interest in active matter systems is the ability of a collection of individually driven components to display large-scale collective motion. A handy example is the spectacular starling mumurations or the swirling shapes formed by schools of fish. The Vicsek model [36] was an early pioneer in modelling these systems.

In actin-myosin motility assays, discussed in Section 1.2 below, clusters of coherently moving filaments have been observed in experiments. See, for example, Schaller *et al.* [28, 37]; Kron and Spudich [38]; Butt *et al.* [39].

Figure 1.1: An example of collective motion is seen here in this image of starling murmerations. Photograph taken by David Tipling, accessed at `https://www.lancswt.org.uk/blog/charlotte-varela/starling-murmuration-facts` on 20/1/2022

1.2 Motility assays

In muscle cells, the main components responsible for muscle contraction are actin filaments and myosin motors. A motility assay is a particular experimental set-up designed to investigate how actin filaments behave when interacting with myosin motors. Motility assays are frequently used to understand muscle contraction [40–43].

In a motility assay, the myosin motors are fixed in place on a glass substrate and free actin filaments, suspended in an aqueous solution, are pushed along by the motors as they attach and detach [26; 28; 29; 38; 44]. Actin filaments are polar and this means that the myosin motors have a preferred direction of movement along actin filaments [2; 38; 39; 41; 45]. See Figure 1.2.

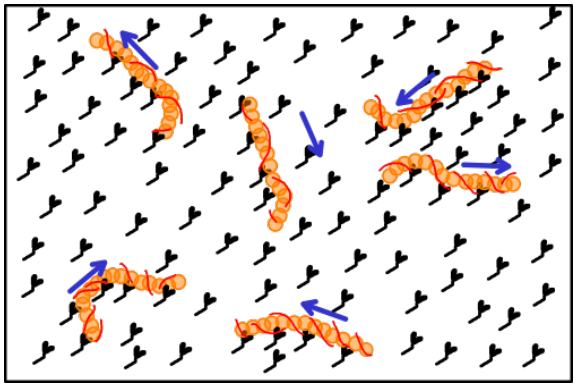

Figure 1.2: In this diagram of a motility assay, the myosin motors are drawn in black and the actin filaments are drawn in orange and red. The blue arrows indicate the preferred direction of motion in which the myosin motors push the actin filaments. Diagram adapted from Batters *et al.* [40] under Creative Commons licence `https://creativecommons.org/licenses/by/4.0/legalcode`.

Actin and myosin are also responsible for a number of other important processes such as cell division and for forming networks to transport vesicles and organelles in the cell [41; 45]. There are several kinds of myosin motors and the different processes involve different myosin motors. For example, muscle contraction and cell division involves actin and myosin II, whereas the transport networks involve actin and myosin V [41; 46; 47].

Biological systems are inherently very complicated and complex. Actin-myosin motility assays are a useful tool for studying the cytoskeleton or muscle contraction since it is a way of studying a particular component in isolation and in a controlled environment. For physicists, it is also simpler to model.

1.3 Calculation justification

Interesting behaviour has been observed in actin-myosin motility assays, however we do not have a complete physical picture of what, on a microscopic level, creates the behaviour.

In this thesis, we propose a microscopic model for the actin filament in an actin-myosin motility assay. Note that although we are trying to build a picture of what happens from the microscopic level, we are still in the realm of classical mechanics. Actin filaments vary in length depending on the cell type, but they are at least several tens of nanometres long and about 6 nm in diameter [45]. Furthermore, the thermal energy (given by Boltzmann's constant k_B multiplied by temperature) at body temperature (310 K) or room temperature (278 K) is around 4×10^{-21} J. If we compare this to the typical quantum energy and length scale, say the Bohr radius (roughly 5×10^{-11} m) and the ground state energy of a hydrogen atom (roughly 2×10^{-18} J), we see that our system is still "large" and "low energy".

From our theoretical study of the system, we hope to discover new length and time scales for this behaviour that may indicate a natural size of the clusters or a natural lifespan of these clusters.

We concentrate on a particular aspect of the motility assay, namely the force a single filament will experience as a result of the other filaments in the assay. This force we model as a drag. This is in line with the observations of Schaller *et al.* [28, 37]. We focus specifically on the situation of the tip of a filament as it explores its surroundings due to the body of the filament being pushed by the myosin motors.

We also bear in mind what is possible to be measured experimentally. After formulating the model, we use it to determine quantities such as the average end-to-end distance of a filament and average density of the filaments since these quantities are possible to be measured experimentally. We mainly look at collective variables (such as density). This is for two reasons. On the one hand, we are primarily interested in the collective behaviour of the filaments. On the other hand, it turns out to be mathematically more tractible to use a collective description.

Other papers have investigated semi-flexible polymers (which is how we describe actin - see section 1.4), but with results more applicable to DNA or chromatin [6; 23; 25] or systems

where the polymers drive their own motion or are in an active bath of particles, rather than being driven [7; 48].

Some work has been done to model actin filaments when they are not constrained by myosin motors, such as in Peterson *et al.* [3] or Eisenstecken *et al.* [7]. The paper by Peterson *et al.* [3] follows a very similar approach to the way we build our model, but it is geared to answer the question about whether sub- or super-diffusive motion of the filaments could be observed if the filaments are placed in a bath of active particles, whereas we are interested in explaining the collective behaviour seen in experiments.

The paper by Kierfeld *et al.* [26] focuses on the constrained motion of actin filaments in a motility assay, but models the actin as stiff rods and focuses on more realistically modelling the myosin motors. This is similar to the approach in Banerjee *et al.* [29]. The paper by Jung *et al.* [49] includes cross-linking, which we do not, and the actin is modelled as joined rigid cylindrical segments. Both Kierfeld *et al.* [26] and Jung *et al.* [49] aim to develop a computational model, whereas we focus on developing an analytical model.

Unlike papers that concentrate on properties of single filaments, such as Liverpool [31] or Munk *et al.* [30], our goal is to describe the dynamics of many filaments at once, with quantities such as average density, by starting from the single-filament, microscopic picture. We wish to provide microscopic motivation for the density clusters seen in experiments.

In a recent 2022 paper, Eisenstecken and Winkler [50] used a formalism very similar to what we shall later employ. However, they used it to study a slightly different system, namely semiflexible polymers composed of active Brownian particles. In our model, the polymer particles are not themselves active and are instead pushed. There is also a difference in how Eisenstecken and Winkler [50] described the forces on the polymer and the way they ensured the polymer is semiflexible, rather than flexible.

1.4 Polymer physics

Active systems, and in the particular system of a motility assay under investigation here, fall under many branches of physics: statistical physics, soft condensed matter physics, biophysics and polymer physics are some of the various fields. Here I will concentrate on giving a background to the necessary polymer physics concepts. Hydrodynamics concepts are also often employed and this will be touched on.

But first, what is a polymer? They are long molecules consisting of repeating units, called monomers. Actin filaments fit this description and are formed out of identical repeating units of a protein known as globular actin [41].

1.4.1 Parametrising the polymer

Figure 1.3 illustrates how polymers are typically parametrised. The polymer is described in terms of a continuous parameter s, known as the arc length and the position vector is a function

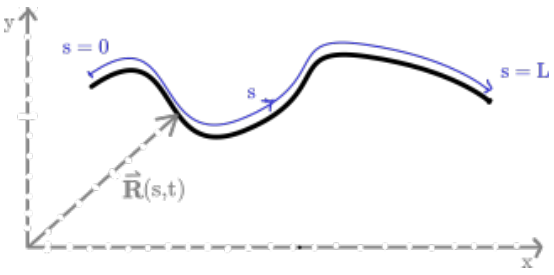

Figure 1.3: Polymers are typically parametrised by a continuous parameter s, known as the arc length, which runs along the body of the polymer. In this case s runs from 0 to L, but polymers can also be parametrised such that s runs from $-L/2$ to $L/2$, where L gives the length of the polymer. The vector $\vec{\mathbf{R}}(s,t)$ gives the position vector relative to a fixed axis to a point s along the polymer at a time t.

of this parameter i.e. $\vec{\mathbf{R}} = \vec{\mathbf{R}}(s)$. If the polymer is not in equilibrium then there is also a time dependence and the position vector is given by

$$\vec{\mathbf{R}} = \vec{\mathbf{R}}(s,t). \tag{1.4.1}$$

The tangent vector $\vec{\mathbf{t}}$ at a point along the polymer is given by

$$\vec{\mathbf{t}}(s,t) = \frac{\partial \vec{\mathbf{R}}(s,t)}{\partial s}. \tag{1.4.2}$$

In the equilibrium case where there is no time dependence, the tangent vector correlation function

$$\langle \vec{\mathbf{t}}(s) \cdot \vec{\mathbf{t}}(0) \rangle \tag{1.4.3}$$

can be used to define a measure of flexibility known as the persistence length. This is denoted by ℓ_{p}. The tangent vector correlation function gives the length scale over which the orientation of different points on the polymer become uncorrelated and we find

$$\langle \vec{\mathbf{t}}(s) \cdot \vec{\mathbf{t}}(0) \rangle \sim \exp\left\{ -\frac{s}{\ell_{\mathrm{p}}} \right\}. \tag{1.4.4}$$

Of course, non-equilibrium analogues can also be defined.

Depending on the length scale under investigation, polymers can appear flexible (the so-called ideal polymer), semiflexible or rigid (also referred to as rod-like) [51; 52]. This can be understood by thinking of a metal ruler that is 2 metres long. If you hold it at one end and consider the entire ruler, it appears bendable. However, if you try bend just 5 centimetres of it, it appears entirely rigid.

The comparison between the persistence length and length scale under investigation determines how flexible the polymer appears. For a polymer of length L, we have that

$$\begin{aligned} \ell_{\mathrm{p}} &\ll L && \text{Flexible polymer} \\ \ell_{\mathrm{p}} &\sim L && \text{Semiflexible polymer} \\ \ell_{\mathrm{p}} &\gg L && \text{Rigid polymer.} \end{aligned} \tag{1.4.5}$$

The persistence length can also be related to physical properties of the polymer in equilibrium, such as the average radius of gyration or average end-to-end distance. For the average end-to-end distance

$$\langle \vec{\mathbf{R}}(t) \rangle = \langle (\vec{\mathbf{R}}(L,t) - \vec{\mathbf{R}}(0,t))^2 \rangle^{\frac{1}{2}} \tag{1.4.6}$$

we have the scaling behaviour

$$\begin{aligned} \langle \vec{\mathbf{R}}(t) \rangle^2 &= L^2 && \text{Rigid polymer} \\ \langle \vec{\mathbf{R}}(t) \rangle^2 &= \ell_{\mathrm{p}}\, L && \text{Flexible polymer.} \end{aligned} \tag{1.4.7}$$

1.4.2 Determining the dynamics of the polymer

On way to study the dynamics of a polymer is to use an equation of motion for the polymer known as a Langevin equation. A general Langevin equation is given by

$$m\ddot{\vec{\mathbf{x}}} = -\gamma\, \dot{\vec{\mathbf{x}}} - \vec{\boldsymbol{\nabla}} V(\vec{\mathbf{x}}) + \vec{\mathbf{f}}(t), \tag{1.4.8}$$

which describes a particle at Cartesian coordinate $\vec{\mathbf{x}}$ experiencing linear drag with drag coefficient γ, an external force given by $-\vec{\boldsymbol{\nabla}} V(\vec{\mathbf{x}})$ and a stochastic force $\vec{\mathbf{f}}(t)$. In the overdamped case of low Reynolds number systems, the time scale $^{m}/_{\gamma}$ is regarded as much shorter than other timescales and the inertial term is omitted. This leaves

$$\vec{\mathbf{0}} = -\gamma\, \dot{\vec{\mathbf{x}}} - \vec{\boldsymbol{\nabla}} V(\vec{\mathbf{x}}) + \vec{\mathbf{f}}(t) \tag{1.4.9}$$

for the general overdamped Langevin equation.

The Reynolds number is a dimensionless number that gives the ratio of inertial to viscous forces. Biological polymers such as actin live in the world of low Reynolds numbers [52–55] and so we use the overdamped Langevin equation to model actin.

The force term $\vec{\boldsymbol{\nabla}} V(\vec{\mathbf{x}})$ is often referred to in terms of a so-called *Hamiltonian*, where the force terms are determined by taking a functional derivative of the Hamiltonian. Typically the position coordinate is time dependent and denoted $\vec{\mathbf{R}}(t)$. The Hamiltonian is then $H(\vec{\mathbf{R}}(t))$ and force terms are given by

$$\frac{\delta H(\vec{\mathbf{R}}(t))}{\delta \vec{\mathbf{R}}(t)}. \tag{1.4.10}$$

We shall see below in equations (1.4.11) and (1.4.15) two energy terms typically used for polymers.

Different models are employed depending on the flexibility of the polymer. The most basic model of a flexible polymer is the known as the Rouse or ideal chain model. The polymer is modelled as a set of N beads on a chain as N goes to infinity. This is known as the continuum limit and the number of beads N is replaced with the chain length L in this limit. The position coordinate $\vec{\mathbf{R}}$ of the polymer is now both dependent on time and on s, which indicates where along the polymer we are. The stretching energy of the polymer is given by

$$E_{\text{stretching}} = \frac{1}{2} k \int_0^L \mathrm{d}s \left(\frac{\partial \vec{\mathbf{R}}(s,t)}{\partial s} \right)^2, \tag{1.4.11}$$

where k can be thought of as an entropic spring constant. In fact, k comes from the entropic elasticity of an ideal chain and is related to the temperature of the system by $^{3\,k_B\,T}/_{l}$ where k_B

is Boltzmann's constant, T is the temperature and l is the distance between two beads on the chain. This distance l is also referred to as the effective bond length [51; 52; 55; 56].

For the Rouse model, the energy term in equation (1.4.11) leads to equation (1.4.9) taking the form

$$0 = -\gamma \frac{\partial \vec{\mathbf{R}}(t)}{\partial t} + k \frac{\partial^2 \vec{\mathbf{R}}(t)}{\partial s^2} + \vec{\mathbf{f}}(t). \qquad \textit{Flexible polymer} \tag{1.4.12}$$

The Rouse model does not include excluded volume interactions (that is, the effects of two segments of the polymer not being able to physically occupy the same region of space), nor hydrodynamic interactions. The Zimm model includes hydrodynamic interactions by introducing a mobility tensor $\mathbf{H}$. This is defined by

$$\vec{\mathbf{v}}(\vec{\mathbf{R}}(s)) = \int \mathrm{d}s' \, \mathbf{H}(\vec{\mathbf{R}}(s) - \vec{\mathbf{R}}(s')) \cdot \vec{\mathbf{F}}(s') \tag{1.4.13}$$

where $\vec{\mathbf{v}}(\vec{\mathbf{R}}(s))$ is the velocity of the polymer at the point s along the polymer and $\vec{\mathbf{F}}(s')$ is the force at the point s' along the polymer. This takes into account that the velocity of a point along the polymer is affected by the forces acting on the rest of the polymer, since the motion due to those forces creates drag in the fluid [52; 55; 57].

In low Reynolds numbers, the mobility tensor can be approximated by the Oseen tensor [52]. The approximation relies on the intertial term being negligible and assumes the fluid is incompressible. The Oseen tensor has the form

$$\mathbf{H}(\vec{\mathbf{R}}(s) - \vec{\mathbf{R}}(s')) = \begin{cases} \zeta^{-1} \, \mathbf{I} & \text{for } s = s' \\ \left(8\pi\eta \left| \vec{\mathbf{R}}_{s\,s'} \right| \right)^{-1} \left(\mathbf{I} + \hat{\mathbf{R}}_{s\,s'} \hat{\mathbf{R}}_{s\,s'} \right) & \text{for } s \neq s'. \end{cases} \tag{1.4.14}$$

Here ζ is the drag coefficient of the fluid, η the viscosity of the fluid, $\vec{\mathbf{R}}_{s\,s'} = \vec{\mathbf{R}}(s) - \vec{\mathbf{R}}(\,s')$ is the distance vector between the point s and the point s' along the polymer. $\hat{\mathbf{R}}_{s\,s'}$ denotes the unit vector corresponding to $\vec{\mathbf{R}}_{s\,s'}$ and $\mathbf{I}$ is the unit tensor $\mathbf{I}_{s\,s'} = \delta(s - s')\,\delta_{\alpha\beta}$. The second delta function takes care of the Cartesian components.

Instead of using the Oseen tensor as presented above, we could also use the *screened* Oseen tensor [52] that describes a more generic situation, but does not change any of our arguments thus far. The screened Oseen tensor still depends on $\vec{\mathbf{R}}(s) - \vec{\mathbf{R}}(s')$, but can describe a situation where there is different flow current for different layers of the fluid whereas the unscreened Oseen tensor assumes a completely free-flowing field. In the paper by Liverpool [31], the screened Oseen tensor is used in favour of the unscreened Oseen tensor.

If the polymer is not entirely flexible, there is an additional energy term from the curvature of the polymer. Physically, this corresponds to the resistance the polymer has to bending. This is given by

$$E_{\,\text{bending}}\,(t) = \frac{1}{2}\kappa \int_0^L \mathrm{d}s \, \left(\frac{\partial^2 \vec{\mathbf{R}}(s,t)}{\partial s^2} \right)^2, \tag{1.4.15}$$

where κ is referred to as the bending rigidity and gives a measure of stiffness. In this case the model is known as the Kratky-Porod or worm-like chain model [52; 58].

For a *semiflexible* polymer, typically the only energy term is the bending energy of equation (1.4.15). One also requires that the absolute value of the tangent is unity at all point along the polymer:

$$\left|\frac{\partial\vec{\mathbf{R}}(s,t)}{\partial s}\right| = 1, \quad \forall s \in [0, L]. \tag{1.4.16}$$

Physically, this encodes inextensibility of the polymer and ensures the polymer does not stretch [25; 31; 59–61]. It is this constraint which makes calculations tricky and gives rise to all the challenges we faced.

We shall be modelling actin filaments as semiflexible polymers as was done, for example, in Liverpool [31]. We focus on a particular aspect of the motility assay, namely the force a single filament will experience as a result of the other filaments in the assay. We model the force of the other filaments as due to a drag. This is in line with the observations of Schaller *et al.* [28, 37].

1.5 Thesis organisation

In this thesis, the terms actin, filament, polymer and chain all refer to the same thing and will be considered interchangeable.

We begin by looking at a single, non-interacting actin filament in a motility assay in Chapter 2.

From there, we move to introducing hydrodnamic interactions due to other filaments in Chapter 3. In this chapter we present our first new results: in the case of a constant flow field, we identify the relevant length and time scales and discuss the behaviour of the actin filaments.

Next, we move to an alternative formalism in Chapter 4 which is appropriate for dense polymer systems. This chapter constitutes the bulk of the thesis. We discuss the formalism in general before applying it to our system. We illustrate the various complications and difficulties encountered while applying this formalism. Finally, we present results for a stripped-down version of the motility-assay.

Lastly, in Chapter 5 we conclude the thesis and discuss possible extensions of this work.

Chapter 2

Summary of work done for a non-interacting single filament

This chapter contains a summary of our investigations into the dynamics of a single non-interacting filament in an actin myosin motility assay. These investigations took place during the course of my honours year.

The basic model was set up and the equations that govern that model were derived. We also looked at the average fluctuations of the angle the tip of the filament makes, with respect to a fixed axis, for both a simple and a more realistic case. The results of this exploration prompted us to continue with this model for the more involved scenario where we include the effects of other filaments in the motility assay.

2.1 The model

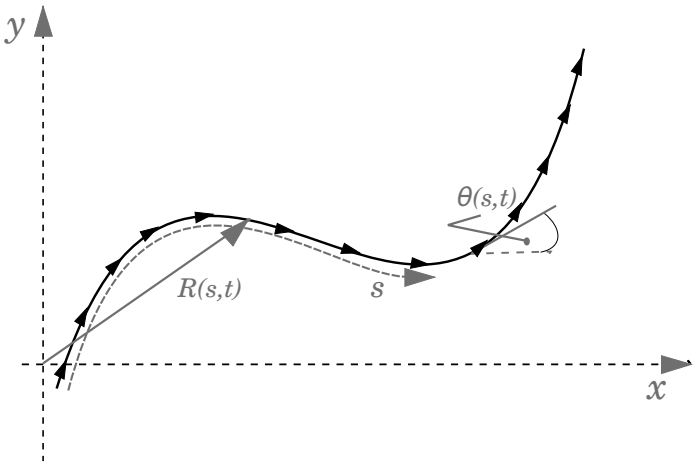

Figure 2.1: Semi-flexible chain model parameterisation. The solid black line represents the actin filament and the arrows along the filament indicate the direction the filament is moving in the motility assay as it is being pushed along by the motors [62].

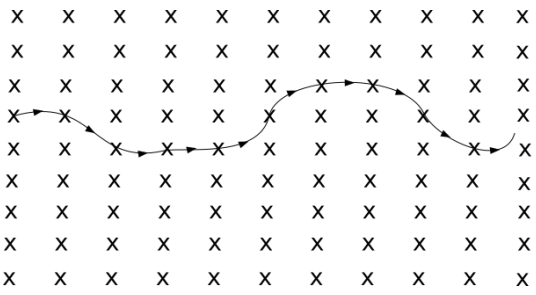

(a) Schematic diagram of a motility assay showing the body essentially fixed in place by the motors (represented by crosses), while the head is free to roam until a motor attaches to it

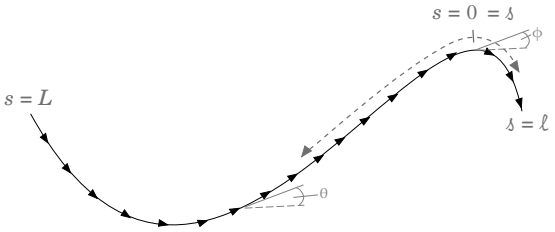

(b) Parameterisation of the head and body of the filament.

Figure 2.2: Schematic diagram of a motility assay (left) and a diagram showing the parameterisation of the head and body of the filament (right). In both diagrams the arrows along the filament indicate the direction the filament is moving as it is pushed along by myosin motors [62].

In a motility assay, movement is largely confined to two dimensions [38; 63]. For this reason, we neglect any three-dimensional considerations and model everything as occurring in a plane. In addition to this, we consider the motion of the head and body of the filament separately. This is because we slightly simplify the way myosin interacts with actin in that we consider only the head of the actin filament free to explore. The body of the actin filament we take to be laterally fixed in place once the myosin has attached to it, but free to move in the direction it was initially orientated when it attached to the motor (see Figure 2.2a). This motion occurs at a constant speed v as the myosin pushes the filament along and moves down the body of the filament. (This is consistent with experimental observation [28; 38; 44].) Thus the motion of the body is predetermined by the exploration of the head and it gives a history of the motion of the head.

2.1.1 Parametrising the filament

We parametrise the filament as illustrated in Figure 2.1, but we distinguish between the head and body as illustrated in Figure 2.2b. We consider a chain of length $L + \ell$, where L is the length of the body and ℓ the length of the head with $L \gg \ell$. We let s run along the backbone from 0 to L and $\mathfrak{s}$ run along the length of the head from 0 to ℓ. We call s and $\mathfrak{s}$ the arc length. We define the tangent angle of the filament for any point on the filament relative to a fixed axis which we call the x-axis. Thus the tangent angle is a function of both arc length and time. For the filament body, we denote this angle $\theta(s,t)$ and we use $\phi(\mathfrak{s},t)$ for the head.

We choose to set $s = 0 = \mathfrak{s}$ at the head-body join. To ensure continuity we must enforce that the angle and curvature at the join are equal i.e.

$$\theta(0,t) = \phi(0,t) \quad \text{and} \quad \left.\frac{\partial\theta(s,t)}{\partial s}\right|_{s=0} = -\left.\frac{\partial\phi(\mathfrak{s},t)}{\partial\mathfrak{s}}\right|_{\mathfrak{s}=0} \quad \text{for all } t. \tag{2.1.1}$$

The minus sign in the second condition arises because s and $\mathfrak{s}$ increase in opposite directions.

As mentioned in Section 1.4, we model actin as a semiflexible polymer. The semiflexible condition, see equation (1.4.16), means that we can choose that the tangent vector is a unit vector i.e.

$$\frac{\partial \vec{\mathbf{R}}(s,t)}{\partial s} = \hat{\mathbf{t}}(s) = \cos(\theta(s,t))\,\hat{\mathbf{i}} + \sin(\theta(s,t))\,\hat{\mathbf{j}} \tag{2.1.2}$$

where $\hat{\mathbf{i}}$ and $\hat{\mathbf{j}}$ are the usual Cartesian unit vectors. This led to some simplification of the calculations, as will be seen later.

2.1.2 Motion of the body of the filament

Now we turn to determining the equation that governs the motion of the body. Since we model the body as following the path of the head, we can relate the value of $\theta(s,t)$ at any point along the chain, for any time, to that of the head-body join at an earlier time. That is to say, we have the condition

$$\theta(s,t) = \theta(0, t - {}^{s}/_{v}). \tag{2.1.3}$$

Equivalently, we can write

$$\frac{\partial \theta(s,t)}{\partial t} = -\,v\,\frac{\partial \theta(s,t)}{\partial s}, \tag{2.1.4}$$

which states that the rate of reorientation of the filament is directly proportional to the curvature of the filament. These relationships will be important later, as it means the motion of the body is determined wholly by the dynamics of the join.

2.1.3 Motion of the head of the filament

The motion of the head requires more care. Here we use an overdamped Langevin equation - see equation (1.4.9) - to model the dynamics of the head. This is a typical approach when dealing with systems, such as motility assays, where there is contact with a substrate [2]. In our case, the head's tangent angle $\phi(\mathfrak{z},t)$ is the relevant degree of freedom. This leads to a bond-orientation Langevin equation for ϕ

$$0 = -\zeta\,\frac{\partial \phi}{\partial t} - \frac{\delta E[\phi]}{\delta \phi(\mathfrak{z})} + f_{\phi}(t). \tag{2.1.5}$$

The second term in this equation is the gradient of the bending energy defined in equation (1.4.15) in terms of the anle ϕ. When we apply the consequence of the semiflexibility condition in equation (2.1.2) to the head, then the bending energy is given by

$$E_{\text{bending}} = \frac{1}{2}\kappa \int_0^{\ell} \mathrm{d}\mathfrak{z}\,\left(\frac{\partial \phi(\mathfrak{z})}{\partial \mathfrak{z}}\right)^2, \tag{2.1.6}$$

which leads to a very simple-looking term as follows:

$$\frac{\delta E[\phi]}{\delta \phi(\mathfrak{z})} = \lim_{\epsilon \to 0^+}\,\frac{1}{\epsilon}\left[\frac{\kappa}{2}\int_0^L \mathrm{d}\mathfrak{z}'\,\left(\frac{\partial \phi}{\partial \mathfrak{z}'} + \epsilon\frac{\partial \delta(\mathfrak{z}'-\mathfrak{z})}{\partial s}\right)^2 - \frac{\kappa}{2}\int_0^L \mathrm{d}\mathfrak{z}'\,\left(\frac{\partial \phi}{\partial \mathfrak{z}'}\right)\right] \tag{2.1.7}$$

$$= \kappa \int_0^L \mathrm{d}\mathfrak{z}' \, \frac{\partial \delta(\mathfrak{z}' - \mathfrak{z})}{\partial \mathfrak{z}'} \, \frac{\partial \phi}{\partial \mathfrak{z}'} \tag{2.1.8}$$

$$= -\kappa \int_0^L \mathrm{d}\mathfrak{z}' \, \delta(\mathfrak{z}' - \mathfrak{z}) \frac{\partial^2 \phi}{\partial \mathfrak{z}'^2} \tag{2.1.9}$$

$$= -\kappa \frac{\partial^2 \phi}{\partial \mathfrak{z}^2}. \tag{2.1.10}$$

The bond-orientation Langevin equation (2.1.5) becomes

$$0 = -\zeta \, \frac{\partial \phi}{\partial t} + \kappa \frac{\partial^2 \phi}{\partial \mathfrak{z}^2} + f_\phi(t). \tag{2.1.11}$$

Here we see the value of the parametrisation discussed earlier and illustrated in Figures 2.1 and 2.2b – the head is described entirely in terms of a single parameter. Note that equation (2.1.11) has the same form as the Rouse model (see equation (1.4.12)).

2.1.4 Description of the filament head in terms of modes

A common analytical technique is the use of modes, in particular for the Rouse model [3; 6; 52; 64]. It amounts to finding the eigenvalues of the Fourier transform. The details can be followed in Appendix A.

The angle of the filament head, $\phi(\mathfrak{z}, t)$ is written in terms of normal modes as follows:

$$\phi(\mathfrak{z}, t) = \sum_{m \text{ odd}} \tilde{\phi}_m(t) \sin(\alpha_m \mathfrak{z}) \tag{2.1.12}$$

with

$$\alpha_m = \frac{m\pi}{2\ell}, \qquad m \text{ odd}. \tag{2.1.13}$$

Although the mathematical form of equation (2.1.11) is exactly the same as the Rouse model, we have different boundary conditions for the head. For the purposes of deriving the modes, we take the exploring end of the head – i.e. where $\mathfrak{z} = \ell$ – to be free of any forces acting on it and we set the angle at the head-body join – where $\mathfrak{z} = 0$ – to be zero. This zero angle is arbitrary and we shall generalise it shortly. The condition that the filament tip is free of any torque is what causes the modes to be only odd.

Following the standard procedure, we obtain

$$\tilde{\phi}_m(t) = \frac{1}{\zeta_m} \int_{-\infty}^{t} \mathrm{d}t' \, e^{-\frac{(t-t')}{\tau_m}} \, \tilde{f}_m(t') \tag{2.1.14}$$

where

$$\tau_m = \frac{\zeta_m}{\kappa_m} = \frac{\left(\frac{1}{2}\zeta\ell\right)}{\left(\frac{\kappa m^2 \pi^2}{8\ell}\right)} = \frac{4\zeta\ell^2}{\kappa\pi^2} \frac{1}{m^2} \tag{2.1.15}$$

and

$$\tilde{f}_m(t) = \frac{\zeta_m}{\zeta} \int_0^\ell \mathrm{d}\mathfrak{z} \, \sqrt{\tfrac{\ell}{2}} \sin\left(\alpha_m \mathfrak{z}\right) f_\phi(t) \tag{2.1.16}$$

for the modes.

To generalise the condition that the head-body join angle is zero we introduce $\Phi_0(t)$ which gives the initial join angle at a time t. Hence

$$\phi(\mathfrak{s},t) = \Phi_0(t) + \sum_{m \text{ odd}} \tilde{\phi}_m(t)\sin(\alpha_m \mathfrak{s}). \tag{2.1.17}$$

2.1.5 Joining the head and the body

Let us now investigate the consequences of imposing continuity of the head and the body. We require both the tangent angle and tangent curvature to be continuous, i.e.

$$\theta(0,t) = \phi(0,t) = \Phi_0(t) \quad \text{for all } t \tag{2.1.18}$$

and

$$\left.\frac{\partial\theta(s,t)}{\partial s}\right|_{s=0} = -\left.\frac{\partial\phi(\mathfrak{s},t)}{\partial\mathfrak{s}}\right|_{\mathfrak{s}=0} \quad \text{for all } t. \tag{2.1.19}$$

Further we have the boundary condition

$$\left.\frac{\partial\phi(\mathfrak{s},t)}{\partial t}\right|_{\mathfrak{s}=0} = v\left.\frac{\partial\phi(\mathfrak{s},t)}{\partial\mathfrak{s}}\right|_{\mathfrak{s}=0} \tag{2.1.20}$$

from applying equation (2.1.4) and the continuity conditions to the point where $s = 0 = \mathfrak{s}$. This has the consequence of coupling the zeroth mode to all the other modes since

$$\begin{aligned}\left.\frac{\partial\phi(\mathfrak{s},t)}{\partial\mathfrak{s}}\right|_{\mathfrak{s}=0} &= \left.\sum_{m \text{ odd}} \tilde{\phi}_m(t)\ \tfrac{\pi m}{2\ell}\ \cos(\pi m\mathfrak{s}/2\ell)\right|_{\mathfrak{s}=0} \\ &= \sum_{m \text{ odd}} \tfrac{\pi m}{2\ell}\ \tilde{\phi}_m(t)\end{aligned} \tag{2.1.21}$$

and

$$\begin{aligned}\left.\frac{\partial\phi(\mathfrak{s},t)}{\partial t}\right|_{\mathfrak{s}=0} &= \dot{\Phi}_0(t) + \left.\sum_{m \text{ odd}} \dot{\tilde{\phi}}_m(t)\ \sin(\pi m\mathfrak{s}/2\ell)\right|_{\mathfrak{s}=0} \\ &= \dot{\Phi}_0(t),\end{aligned} \tag{2.1.22}$$

we have that

$$\dot{\Phi}_0(t) = v\sum_{m \text{ odd}} \tfrac{\pi m}{2\ell}\ \tilde{\phi}_m(t). \tag{2.1.23}$$

2.1.6 Motion of the exploring filament tip

We have derived equations that govern the motion of the body, the motion of the force-free head in terms of modes and explored the consequences of the continuity of these two regimes. What we have yet to do is take into account the forces acting on the tip of the head as it explores its environment.

The head experiences a drag from the surrounding fluid and is also pushed forward by the body. We model the head as being like a bead on a chain with the drag only acting on the bead. The Langevin equation that describes this is

$$\vec{\mathbf{0}} = -\varsigma \frac{\partial \vec{\mathbf{R}}(\ell, t)}{\partial t} - \frac{\partial E}{\partial \vec{\mathbf{R}}(\ell, t)} + \vec{\mathbf{f}}_h, \tag{2.1.24}$$

where E is the bending energy and $\vec{\mathbf{f}}_h$ is the stochastic force, which we assume acts only on the bead at the head of the filament. This is reasonable, given our assumption that $\ell \ll L$ – in other words that the myosin motors in the actin-mosin motility assay are sufficiently dense so that the polymer does not remain untethered for long. In keeping with this assumption, we shall also only consider the head tangent angle up to the first mode i.e.

$$\phi(\mathfrak{z}, t) = \Phi_0(t) + \tilde{\phi}_1(t) \sin\left({}^{\pi\mathfrak{z}}/_{2\ell}\right). \tag{2.1.25}$$

This makes the assumption that the head does not bend into very convoluted shapes and instead that the head configuration remains simple. This is also the leading order bending energy contribution, see equation (2.1.6), as can be seen below:

$$E_{\text{bending}} = \frac{1}{2}\kappa \int_0^\ell \mathrm{d}\mathfrak{z} \left(\frac{\partial \phi(\mathfrak{z}, t)}{\partial \mathfrak{z}}\right)^2 \tag{2.1.26}$$

$$= \frac{1}{2}\kappa \int_0^\ell \mathrm{d}\mathfrak{z} \left(\frac{\partial \left(\Phi_0(t) + \sum_{m \text{ odd}} \tilde{\phi}_m(t) \sin\left({}^{m\pi\mathfrak{z}}/_{2\ell}\right)\right)}{\partial \mathfrak{z}}\right)^2 \tag{2.1.27}$$

$$= \frac{1}{2}\kappa \int_0^\ell \mathrm{d}\mathfrak{z} \left(\sum_{m \text{ odd}} \tilde{\phi}_m(t) \left({}^{\pi m}/_{2\ell}\right) \cos\left({}^{m\pi\mathfrak{z}}/_{2\ell}\right)\right)^2 \tag{2.1.28}$$

$$\approx \frac{1}{2}\kappa \int_0^\ell \mathrm{d}\mathfrak{z} \left(\frac{\pi}{2\ell}\tilde{\phi}_1(t) \cos\left({}^{\pi\mathfrak{z}}/_{2\ell}\right)\right)^2 \tag{2.1.29}$$

$$= \frac{\kappa\pi^2}{16\ell}\, \tilde{\phi}_1^2(t). \tag{2.1.30}$$

We see here that the bending energy is in terms of ϕ, whereas the bending energy force term in equation (2.1.24) is in terms of $\vec{\mathbf{R}}$. To get round this, we use the chain rule to write

$$\frac{\partial E}{\partial \vec{\mathbf{R}}(\ell, t)} = \frac{\partial E}{\partial \phi}\frac{\partial \phi}{\partial x}\hat{\mathbf{i}} + \frac{\partial E}{\partial \phi}\frac{\partial \phi}{\partial y}\hat{\mathbf{j}} \tag{2.1.31}$$

From equation (2.1.30), we have that

$$\frac{\partial E}{\partial \phi} = \frac{\partial E}{\partial \tilde{\phi}_1} = \frac{\kappa\pi^2}{8\ell}\, \tilde{\phi}_1(t). \tag{2.1.32}$$

and so we need only determine $\frac{\partial \phi_1}{\partial x}$ and $\frac{\partial \phi_1}{\partial y}$ in equation (2.1.31). The details of this calculation and the calculation of $\frac{\partial \vec{\mathbf{R}}(\ell,t)}{\partial t}$ in equation (2.1.31) can be followed in Appendix B. The result is

$$\vec{\mathbf{0}} = \left\{ -\varsigma v \cos(\Phi_0) + \left(\frac{\kappa\pi^3}{16\ell^2}\frac{1}{\sin\Phi_0} + \frac{\varsigma v \pi}{2}\sin\Phi_0\right)\tilde{\phi}_1 + \left(\frac{2\varsigma\ell}{\pi}\sin\Phi_0\right)\dot{\tilde{\phi}}_1 \right\}\hat{\mathbf{i}} \; +$$

$$\left\{-\varsigma v\sin(\Phi_0)+\left(-\frac{\kappa\pi^3}{16\ell^2}\frac{1}{\cos\Phi_0}-\frac{\varsigma v\pi}{2}\cos\Phi_0\right)\tilde{\phi}_1-\left(\frac{2\varsigma\ell}{\pi}\cos\Phi_0\right)\dot{\tilde{\phi}}_1\right\}\hat{\mathbf{j}}\ +\ \vec{\mathbf{f}}_h.\prime \tag{2.1.33}$$

At this point we introduce the projection unit vector

$$\hat{\mathbf{\Phi}}_\perp=-\sin\Phi_0\hat{\mathbf{i}}+\cos\Phi_0\hat{\mathbf{j}} \tag{2.1.34}$$

that projects perpendicularly to the tangent angle. If we project equation (2.1.33) in this direction then we have a very simple differential equation for $\tilde{\phi}_1$, as can be seen below:

$$\frac{2\varsigma\ell}{\pi}\dot{\tilde{\phi}}_1=-\left(\frac{\kappa\pi^3}{8\ell^2}+\frac{\varsigma v\pi}{2}\right)\tilde{\phi}_1+f_{\text{proj}}. \tag{2.1.35}$$

We have renamed $\vec{\mathbf{f}}_h\cdot\hat{\mathbf{\Phi}}_\perp$ as f_{proj} and we consider this projection as still being Gaussian distributed with probability

$$\mathrm{P}[f]=\mathcal{N}\ \exp\left\{-\frac{1}{2\lambda}\int_0^\infty \mathrm{d}\tau\ f_{\text{proj}}^{\,2}(\tau)\right\}. \tag{2.1.36}$$

This assumes that the stochastic force is not biased towards a particular direction and that the stochastic force is faster than any reorientation of the head.

The form of equation (2.1.35) is the same as a one-dimensional motion of a Brownian particle in a harmonic potential [52]. The formal solution of this differential equation is

$$\tilde{\phi}_1(t)=\tilde{\phi}_1(0)e^{-t/a}\ +\ \frac{1}{\xi}\int_0^t \mathrm{d}t'\ e^{-(t-t')/a}\ f_{\text{proj}}(t') \tag{2.1.37}$$

where

$$a=\frac{\xi}{k}\quad\text{and}\quad\xi=\frac{2\varsigma\ell}{\pi}\qquad k=\left(\frac{\kappa\pi^3}{8\ell^2}+\frac{\varsigma v\pi}{2}\right). \tag{2.1.38}$$

Note that a is a time scale (see Appendix C) and that the effective spring coefficient k depends on the bending rigidity κ, drag ς and filament head extension ℓ in an intuitive way. Note that it also contains the active velocity term v of the body pushing the head. The effective drag coefficient depends on the original drag coefficient ς and the head extension ℓ, which also seems intuitive.

Without loss of generality, we may choose to set $\tilde{\phi}_1(0)$ in equation (2.1.37) to zero and just work with

$$\tilde{\phi}_1(t)=\frac{1}{\xi}\int_0^t \mathrm{d}t'\ e^{-(t-t')/a}\ f_{\text{proj}}(t'). \tag{2.1.39}$$

We may also obtain a formal solution for Φ_0 from equation (2.1.39) since, by equation (2.1.23),

$$\Phi_0(t)=\Phi_0(0)+\frac{v\pi}{2\ell}\int_0^t \mathrm{d}t'\ \tilde{\phi}_1(t'). \tag{2.1.40}$$

.

2.2 Calculating the average end-to-end distance

One of the experimentally measurable quantities in an actin-myosin motility assay is the average end-to-end distance of the filaments. It also gives insight into how the filament is moving.

We ignore the extension ℓ of the head when we calculate the average end-to-end distance of the polymer (recall equation (1.4.6)). That is to say, we consider $\langle(\vec{\mathbf{R}}(L,t) - \vec{\mathbf{R}}(0,t))^2\rangle$ instead of $\langle(\vec{\mathbf{R}}(L+\ell,t) - \vec{\mathbf{R}}(0,t))^2\rangle$. This is in keeping with our $L \gg \ell$ assumption. However, the effect of the exploring head is taken into account by coupling the body to equation (2.1.35) that governs the head.

Using equation (2.1.2), which relates the position vector to the orientation angle, we can integrate to obtain

$$\vec{\mathbf{R}}(L,t) - \vec{\mathbf{R}}(0,t) = \int_0^L \mathrm{d}s \, \left(\cos(\theta(s,t))\,\hat{\mathbf{i}} + \sin(\theta(s,t))\,\hat{\mathbf{j}}\right). \tag{2.2.1}$$

Now we square this term and bring in the averaging. If we rewrite $\theta(s,t)$ as $\theta(0, t - {}^{s}/_{v})$, as per equation (2.1.3), and make the change of variables $\tau = t - {}^{s}/_{v}$, we find that

$$\begin{aligned}&\langle(\vec{\mathbf{R}}(L,t) - \vec{\mathbf{R}}(0,t))^2\rangle \\ &= \langle v^2 \int_{t-\frac{L}{v}}^{t}\int_{t-\frac{L}{v}}^{t} \mathrm{d}\tau\mathrm{d}\tau' \left[\cos\left(\theta(0,\tau)\right)\cos\left(\theta(0,\tau')\right) + \sin\left(\theta(0,\tau)\right)\sin\left(\theta(0,\tau')\right)\right]\rangle.\end{aligned} \tag{2.2.2}$$

It is convenient to rewrite the trigonometric terms in terms of exponential functions in order to evaluate this integral. If we simplify notation and set $\theta(0,\tau) = \theta$ and $\theta(0,\tau') = \theta'$, we have

$$\begin{aligned}\cos\left(\theta(0,\tau)\right)\cos\left(\theta(0,\tau')\right) &= \frac{1}{4}\left(e^{+i\theta} + e^{-i\theta}\right)\left(e^{+i\theta'} + e^{-i\theta'}\right) \\ \sin\left(\theta(0,\tau)\right)\sin\left(\theta(0,\tau')\right) &= -\frac{1}{4}\left(e^{+i\theta} - e^{-i\theta}\right)\left(e^{+i\theta'} - e^{-i\theta'}\right),\end{aligned}$$

which results in terms of the type $e^{\pm i(\theta+\theta')}$ and $e^{\pm i(\theta-\theta')}$ in equation (2.2.2).

At this point we can see how the head couples. From equations (2.1.20), (2.1.25) and (2.1.39), we have

$$\frac{\partial\theta(0,t)}{\partial t} = \frac{\partial\phi(0,t)}{\partial t} = v\,\frac{\partial\phi}{\partial s}\bigg|_{s=0} = \frac{v\pi}{2\ell}\tilde{\phi}_1(t) = \tfrac{1}{\zeta}\int_0^t \mathrm{d}t'\, e^{-(t-t')/a}\, f_{\text{proj}}(t') \tag{2.2.3}$$

with

$$\frac{v\pi}{2\ell\xi} = \frac{1}{\zeta}. \tag{2.2.4}$$

Now

$$\theta - \theta' = \tfrac{1}{\zeta}\int_{\tau'}^{\tau} \mathrm{d}t\, \tilde{\phi}_1(t) = \tfrac{1}{\zeta}\int_{\tau'}^{\tau} \mathrm{d}t_2 \int_0^{t_2} \mathrm{d}t_1\, e^{-(t_2-t_1)/a}\, f_{\text{proj}}(t_1) \tag{2.2.5}$$

and hence

$$\langle e^{\pm i(\theta-\theta')}\rangle = N\int [\mathrm{d}f]\exp\left\{\pm {}^{i}\!/_{\zeta}\int_{\tau'}^{\tau}\mathrm{d}t\int_{0}^{t}\mathrm{d}t_1\, e^{-(t-t_1)/a}\, f_{\mathrm{proj}}(t_1) - {}^{1}\!/_{2\lambda}\int \mathrm{d}t\, f_{\mathrm{proj}}^{2}(t)\right\} \tag{2.2.6}$$

with N a normalisation coefficient.

The calculation from this point onwards becomes quite involved. During the calculation, an analogue of the persistence length (see equation (1.4.4) and equation (1.4.7)) emerged that depended on the active velocity v of the body as it is pushed by myosin motors and, in turn, pushes the head. Despite neglecting the extension of the head in $\langle(\vec{\mathbf{R}}(L,t)-\vec{\mathbf{R}}(0,t))^2\rangle$, it still plays a role: the persistence length depended on the extension of the head, ℓ, as well as the drag, ς, on the head. The stiffness of the polymer (via κ) and the stochastic force (via λ) also plays a role in this persistence length:

$$\ell_{\mathrm{p}} = \frac{2\zeta^2 v}{a^2\lambda} = \frac{\left(\kappa\pi^3 + 4\pi v\ell^3\varsigma\right)^2}{8\pi^2 v\ell^4\lambda}. \tag{2.2.7}$$

We investigated $\langle(\vec{\mathbf{R}}(L,t)-\vec{\mathbf{R}}(0,t))^2\rangle$ for various limits and found

$$\text{(a)}\ \langle(\vec{\mathbf{R}}(L,t)-\vec{\mathbf{R}}(0,t))^2\rangle \sim \tfrac{1}{2}L^2 \quad \text{when } {}^{L}\!/_{v} \ll a \tag{2.2.8}$$

$$\text{(b)}\ \langle(\vec{\mathbf{R}}(L,t)-\vec{\mathbf{R}}(0,t))^2\rangle \sim \tfrac{1}{2}L^2 \quad \text{when } {}^{L}\!/_{v} \gg a \text{ and } L/\ell_{\mathrm{p}} \ll 1 \tag{2.2.9}$$

$$\text{(c)}\ \langle(\vec{\mathbf{R}}(L,t)-\vec{\mathbf{R}}(0,t))^2\rangle \sim (\ell_{\mathrm{p}}+av)L \quad \text{when } {}^{L}\!/_{v} \gg a \text{ and } L/\ell_{\mathrm{p}} \gg 1. \tag{2.2.10}$$

We see that we recover the equilibrium rigid rod behaviour for short times or long times, but short lengths ((a) and (b), respectively) and in (c) we have equilibrium flexible behaviour for long times and long lengths.

Chapter 3

Introducing hydrodynamics

In the previous chapter, we outlined the work where we looked at a single actin filament in a motility assay without considering the interactions with other filaments. However, we would really like to investigate the dynamics of the actin filaments as they interact with each other and so we need to include the interactions of the filaments with each other in our equations.

Recalling that the filaments in a motility assay move about in an aqueous environment, the logical way to model the interaction of the filaments is to take hydrodynamic effects into account. There also short-range direct interactions which we do not take into account but which we could, in principle, include. We keep our focus on the single actin filament, as before, but now we introduce an additional drag term to model the effect of the other filaments. This approach is supported by the work of Schaller *et al.* [28, 37] in that those papers observed hydrodynamic effects in the motility assays. Effectively, we postulate that the fluid of the motility assay will mediate the interaction between the filaments: the movement of the other filaments will create a current in the fluid of the motility assay which will result in the filament under consideration experiencing a drag force. Different points of this filament may experience a different force and so we must include the position dependence of this force. That is to say, the drag experienced by a filament tip is now relative to the flow field:

$$\vec{\mathbf{f}}_{\text{drag}} = -\varsigma \left(\frac{\partial \vec{\mathbf{R}}(\ell, t)}{\partial t} - \vec{\mathbf{v}}_f \left(\vec{\mathbf{R}}(\ell, t) \right) \right) \tag{3.0.1}$$

We can separate out the interaction flow term

$$\vec{\mathbf{f}}_{\text{interaction}} = \varsigma \, \vec{\mathbf{v}}_f \left(\vec{\mathbf{R}}(\ell, t) \right), \tag{3.0.2}$$

where ς is the drag coefficient and we see that the flow field $\vec{\mathbf{v}}_f$ depends on the position $\vec{\mathbf{R}}(\imath, t)$ of our focus filament.

Recall that we have modelled the head of the filament as the exploratory part and the body as simply following the path of the head. This is why we focus on the tip $\vec{\mathbf{R}}(\ell, t)$ of the filament.

3.1 Constant flow field

We start with the case of a homogeneous flow field i.e. $\vec{\mathbf{v}}_f\left(\vec{\mathbf{R}}(\mathfrak{z},t)\right) = \vec{\mathbf{v}}_f$, a constant. This models a filament that is isolated, but still experiencing some constant flow field. This is not yet the situation we would most like to model, but we start by investigating this case for two reasons: it is simpler mathematically; and should give us some insight into how to continue our calculations when the velocity field becomes more complicated.

Previously, we had equation (2.1.24)

$$\vec{\mathbf{0}} = -\varsigma\frac{\partial\vec{\mathbf{R}}(\ell,t)}{\partial t} - \frac{\delta E}{\delta\vec{\mathbf{R}}(\ell,t)} + \vec{\mathbf{f}}_h$$

at the tip of the filament.

Now, as discussed above, we investigate the case where the drag term is replaced so that the equation is the following:

$$\vec{\mathbf{0}} = -\varsigma\left(\frac{\partial\vec{\mathbf{R}}(\ell,t)}{\partial t} - \vec{\mathbf{v}}_f\right) - \frac{\delta E}{\delta\vec{\mathbf{R}}(\ell,t)} + \vec{\mathbf{f}}_h. \tag{3.1.1}$$

Up to first order in ϕ, equation (2.1.33) now reads

$$\begin{aligned}\vec{\mathbf{0}} = &\left\{-\varsigma v\cos(\Phi_0) + \left(\frac{\kappa\pi^3}{16\ell^2}\frac{1}{\sin\Phi_0} + \frac{\varsigma v\pi}{2}\sin\Phi_0\right)\tilde{\phi}_1 + \left(\frac{2\varsigma\ell}{\pi}\sin\Phi_0\right)\tilde{\phi}_1'\right\}\hat{\mathbf{i}}\\ &\left\{-\varsigma v\sin(\Phi_0) + \left(-\frac{\kappa\pi^3}{16\ell^2}\frac{1}{\cos\Phi_0} - \frac{\varsigma v\pi}{2}\cos\Phi_0\right)\tilde{\phi}_1 - \left(\frac{2\varsigma\ell}{\pi}\cos\Phi_0\right)\tilde{\phi}_1'\right\}\hat{\mathbf{j}}\\ &+\ \varsigma\,\vec{\mathbf{v}}_f\ +\ \vec{\mathbf{f}}_h.\end{aligned} \tag{3.1.2}$$

If, again, we project onto the direction of $\hat{\mathbf{\Phi}}_\perp = -\sin\Phi_0\hat{\mathbf{i}} + \cos\Phi_0\hat{\mathbf{j}}$ we obtain

$$\xi\tilde{\phi}_1' = -k\tilde{\phi}_1\ +\ \varsigma\,\vec{\mathbf{v}}_f\cdot\hat{\mathbf{\Phi}}_\perp\ +\ \vec{\mathbf{f}}_h\cdot\hat{\mathbf{\Phi}}_\perp. \tag{3.1.3}$$

Without loss of generality, let us also orientate our axes such that $\vec{\mathbf{v}}_f = v_f\hat{\mathbf{i}}$. Then we have

$$\xi\ \tilde{\phi}_1'(t) = -\ k\ \tilde{\phi}_1(t)\ -\ \varsigma v_f\sin\Phi_0(t)\ +\ f_{\text{proj}} \tag{3.1.4}$$

with ξ and k defined as before in (2.1.38).

We should note, however, that Φ_0 depends on $\tilde{\phi}_1$ via (2.1.23). We rewrite (3.1.4) now in terms of this to get a linear, second-order differential equation in Φ_0

$$\xi\ \Phi_0''(t) = -\ k\ \Phi_0'(t)\ -\ \tfrac{\varsigma v_f v\pi}{2\ell}\sin\Phi_0(t)\ +\ \tfrac{v\pi}{2\ell}f_{\text{proj}} \tag{3.1.5}$$

and we recognise the equation for a damped pendulum driven by a stochastic force. Unfortunately this equation is for an anharmonic pendulum and is not simple to solve analytically. The behaviour of the harmonic pendulum equation, however, are well known. We can retrieve the

harmonic pendulum equation if we linearise the sine function . This would be an acceptable approximation in the case of small $\Phi_0(t)$. The linear version now reads

$$\xi\ \Phi_0''(t) = -\ k\ \Phi_0'(t)\ -\ \tfrac{\varsigma v_f v\pi}{2\ell}\ \Phi_0(t)\ +\ \tfrac{v\pi}{2\ell} f_{\text{proj}}(t). \tag{3.1.6}$$

At this point it is helpful to rewrite this equation in a simpler form so that we can separate the underdamped and overdamped scenarios. Consider now

$$\Phi_0''(t) + a\ \Phi_0'(t)\ + b\ \Phi_0(t)\ = \tfrac{v\pi}{2\ell\xi} f_{\text{proj}}(t), \tag{3.1.7}$$

where

$$a = {}^{k}\!/_{\xi}, \tag{3.1.8}$$

as before, and we define

$$b = {}^{\varsigma v_f v\pi}\!/_{2\xi\ell}. \tag{3.1.9}$$

We see that a depends only on the filament properties, whereas b is additionally directly proportional to the speed of the flow field, v_f. Note also that a has a dimension of ${}^{1}\!/_{t}$ and b has a dimension of ${}^{1}\!/_{t^2}$. Whether or not we have over- or underdamping depends on how these rates compare. We introduce the dimensionless ratio

$$r = {}^{4b}\!/_{a^2}. \tag{3.1.10}$$

Then over- and underdamping is a simple matter of whether or not the ratio r is greater or less than 1.

$$\begin{aligned} &\text{Overdamping:} && r\ <\ 1 \\ &\text{Underdamping:} && r\ >\ 1 \end{aligned} \tag{3.1.11}$$

In order to solve for $\Phi_0(t)$, we introduce the Fourier transform of $\Phi_0(t)$

$$\overline{\Phi}_0(\omega) = \int_{-\infty}^{\infty} \mathrm{d}t\ \Phi_0(t)\ e^{-i\omega t} \tag{3.1.12}$$

and find

$$-\omega^2\ \overline{\Phi}_0 + ia\,\omega\ \overline{\Phi}_0 + b\ \overline{\Phi}_0 = \tfrac{v\pi}{2\ell\xi}\ \overline{f}_{\text{proj}}(\omega) \tag{3.1.13}$$

$$\implies \qquad \overline{\Phi}_0 = \frac{\frac{v\pi}{\xi 2\ell}\ \overline{f}_{\text{proj}}(\omega)}{-\omega^2 + ia\,\omega + b} \equiv \wr(\omega)\ \overline{f}_{\text{proj}}(\omega) \tag{3.1.14}$$

where

$$\overline{f}_{\text{proj}}(\omega) = \int_{-\infty}^{\infty} \mathrm{d}t\ f_{\text{proj}}(t)\ e^{-i\omega t}.$$

A quick check shows that

$$\langle \overline{f}(\omega) \rangle = 0 \tag{3.1.15}$$

$$\langle \overline{f}(\omega_1)\overline{f}(\omega_2)\rangle = 2\pi\ \delta(\omega_1+\omega_2). \tag{3.1.16}$$

We calculate

$$\left\langle (\Phi_0(t_2)-\Phi_0(t_1))^2\right\rangle = \left\langle \Phi_0^2(t_2) - 2\ \Phi_0(t_1)\Phi_0(t_2) + \Phi_0^2(t_2)\right\rangle \tag{3.1.17}$$

via the inverse Fourier transform

$$\Phi_0(t) = \tfrac{1}{2\pi}\int_{-\infty}^{\infty} \mathrm{d}\omega\ \overline{\Phi}_0(\omega)\ e^{i\omega t}. \tag{3.1.18}$$

Then we have

$$\begin{aligned}
\left\langle \Phi_0^2(t)\right\rangle &= \left\langle \tfrac{1}{4\pi^2}\int_{-\infty}^{\infty}\mathrm{d}\omega_1\ \int_{-\infty}^{\infty}\mathrm{d}\omega_2\ e^{i(\omega_1+\omega_2)t}\overline{\Phi}_0(\omega_1)\overline{\Phi}_0(\omega_2)\right\rangle \\
&= \tfrac{1}{4\pi^2}\int_{-\infty}^{\infty}\mathrm{d}\omega_1\ \int_{-\infty}^{\infty}\mathrm{d}\omega_2\ e^{i(\omega_1+\omega_2)t}\int(\omega_1)\int(\omega_2)\left\langle \overline{f}_{\text{proj}}(\omega_1)\overline{f}_{\text{proj}}(\omega_2)\right\rangle \\
&= \tfrac{1}{4\pi^2}\int_{-\infty}^{\infty}\mathrm{d}\omega_1\ \int_{-\infty}^{\infty}\mathrm{d}\omega_2\ e^{i(\omega_1+\omega_2)t}\int(\omega_1)\int(\omega_2)\ 2\pi\lambda\,\delta(\omega_1+\omega_2) \\
&= \tfrac{\lambda}{2\pi}\int_{-\infty}^{\infty}\mathrm{d}\omega\ \int(\omega)\int(-\omega) = \tfrac{\lambda}{2\pi}\int_{-\infty}^{\infty}\mathrm{d}\omega\ \int(\omega)\int^*(\omega)
\end{aligned} \tag{3.1.19}$$

and

$$\begin{aligned}
\langle \Phi_0(t_1)\Phi_0(t_2)\rangle &= \left\langle \tfrac{1}{4\pi^2}\int_{-\infty}^{\infty}\mathrm{d}\omega_1\ \int_{-\infty}^{\infty}\mathrm{d}\omega_2\ e^{i(\omega_1 t_1+\omega_2 t_2)}\ \overline{\Phi}_0(\omega_1)\overline{\Phi}_0(\omega_2)\right\rangle \\
&= \tfrac{1}{4\pi^2}\int_{-\infty}^{\infty}\mathrm{d}\omega_1\ \int_{-\infty}^{\infty}\mathrm{d}\omega_2\ e^{i(\omega_1 t_1+\omega_2 t_2)}\int(\omega_1)\int(\omega_2)\left\langle \overline{f}_{\text{proj}}(\omega_1)\overline{f}_{\text{proj}}(\omega_2)\right\rangle \\
&= \tfrac{1}{4\pi^2}\int_{-\infty}^{\infty}\mathrm{d}\omega_1\ \int_{-\infty}^{\infty}\mathrm{d}\omega_2\ e^{i(\omega_1 t_1+\omega_2 t_2)}\int(\omega_1)\int(\omega_2)\ 2\pi\lambda\,\delta(\omega_1+\omega_2) \\
&= \tfrac{\lambda}{2\pi}\int_{-\infty}^{\infty}\mathrm{d}\omega\ e^{i\omega|t_1-t_2|}\int(\omega)\int(-\omega).
\end{aligned} \tag{3.1.20}$$

The integrals in equations (3.1.19) and (3.1.20) can be evaluated. We introduce another dimensionless ratio $\tau = \frac{|t_2-t_1|\,a}{2}$. This ratio is the comparison between the length of the observation time and the rate a, which depends on filament properties. We obtain

$$\left\langle (\Phi_0(t_2)-\Phi_0(t_1))^2\right\rangle = \frac{2\lambda v^2\pi^2\xi}{\ell^2 k^3}\,\frac{1}{r}\begin{cases} 1-e^{-\tau}\left[\cosh\left(\sqrt{1-r}\,\tau\right)+\frac{1}{\sqrt{1-r}}\sinh\left(\sqrt{1-r}\,\tau\right)\right] & \text{overdamped, } r<1 \\ 1-e^{-\tau}\left[\cos\left(\sqrt{r-1}\,\tau\right)+\frac{1}{\sqrt{r-1}}\sin\left(\sqrt{r-1}\,\tau\right)\right] & \text{underdamped, } r>1. \end{cases} \tag{3.1.21}$$

This is clearly real, as it should be. We also need to make sure that it is positive. We shall investigate this result by taking a look at some limits and making a few plots. We see, also, that the second term is exponentially suppressed for longer observation times and that the first

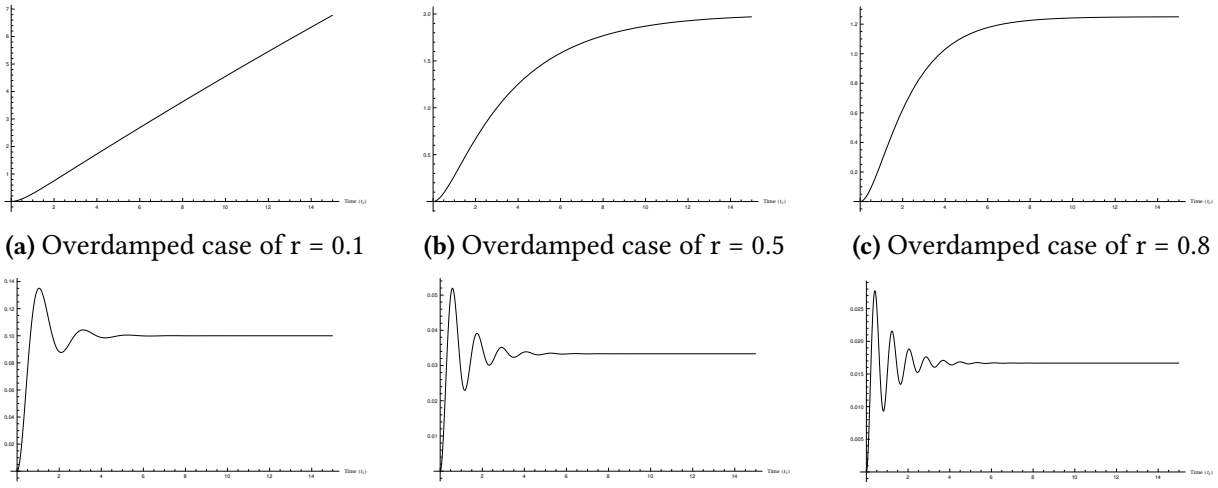

(a) Overdamped case of r = 0.1 **(b)** Overdamped case of r = 0.5 **(c)** Overdamped case of r = 0.8

(d) Underdamped case of r = 10 **(e)** Underdamped case of r = 30 **(f)** Underdamped case of r = 60

Figure 3.1: Plots showing $\langle(\Phi_0(t_2) - \Phi_0(t_1))^2\rangle$ for different values of r as $\tau = \frac{|t_2 - t_1|\, a}{2}$ goes from 0 to 15.

term is independent of time. The first term is only dependent on the ratio r, which compares the filament rate a with the rate b that depends on the flow velocity.

However, before we investigate further, we recall equation (3.1.7). To be consistent with our linear approximation in equation (3.1.7), we must make sure that Φ_0 is small. We can consider Φ_0 being well approximated by

$$\begin{aligned}\Phi_0 &= \langle\Phi_0\rangle + \Delta\Phi_0 \\ &= \langle\Phi_0\rangle + \sqrt{\langle(\Phi_0 - \langle\Phi_0\rangle)^2\rangle} \\ &= \langle\Phi_0\rangle + \sqrt{\langle\Phi_0^2\rangle - \langle\Phi_0\rangle^2}.\end{aligned} \tag{3.1.22}$$

In other words, we approximate Φ_0 by saying it is equal to its average value plus fluctuations around that average.

It is quick to show that $\langle\Phi_0\rangle = 0$ (see Appendix D). This is the expected behaviour, given that the flow field is homogenous and orientated along the x-axis.

Hence the above equation (3.1.22) simplifies to

$$\begin{aligned}\Phi_0 &= \sqrt{\langle\Phi_0^2\rangle} \\ &= \left(\frac{2\lambda v^2 \pi^2 \xi}{\ell^2 k^3}\,\frac{1}{r}\right)^{1/2}.\end{aligned} \tag{3.1.23}$$

We have already outlined this calculation in equation (3.1.19). Since $\Phi_0(t)$ must be small, we have that our approximation is only valid for large enough r or, equivalently, large enough v_f.

Now that we know the situations where our linear approximation is appropriate, we return to our investigation of equation (3.1.21).

We can see a few sample plots of $\langle(\Phi_0(t_2) - \Phi_0(t_1))^2\rangle$ in figure Figure 3.1. The oscillatory behaviour in the underdamped case can clearly be seen. It should also be noted that the plots are purely positive, as they should be.

We turn to an investigation of equation (3.1.21) in various limiting scenarios, namely the large and small v_f cases for both long and short time scales τ.

If the flow field v_f is very large in comparison, this corresponds to the underdamped case with $r \to \infty$. If we perform this limit on equation (3.1.21), we find

$$\lim_{r\to\infty} \langle (\Phi_0(t_2) - \Phi_0(t_1))^2 \rangle = \infty. \tag{3.1.24}$$

This corresponds to our intuition that a strong flow field should cause the filament to align totally and hence there will be no average fluctuations.

If the flow field v_f is very small in comparison, we expect to recover the flexible behaviour seen for long filaments over long times in equation (2.2.8). This scenario corresponds to the overdamped case with $r \to 0$. If we perform this limit, we get

$$\lim_{r\to 0} \langle (\Phi_0(t_2) - \Phi_0(t_1))^2 \rangle = \tfrac{1}{4} \left(2\tau + e^{-2\tau} - 1\right). \tag{3.1.25}$$

What we see is modified random walk behaviour and therefore we are able to recover the $v_f = 0$ behaviour investigated earlier when we take this limit.

Since this limit is still dependent on time, we can further investigate the (comparatively) long and short $\tau = \frac{|t_2 - t_1|a}{2}$ limits. For cases where the differences between the observational time difference is sufficiently larger than the intrinsic a time scale, we obviously see $\langle (\Phi_0(t_2) - \Phi_0(t_1))^2 \rangle$ going off to infinity, but for the $\tau \to 0$ case we recover rigid rod behaviour in that

$$\lim_{\tau\to 0} \tfrac{1}{4} \left(2\tau + e^{-2\tau} - 1\right) \sim \tau^2. \tag{3.1.26}$$

This is simply the known result that on sufficiently short length and time scales, we see rigid rod behaviour.

3.2 Non-homogenous flow fields

The results for the homogenous flow field are promising and a natural next step is to investigate non-homogenous flow fields. We began by investigating the case of a flow field with a constant gradient. However, the approach we followed for the homogenous case no longer became tractible when introducing non-homogeneity. Further, we really want to investigate the dynamics in terms of *collective* variables and to include a more physical model of the interaction drag force since this is caused by the active motion of the other filaments..

It is at this point, then, that we turn to a alternative formalism to gain some headway. This is the subject of the next chapter.

Chapter 4

Collective coordinates for dense systems

In Chapter 3 we motivated including the effects of other filaments by introducing hydrodynamic interactions. Now we look at an alternative way to formulate the equations of motion and the hydrodynamics of our system to deal with the coupling between different filaments that this hydrodynamic interaction produces.

One method that has been employed to study a system such as ours is to use continuum fields to represent densities and orientations of the filaments. This can be done in different ways, one approach of which is detailed in, for example, Giomi and Marchetti [63] or Elgeti *et al.* [5]. We follow a different approach based mainly on the paper by Fredrickson and Helfand [65].

Both approaches use continuum fields to understand the system, but the starting points are different. In the approach we follow, we derive properties of the continuum fields based on a Langevin equation which we have set up from considering the system on a microscopic scale. As such, we try to make an explicit connection between the microscopic picture of the system and the macroscopic behaviour of the system that is contained in the continuum fields. In the approach of the papers by Giomi and Marchetti [63] and Elgeti *et al.* [5], the authors begin immediately with hydrodynamic equations of motion for the macroscopic continuum fields, but include tuneable parameters in these equations. These parameters are then analysed, however the explicit connection to the microscopic is lost.

In the approach of the papers by Giomi and Marchetti [63] and Elgeti *et al.* [5], the coupled hydrodynamic equations are derived from a "free energy" given in terms of a polarisation vector field $\vec{\mathbf{P}}(\vec{\mathbf{r}}, t)$ that is simply defined without being based on an explicit model of dynamics of individual filaments. This "free energy" has a term that is quadratic in $\vec{\mathbf{P}}(\vec{\mathbf{r}}, t)$ and another that is quartic in $\vec{\mathbf{P}}(\vec{\mathbf{r}}, t)$, with coefficients a_2 and a_4 respectively. These coefficients take on the role of tuneable parameters. A third tuneable parameter λ is also introduced to describe the coupling of the filament orientation and the flow field.

In contrast, we formulate the Langevin equation – equation (1.4.9) – via the Hamiltonian with stretching energy given by equation (1.4.11) and bending energy given by equation (1.4.15). We also have a connection – equations (2.1.3) and (2.1.4) – between the position, s, along the

filament and the time, t, in our model so that we can always rewrite s in terms of t and vice versa. Instead of the polarisation vector field $\vec{\mathbf{P}}$ of Giomi and Marchetti [63] and Elgeti *et al.* [5], we have an orientational density field, $\vec{\pi}\left(\vec{\mathbf{R}}, t\right)$, which we define later in equation (4.2.17). We determine the fluctuations of these fields based on the Langevin equation. Instead of tuneable parameters, the coefficients in our work arise from microscopic considerations.

The tuneable parameters of Giomi and Marchetti [63] and Elgeti *et al.* [5] allow the authors to create phase diagrams for the system. While the method we employ – outlined below – is not able to produce detailed phase diagrams, analogous information can still be obtained by seeing where the method breaks down. If divergence appears, this is a signal of a phase change in the system.

These papers also introduce a Navier-Stokes equation to describe the evolution of the flow velocity. The Fredrickson and Helfand [65] paper we follow also uses an additional hydrodynamics equation to describe the flow velocity. The collective density variables are coupled to an underlying velocity field for the hydrodynamical medium, also modelled through a Navier-Stokes equation. We rather include the hydrodynamics of the flow velocity via the Oseen tensor, as Fredrickson and Helfand [65] suggested as an alternative and as detailed in Doi and Edwards [52].

4.1 Summary of the Martin-Siggia-Rose formalism

The Martin-Siggia-Rose (MSR) formalism [66] is a functional integral formalism. First we rewrite our equations in this functional integral formalism and then we follow that up by transforming to collective coordinates. We follow the approach outlined by Jensen [67] and Fredrickson and Helfand [65], that builds on the work of Martin, Siggia and Rose [66] and Jouvet and Phythian [68].

Suppose we have a Langevin equation $\vec{\mathcal{L}}(\vec{\mathbf{r}}(t)) = 0$, for all time t. Let $\vec{\mathbf{r}}(t)$ be a solution to the Langevin equation and consider

$$Z[\vec{\mathbf{r}}(t)] = \int [\mathrm{d}\vec{\mathbf{r}}(t)]\, \delta\left[\vec{\mathbf{r}}(t) - \vec{\mathbf{r}}(t)\right] \tag{4.1.1}$$

where $\int [\mathrm{d}\vec{\mathbf{r}}(t)]$ is a functional integral[1]. The delta functional in the integral means we may make a change of variables, since $\vec{\mathbf{r}}(t) - \vec{\mathbf{r}}(t)$ and $\vec{\mathcal{L}}(\vec{\mathbf{r}}(t))$will be zero at the same values of $\vec{\mathbf{r}}(t)$, for all t:

$$Z[\vec{\mathbf{r}}(t)] = \int [\mathrm{d}\vec{\mathbf{r}}(t)]\, \delta\left[\vec{\mathcal{L}}(\vec{\mathbf{r}}(t))\right]. \tag{4.1.2}$$

[1]The functional integral can be understood as integrating over all values of a function or, more formally, as the limit of a product of ordinary integrals as the function variable runs over the entire domain, where the domain has been discretised into N pieces of size ϵ: $\int [\mathrm{d}f(x)] \ldots = \lim_{\epsilon \to 0} \prod_{i=1}^{N} \int \mathrm{d}f(x_i) \ldots$The precise way the domain has been discretised will not be important in our case, because when calculating average values the prefactors this discretisation introduces will cancel.

We can ignore the Jacobian this produces if we obey certain causality rules as set out by Jensen [67]. The causality rules will be elaborated on later in this section.

Now we introduce what is known as the auxillary or response field $\hat{\vec{\mathbf{r}}}(t)$ by writing the Fourier transform of the delta functional:

$$Z[\vec{\mathbf{r}}(t)] = \int [\mathrm{d}\vec{\mathbf{r}}(t)][\mathrm{d}\hat{\vec{\mathbf{r}}}(t)]\ \exp\left\{ i \int \mathrm{d}t\ \hat{\vec{\mathbf{r}}}(t) \cdot \vec{\mathcal{L}}(\vec{\mathbf{r}}(t)) \right\}. \tag{4.1.3}$$

The average value over all possible realisations of $\vec{\mathbf{r}}(t)$ of some function $F(\vec{\mathbf{r}}(t))$ is given by

$$\langle F(\vec{\mathbf{r}}(t)) \rangle = Z[\vec{\mathbf{r}}(t)]^{-1} \int [\mathrm{d}\vec{\mathbf{r}}(t)][\mathrm{d}\hat{\vec{\mathbf{r}}}(t)]\ F(\vec{\mathbf{r}}(t))\ \exp\left\{ i \int \mathrm{d}t\ \hat{\vec{\mathbf{r}}}(t) \cdot \vec{\mathcal{L}}(\vec{\mathbf{r}}(t)) \right\}. \tag{4.1.4}$$

We can link equation (4.1.4) to equation (4.1.3) in the following way:

$$\begin{aligned} \langle F(\vec{\mathbf{r}}(t)) \rangle &= Z[\vec{\mathbf{r}}(t)]^{-1} \frac{\delta}{\delta G(t)} \int [\mathrm{d}\vec{\mathbf{r}}(t)][\mathrm{d}\hat{\vec{\mathbf{r}}}(t)] \times \\ &\qquad \exp\left\{ i \int \mathrm{d}t\ \left(\hat{\vec{\mathbf{r}}}(t) \cdot \vec{\mathcal{L}}(\vec{\mathbf{r}}(t)) + G(t) F(\vec{\mathbf{r}}(t)) \right) \right\} \Bigg|_{G=0} \\ &= Z[\vec{\mathbf{r}}(t)]^{-1}\ \frac{\delta Z[G(t)]}{\delta G(t)} \Bigg|_{G=0} \end{aligned} \tag{4.1.5}$$

The function $G(t)$ is arbitrary and the functional $Z[G(t)]$ that is being derived in equation (4.1.5) is often referred to as the generating functional as it can be used to generate average values.

It is when calculating averages that the causality rules come into play. These causality rules also ensure normalisation when averaging. The first rule is that averages over a product containing a hatted field $\hat{\vec{\mathbf{r}}}(t)$ is zero if t is the latest time appearing in the product. The second rule is that products with hatted variables, e.g. $\hat{\vec{\mathbf{r}}}(t)\vec{\mathbf{r}}(t)$, are interpreted as if the time t in the hatted variable is at an infinitesimally later time. Thus by the first rule, these products will average to zero [65; 67].

4.1.1 Collective variables

In the paper by Fredrickson and Helfand [65], the ideas outlined above are extended to deal with collective variables. The idea is to introduce the collective variables via integration over a delta functional.

For example, suppose we have a collection of particles labelled by an integer j and described by the position vector $\vec{\mathbf{r}}_j(t)$. We can define a particle density $\rho(\vec{\mathbf{r}}, t)$ as

$$\rho(\vec{\mathbf{r}}, t) = \sum_j \delta\left(\vec{\mathbf{r}} - \vec{\mathbf{r}}_j(t)\right). \tag{4.1.6}$$

We can introduce this into equation (4.1.3) in the following way:

$$\prod_j \int [\mathrm{d}\vec{\mathbf{r}}(t)][\mathrm{d}\hat{\vec{\mathbf{r}}}(t)][\mathrm{d}\rho(\vec{\mathbf{r}}, t)]\ \delta\left[\rho(\vec{\mathbf{r}}, t) - \textstyle\sum_j \delta\left(\vec{\mathbf{r}} - \vec{\mathbf{r}}_j(t)\right)\right]\ \exp\left\{ i \int \mathrm{d}t\ \hat{\vec{\mathbf{r}}}(t) \cdot \vec{\mathcal{L}}(\vec{\mathbf{r}}(t)) \right\}. \tag{4.1.7}$$

As before, we can rewrite the delta functional via the Fourier transform to bring the collective variable into the exponential:

$$\prod_j \int [\mathrm{d}\vec{\mathbf{r}}(t)][\mathrm{d}\hat{\vec{\mathbf{r}}}(t)][\mathrm{d}\rho(\vec{\mathbf{r}},t)][\mathrm{d}P(\vec{\mathbf{r}},t)] \times$$
$$\exp\left\{ i \int \mathrm{d}t\; P(\vec{\mathbf{r}},t) \left(\rho(\vec{\mathbf{r}},t) - \textstyle\sum_j \delta\left(\vec{\mathbf{r}} - \vec{\mathbf{r}}_j(t)\right) \right) + \hat{\vec{\mathbf{r}}}(t) \cdot \vec{\mathcal{L}}(\vec{\mathbf{r}}(t)) \right\}. \tag{4.1.8}$$

If we then integrate over $\vec{\mathbf{r}}(t)$ and $\hat{\vec{\mathbf{r}}}(t)$, we shall be left with a generating functional in terms of the collective variable $\rho(\vec{\mathbf{r}},t)$ and its response field $P(\vec{\mathbf{r}},t)$, as outlined in equation (4.1.5). In other words, we have used the delta functionals to make a change of variables. This will allow us to calculate average values of the collective variables and their correlation functions. These collective variables allow for a compact formulation of the hydrodynamic interaction between the filament tips and the bodies of the other filaments, as will be seen later – particularly in equation (4.2.18). We shall be approximating to quadratic order in the fluctuations of the density field, as has successfully been done before for dense systems. (The paper by Fredrickson and Helfand [65] is a prime example.) The approximation we employ is discussed in Section 4.3.

4.2 Applying the MSR formalism to our system

Recalling equation (3.1.1), we can write the Langevin equation for the tip of the j^{th} filament. First, however, we refine our notation so that

$$\vec{\mathbf{R}}_j(\ell,t) = \vec{\mathbf{R}}_j(0,t) + \vec{\mathbf{r}}_j(\ell,t) \tag{4.2.1}$$
$$\vec{\mathbf{r}}_j(\ell,t) = \ell\left[\cos\Phi_{0,j}(t) - \tfrac{2\ell}{\pi}\,\phi_{1,j}(t)\sin\Phi_{0,j}(t)\right]\hat{\mathbf{i}} + \ell\left[\sin\Phi_{0,j}(t) + \tfrac{2\ell}{\pi}\,\phi_{1,j}(t)\cos\Phi_{0,j}(t)\right]\hat{\mathbf{j}} \tag{4.2.2}$$
$$\frac{\partial}{\partial t}\vec{\mathbf{R}}_j(\ell,t) = \dot{\vec{\mathbf{R}}}_j(\ell,t) = \dot{\vec{\mathbf{R}}}_j(0,t) + \dot{\vec{\mathbf{r}}}_j(\ell,t) = \vec{\mathbf{v}}_{\mathrm{a},j}(t) + \dot{\vec{\mathbf{r}}}_j(\ell,t) \tag{4.2.3}$$

where the tilde over $\phi_{1,j}$ has been dropped and where

$$\vec{\mathbf{v}}_{\mathrm{a},j} = v\cos\Phi_{0,i}(t)\hat{\mathbf{i}} + v\sin\Phi_{0,i}(t)\hat{\mathbf{j}} \tag{4.2.4}$$

is the active velocity term that results from the body of the filament being pushed by the myosin motors. $\vec{\mathbf{R}}_j(\ell,t)$ is the absolute position of the tip of the j^{th} filament, $\vec{\mathbf{r}}_j(\ell,t)$ is the relative position vector between the head-body join of the filament and the tip of the j^{th} filament and $\frac{\partial}{\partial t}\vec{\mathbf{R}}_j(\ell,t)$ is the velocity of the tip of the j^{th} filament. See Figure 4.1.

With this in mind, we rewrite the equation for the dynamics of the tip of the j^{th} filament, previously equation (3.1.1), as

$$0 = -\varsigma\left(\vec{\mathbf{v}}_{\mathrm{a},j}(t) + \dot{\vec{\mathbf{r}}}_j(\ell,t) - \vec{\mathbf{v}}_f(\vec{\mathbf{r}}_j(\ell,t))\right) - \frac{\delta E}{\delta\vec{\mathbf{r}}_j(\ell,t)} + \vec{\mathbf{f}}_{h,j}$$

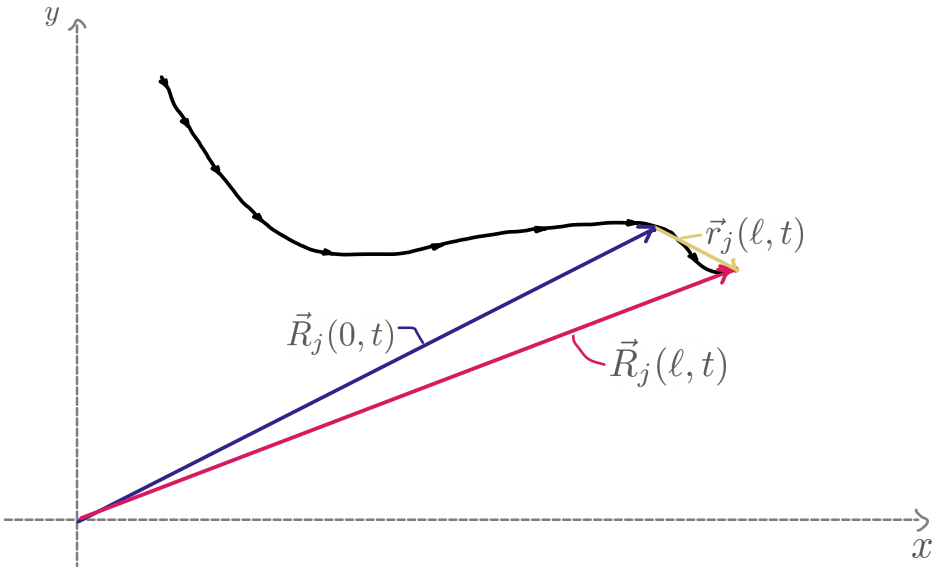

Figure 4.1: Diagram showing how notation has been refined for the position vectors. The vector $\vec{\mathbf{R}}_j(\ell,t)$ points from the origin to the tip of the j^{th} filament, $\vec{\mathbf{R}}_j(0,t)$ points from the origin to the head-body join and the vector $\vec{\mathbf{r}}_j(\ell,t)$ points from the join to the tip of the j^{th} filament.

$$= \underbrace{-\varsigma\left(\vec{\mathbf{v}}_{\mathrm{a},j}(t)+\dot{\vec{\mathbf{r}}}_j(\ell,t)\right)-\frac{\delta E}{\delta\vec{\mathbf{r}}_j(\ell,t)}+\vec{\mathbf{f}}_{h,j}}_{\text{no interactions}} + \overbrace{\varsigma\,\vec{\mathbf{v}}_f(\vec{\mathbf{r}}_j(\ell,t))}^{\text{hydrodynamic interactions}} \tag{4.2.5}$$

where we have separated out the drag term that comes from interactions with other filaments. We model this drag as being due to the motion of the bodies of the other filaments as they move through the surrounding fluid. Since this is a hydrodynamic interaction, we model this term as discussed in equation (1.4.13) using the Oseen tensor [31; 52] defined in equation (1.4.14):

$$\vec{\mathbf{v}}_f(\vec{\mathbf{r}}_j(\ell,t)) = \sum_i \int \mathrm{d}s\ \mathbf{H}\left(\vec{\mathbf{r}}_j(t)-\vec{\mathbf{R}}_i(s,t)\right)\cdot\vec{\mathbf{F}}_i(s) \tag{4.2.6}$$

where $\vec{\mathbf{F}}_i(s)$ are the forces acting on the i^{th} filament body at the point s along the body. We postulate that we need only include the active force of the bodies being pushed through the fluid by the myosin motors. We say this force has a constant magnitude and points tangentially to the body. We take the magnitude as constant, since the force arises from the experimentally observed constant velocity of the filament bodies. Hence

$$\vec{\mathbf{F}}_i(s) = f_a\,\frac{\partial\vec{\mathbf{R}}_i(s,t)}{\partial s} \tag{4.2.7}$$

and

$$\vec{\mathbf{v}}_f(\vec{\mathbf{r}}_j(\ell,t)) = f_a\sum_i \int \mathrm{d}s\ \mathbf{H}\left(\vec{\mathbf{r}}_j(t)-\vec{\mathbf{R}}_i(s,t)\right)\cdot\frac{\partial\vec{\mathbf{R}}_i(s,t)}{\partial s}. \tag{4.2.8}$$

The non-interacting part we deal with exactly as in previous sections. To linear order in $\phi_{1,j}$, as before, the non-interacting part looks as follows:

$$\begin{aligned}\vec{\mathcal{L}}_j = &-\varsigma\left[v\,\cos(\Phi_{0,j}(t)) - \tfrac{\pi}{2}\,v\,\phi_{1,j}(t)\,\sin(\Phi_{0,j}(t)) - \tfrac{2\ell}{\pi}\,\dot{\phi}_{1,j}\,\sin(\Phi_{0,j}(t))\right]\,\hat{\mathbf{i}}\\ &-\varsigma\left[v\,\sin(\Phi_{0,j}(t)) - \tfrac{\pi}{2}\,v\,\phi_{1,j}(t)\,\cos(\Phi_{0,j}(t)) - \tfrac{2\ell}{\pi}\,\dot{\phi}_{1,j}\,\cos(\Phi_{0,j}(t))\right]\,\hat{\mathbf{i}}\\ &-\frac{\kappa\pi^3}{16\ell^2}\,\phi_{1,j}(t)\left[-\frac{1}{\sin\Phi_{0,j}(t)}\,\hat{\mathbf{i}} + \frac{1}{\cos\Phi_{0,j}(t)}\,\hat{\mathbf{j}}\right] + \vec{\mathbf{f}}_{\mathrm{h}}.\end{aligned} \tag{4.2.9}$$

We recall the perpendicular projection operator $\hat{\mathbf{\Phi}}_{\perp}$ in equation (2.1.34) and introduce a tangential projection operator. The subscript j refers to the fact that we now need to keep track of the particular filament in question.

$$\hat{\mathbf{\Phi}}_{\perp,j}(t) = \hat{\mathbf{\Phi}}_{\perp,j} = -\sin(\Phi_{0,j}(t))\,\hat{\mathbf{i}} + \cos(\Phi_{0,j}(t))\,\hat{\mathbf{j}} \tag{4.2.10}$$

$$\hat{\mathbf{\Phi}}_{\parallel,j}(t) = \cos(\Phi_{0,j}(t))\,\hat{\mathbf{i}} + \sin(\Phi_{0,j}(t))\,\hat{\mathbf{j}} \tag{4.2.11}$$

Ignoring the stochastic force $\vec{\mathbf{f}}_{\mathrm{h}}$ for the moment, projections of equation (4.2.9) onto $\hat{\mathbf{\Phi}}_{\perp,j}(t)$ and $\hat{\mathbf{\Phi}}_{\parallel,j}(t)$ yield

$$\mathcal{L}_{\perp,j}(t) = -\tfrac{2\ell\varsigma}{\pi}\,\dot{\phi}_{1,j}(t) \;-\; \left(\tfrac{\kappa\pi^3}{\varsigma\ell^2} + \tfrac{\varsigma\pi}{2}\,v\right)\phi_{1,j}(t) = -\,\xi\,\dot{\phi}_{1,j}(t) \;-\; k\,\phi_{1,j}(t) \tag{4.2.12}$$

$$\mathcal{L}_{\parallel,j}(t) = -\,\varsigma\,v + \tfrac{\kappa\pi^3}{16\ell^2}\,\phi_{1,i}(t)\,\cot(2\Phi_{0,j}(t)) \tag{4.2.13}$$

remembering ξ and k that were defined previously in equation (2.1.38).

4.2.1 Collective variables for our system

Let us now define collective variables for our system. We define density of the filament tips ρ, density of the filament bodies ρ_R, the auxiliary density of the filament tips $\hat{\vec{\rho}}$ (defined in the usual manner [65]) and an orientational density of the filament bodies $\vec{\pi}$. The densities ρ and ρ_R are standard fields to define, since they can be experimentally observed. The auxillary field $\hat{\vec{\rho}}$ is the type of field that always arises naturally in this formalism. The orientational density field $\vec{\pi}$ arises also naturally when considering the hydrodynamical interactions in equation (4.2.18).

$$\rho\,(\vec{\mathbf{r}},t) = \sum_j \delta(\vec{\mathbf{r}} - \vec{\mathbf{R}}_j(\ell,t)) = \sum_j \delta(\vec{\mathbf{r}} - \vec{\mathbf{R}}_j(0,t) - \vec{\mathbf{r}}_j(t)) \tag{4.2.14}$$

$$\hat{\vec{\rho}}\,(\vec{\mathbf{r}},t) = \sum_j \hat{\vec{\mathbf{r}}}_j(t)\,\delta(\vec{\mathbf{r}} - \vec{\mathbf{R}}_j(\ell,t)) = \sum_j \hat{\vec{\mathbf{r}}}_j(t)\,\delta(\vec{\mathbf{r}} - \vec{\mathbf{R}}_j(0,t) - \vec{\mathbf{r}}_j(t)) \tag{4.2.15}$$

$$\rho_R\,(\vec{\mathbf{R}},t) = \sum_i \int_0^L \mathrm{d}s\,\delta(\vec{\mathbf{R}} - \vec{\mathbf{R}}_i(t)) \tag{4.2.16}$$

$$\vec{\pi}\,(\vec{\mathbf{R}},t) = \sum_i \int_0^L \mathrm{d}s\,\frac{\partial\vec{\mathbf{R}}_i(s,t)}{\partial s}\,\delta(\vec{\mathbf{R}} - \vec{\mathbf{R}}_i(s,t)) \tag{4.2.17}$$

We can now rewrite the interaction term in equation (4.2.5) in terms of the collective variables using equation (4.2.8)

$$\vec{\mathcal{L}}_{\mathrm{int}}(t) = \varsigma\,\vec{\mathbf{v}}_f(\vec{\mathbf{r}}_j(\ell,t)) = \varsigma\,f_a\int \mathrm{d}\vec{\mathbf{r}}\,\mathrm{d}\vec{\mathbf{R}}\;\hat{\vec{\rho}}(\vec{\mathbf{r}},t)\cdot\mathbf{H}(\vec{\mathbf{r}} - \vec{\mathbf{R}})\cdot\vec{\pi}(\vec{\mathbf{R}},t) \tag{4.2.18}$$

and write our total Langevin equation as

$$\vec{\mathcal{L}}(t) = \sum_j \left(\mathcal{L}_{\perp,j}(t)\, \hat{\mathbf{\Phi}}_{\perp,j}(t) + \mathcal{L}_{\parallel,j}(t)\, \hat{\mathbf{\Phi}}_{\parallel,j}(t) \right) + \vec{\mathcal{L}}_{\text{int}}(t) \tag{4.2.19}$$

The expression for the interacting terms obtained in equation (4.2.18) is really the highlight of this section. It expresses the nature of the hydrodynamic interaction of the filaments: the filament tips – described by $\hat{\vec{\rho}}$ – are influenced by the orientations of the bodies of the surrounding filaments – described by $\vec{\pi}$ – and this interaction is mediated by the hydrodynamics contained in the Oseen tensor, $\mathbf{H}$. This ties in with the results of the previous approach in Section 3.1 where we saw that, for a constant flow field, the filament tips tend to align themselves in the direction of the low field the filament bodies create. The expression also indicates that it may be practical to use the RPA approach, since we see that the interaction is quadratic in the collective variables.

4.2.2 Returning to the primary expression

We wish to move to an expression for a generating functional like that in equation (4.1.8). We use variables P_i to write the collective variables in terms of the Fourier transform.

$$\begin{aligned}
\mathcal{Z} = &\prod_j \int [\mathrm{d}\vec{\mathbf{r}}_j(t)][\mathrm{d}\hat{\vec{\mathbf{r}}}_j(t)][\mathrm{d}\rho(\vec{\mathbf{r}},t)][\mathrm{d}P_1(\vec{\mathbf{r}},t)][\mathrm{d}\hat{\vec{\rho}}(\vec{\mathbf{r}},t)][\mathrm{d}\vec{\mathbf{P}}_2(\vec{\mathbf{r}},t)] \times \\
&\int [\mathrm{d}\vec{\mathbf{R}}_i(s,t)][\mathrm{d}\rho_R(\vec{\mathbf{R}},t)][\mathrm{d}P_3(\vec{\mathbf{R}},t)][\mathrm{d}\vec{\pi}(\vec{\mathbf{R}},t)][\mathrm{d}\vec{\mathbf{P}}_4(\vec{\mathbf{R}},t)] \times \\
&\exp\left\{ i \int \mathrm{d}t\; P_1(\vec{\mathbf{r}},t) \left(\rho(\vec{\mathbf{r}},t) - \sum_j \delta\left(\vec{\mathbf{r}} - \vec{\mathbf{R}}_j(\ell,t)\right)\right)\right\} \times \\
&\exp\left\{ i \int \mathrm{d}t\; \vec{\mathbf{P}}_2(\vec{\mathbf{r}},t) \cdot \left(\hat{\vec{\rho}}(\vec{\mathbf{r}},t) - \sum_j \hat{\vec{\mathbf{r}}}_j\, \delta\left(\vec{\mathbf{r}} - \vec{\mathbf{R}}_j(\ell,t)\right)\right)\right\} \times \\
&\exp\left\{ i \int \mathrm{d}t\; P_3(\vec{\mathbf{R}},t) \left(\rho_R(\vec{\mathbf{R}},t) - \sum_i \int_0^L \mathrm{d}s\; \delta\left(\vec{\mathbf{R}} - \vec{\mathbf{R}}_i(t)\right)\right)\right\} \times \\
&\exp\left\{ i \int \mathrm{d}t\; \vec{\mathbf{P}}_4(\vec{\mathbf{r}},t) \cdot \left(\vec{\pi}(\vec{\mathbf{R}},t) - \sum_i \int_0^L \mathrm{d}s\; \frac{\partial \vec{\mathbf{R}}_i(s,t)}{\partial s}\, \delta(\vec{\mathbf{R}} - \vec{\mathbf{R}}_i(s,t))\right)\right\} \times \\
&\exp\left\{ i \int \mathrm{d}t\; \hat{\vec{\mathbf{r}}}_j(t) \cdot \left(\sum_j \left(\mathcal{L}_{\perp,j}(t)\, \hat{\mathbf{\Phi}}_{\perp,j}(t) + \mathcal{L}_{\parallel,j}(t)\, \hat{\mathbf{\Phi}}_{\parallel,j}(t)\right) + \vec{\mathcal{L}}_{\text{int}}(t)\right)\right\}.
\end{aligned} \tag{4.2.20}$$

We would also like to exploit the simplicity of the perpendicularly projected Langevin equation (4.2.12). The tangential Langevin, unfortunately, does not simplify as nicely - the cotangent introduces complicated non-linearity. However, most of the interesting effects should be contained in the perpendicular projection and so we focus our attention onto this direction. This ties in with our earlier assumption that the extension of the head is very short and that $\phi_{1,j}$ is suitably small. For $\mathcal{L}_{\parallel,j}$ to contribute, it would need to be larger or of comparable magnitude with the $\mathcal{L}_{\perp,j}$ terms.

With this in mind, we ignore the tangential projection and take the non-interacting part of the Langevin equation as $\mathcal{L}_{\perp,j}$ only.

As before in Chapters 2 and 3, we express $\mathcal{Z}$ in terms of the angles $\phi_{1,j}$ and $\Phi_{0,j}$, to lowest order in $\phi_{1,j}$, by integrating over delta functionals

$$\delta\left[\phi_{1,j}(t) - \tfrac{2\ell}{v\pi}\dot{\Phi}_{0,j}(t)\right] \tag{4.2.21}$$

$$\delta\Big[\vec{\mathbf{r}}_j(t) - \left[\ell\cos\Phi_{0,j}(t) - \tfrac{2\pi}{\ell},\ \phi_{1,j}(t)\sin\Phi_{0,j}(t)\right]\hat{\mathbf{i}} - \left[\ell\sin\Phi_{0,j}(t) - \tfrac{2\pi}{\ell}\ \phi_{1,j}(t)\cos\Phi_{0,j}(t)\right]\hat{\mathbf{j}}\Big] \tag{4.2.22}$$

and

$$\delta\left[\vec{\mathbf{R}}_i(t) - \vec{\mathbf{R}}_i(0,0) - v\int_0^t \mathrm{d}T\ \cos(\Phi_{0,i}(T))\hat{\mathbf{i}} + \sin(\Phi_{0,i}(T))\hat{\mathbf{j}}\right]. \tag{4.2.23}$$

The delta functional in equation (4.2.21) captures the relationship between the angles $\phi_{1,j}$ and $\Phi_{0,j}$ and the latter two delta functionals in equations (4.2.22) and (4.2.23) simply relate the position vectors to the angles.

In total, we now have the following expression:

$$\begin{aligned}
\mathcal{Z} = \prod_j \int &[\mathrm{d}\vec{\mathbf{r}}_j(t)][\mathrm{d}\rho(\vec{\mathbf{r}},t)][\mathrm{d}P_1(\vec{\mathbf{r}},t)][\mathrm{d}\hat{\vec{\rho}}(\vec{\mathbf{r}},t)][\mathrm{d}\vec{\mathbf{P}}_2(\vec{\mathbf{r}},t)] \times \\
&\int [\mathrm{d}\vec{\mathbf{R}}_i(s,t)][\mathrm{d}\rho_R(\vec{\mathbf{R}},t)][\mathrm{d}P_3(\vec{\mathbf{R}},t)][\mathrm{d}\vec{\pi}(\vec{\mathbf{R}},t)][\mathrm{d}\vec{\mathbf{P}}_4(\vec{\mathbf{R}},t)] \times \\
&\int [\mathrm{d}\hat{\mathbf{r}}_j(t)][\mathrm{d}\Phi_{0,j}(t)][\mathrm{d}\phi_{1,j}(t)]\ \delta\left(\phi_{1,j}(t) - \tfrac{2\ell}{v\pi}\dot{\Phi}_{0,j}(t)\right) \times \\
&\delta\left(\vec{\mathbf{r}}_j(t) - \left[\ell\cos\Phi_{0,j}(t) - \tfrac{2\pi}{\ell}\ \phi_{1,j}(t)\sin\Phi_{0,j}(t)\right]\hat{\mathbf{i}} - \left[\ell\sin\Phi_{0,j}(t) - \tfrac{2\pi}{\ell}\ \phi_{1,j}(t)\cos\Phi_{0,j}(t)\right]\hat{\mathbf{j}}\right) \times \\
&\delta\left(\vec{\mathbf{R}}_i(t) - \vec{\mathbf{R}}_i(0,0) - v\int_0^t \mathrm{d}T\ \cos(\Phi_{0,i}(T))\hat{\mathbf{i}} + \sin(\Phi_{0,i}(T))\hat{\mathbf{j}}\right) \times \\
&\exp\left\{i\int \mathrm{d}t\ P_1(\vec{\mathbf{r}},t)\left(\rho(\vec{\mathbf{r}},t) - \sum_j \delta\left(\vec{\mathbf{r}} - \vec{\mathbf{r}}_j(t)\right)\right)\right\} \times \\
&\exp\left\{i\int \mathrm{d}t\ \vec{\mathbf{P}}_2(\vec{\mathbf{r}},t)\cdot\left(\hat{\vec{\rho}}(\vec{\mathbf{r}},t) - \sum_j \hat{\vec{\mathbf{r}}}_j\ \delta\left(\vec{\mathbf{r}} - \vec{\mathbf{r}}_j(t)\right)\right)\right\} \times \\
&\exp\left\{i\int \mathrm{d}t\ P_3(\vec{\mathbf{R}},t)\left(\rho_R(\vec{\mathbf{R}},t) - \sum_i \int_0^L \mathrm{d}s\ \delta\left(\vec{\mathbf{R}} - \vec{\mathbf{R}}_i(t)\right)\right)\right\} \times \\
&\exp\left\{i\int \mathrm{d}t\ \vec{\mathbf{P}}_4(\vec{\mathbf{r}},t)\cdot\left(\vec{\pi}(\vec{\mathbf{R}},t) - \sum_i \int_0^L \mathrm{d}s\ \frac{\partial\vec{\mathbf{R}}_i(s,t)}{\partial s}\,\delta(\vec{\mathbf{R}} - \vec{\mathbf{R}}_i(s,t))\right)\right\} \times \\
&\exp\left\{i\int \mathrm{d}t\ \hat{\vec{\mathbf{r}}}_j(t)\cdot\left(\sum_j \mathcal{L}_{\perp,j}(t)\ \hat{\mathbf{\Phi}}_{\perp,j}(t) + \vec{\mathcal{L}}_{\text{int}}(t)\right)\right\}.
\end{aligned} \tag{4.2.24}$$

4.3 Random phase approximation

In addition to the MSR formalism, we shall also be employing a Gaussian approximation which is an analogue of the random phase approximation (RPA). The RPA was first introduced by

Bohm and Pines [69] when investigating electron interactions. However, the RPA has been applied to other systems as well, including dynamic polymer systems [65; 70; 71]. We shall follow the method as outlined by Fredrickson and Helfand [65]. The RPA is known to be a suitable approximation for dense systems of polymers.

The reason for this is that the expression obtained in equation (4.2.24) is not able to be calculated analytically without making some kind of approximation. The RPA is a tried and tested method that gives us a systematic and controlled way of approaching the calculation.

To employ the RPA, first we take a Taylor series representation of the exponentials in equation (4.2.20) up to quadratic order in the density fields. This results in the following:

$$
\begin{aligned}
\mathcal{Z} = \prod_j \int [\mathrm{d}\vec{\mathbf{R}}_i(s,t)][\mathrm{d}\vec{\mathbf{r}}_j(t)][\mathrm{d}\hat{\vec{\mathbf{r}}}_j(t)][\mathrm{d}\rho(\vec{\mathbf{r}},t)][\mathrm{d}P_1(\vec{\mathbf{r}},t)][\mathrm{d}\hat{\vec{\rho}}(\vec{\mathbf{r}},t)][\mathrm{d}\vec{\mathbf{P}}_2(\vec{\mathbf{r}},t)] \times \\
\int [\mathrm{d}\rho_R(\vec{\mathbf{R}},t)][\mathrm{d}P_3(\vec{\mathbf{R}},t)][\mathrm{d}\vec{\pi}(\vec{\mathbf{R}},t)][\mathrm{d}\vec{\mathbf{P}}_4(\vec{\mathbf{R}},t)] \times \\
\int [\mathrm{d}\hat{\mathbf{r}}_j(t)][\mathrm{d}\Phi_{0,j}(t)][\mathrm{d}\phi_{1,j}(t)]\, \delta\left[\phi_{1,j}(t) - \tfrac{2\ell}{v\pi}\dot{\Phi}_{0,j}(t)\right] \times \\
\delta\left(\vec{\mathbf{r}}_j(t) - \left[\ell\cos\Phi_{0,j}(t) - \tfrac{2\pi}{\ell}\,\phi_{1,j}(t)\sin\Phi_{0,j}(t)\right]\hat{\mathbf{i}} - \left[\ell\sin\Phi_{0,j}(t) - \tfrac{2\pi}{\ell}\,\phi_{1,j}(t)\cos\Phi_{0,j}(t)\right]\hat{\mathbf{j}}\right) \times \\
\delta\left(\vec{\mathbf{R}}_i(t) - \vec{\mathbf{R}}_i(0,0) - v\int_0^t \mathrm{d}T\, \cos(\Phi_{0,i}(T))\hat{\mathbf{i}} + \sin(\Phi_{0,i}(T))\hat{\mathbf{j}}\right) \times \\
\exp\left\{i\int \mathrm{d}t\, P_1(\vec{\mathbf{r}},t)\rho(\vec{\mathbf{r}},t)\right\}\Big(1 \underbrace{-i\int \mathrm{d}t\, P_1(\vec{\mathbf{r}},t)\left(-\sum_j \delta\left(\vec{\mathbf{r}} - \vec{\mathbf{R}}_j(\ell,t)\right)\right)}_{①} \\
\underbrace{-\frac{1}{2}\left[\int \mathrm{d}t\, P_1(\vec{\mathbf{r}},t)\left(-\sum_j \delta\left(\vec{\mathbf{r}} - \vec{\mathbf{R}}_j(\ell,t)\right)\right)\right]^2}_{①^2} \ldots\Big) \times \\
\exp\left\{i\int \mathrm{d}t\, \vec{\mathbf{P}}_2(\vec{\mathbf{r}},t)\cdot\hat{\vec{\rho}}(\vec{\mathbf{r}},t)\right\}\Big(1 \underbrace{-i\int \mathrm{d}t\, \vec{\mathbf{P}}_2(\vec{\mathbf{r}},t)\cdot\left(-\sum_j \hat{\vec{\mathbf{r}}}_j\, \delta\left(\vec{\mathbf{r}} - \vec{\mathbf{R}}_j(\ell,t)\right)\right)}_{②} \\
\underbrace{-\frac{1}{2}\left[\int \mathrm{d}t\, \vec{\mathbf{P}}_2(\vec{\mathbf{r}},t)\cdot\left(-\sum_j \hat{\vec{\mathbf{r}}}_j\, \delta\left(\vec{\mathbf{r}} - \vec{\mathbf{R}}_j(\ell,t)\right)\right)\right]^2}_{②^2} \ldots\Big) \times \\
\exp\left\{i\int \mathrm{d}t\, P_3(\vec{\mathbf{R}},t)\rho_R(\vec{\mathbf{R}},t)\right\}\Big(1 \underbrace{-i\int \mathrm{d}t\, P_3(\vec{\mathbf{R}},t)\left(-\sum_i \int_0^L \mathrm{d}s\, \delta\left(\vec{\mathbf{R}} - \vec{\mathbf{R}}_i(t)\right)\right)}_{③}
\end{aligned}
$$

$$\underbrace{-\frac{1}{2}\left[\int \mathrm{d}t\; P_3(\vec{\mathbf{R}},t)\left(-\sum_i \int_0^L \mathrm{d}s\;\delta\left(\vec{\mathbf{R}}-\vec{\mathbf{R}}_i(t)\right)\right)\right]^2 \dots}_{(3^2)}\Big) \times$$

$$\exp\left\{i\int \mathrm{d}t\;\vec{\mathbf{P}}_4(\vec{\mathbf{r}},t)\cdot\vec{\pi}(\vec{\mathbf{R}},t)\right\}\Big(1\underbrace{-i\int \mathrm{d}t\;\vec{\mathbf{P}}_4(\vec{\mathbf{r}},t)\cdot\left(-\sum_i\int_0^L \mathrm{d}s\;\frac{\partial\vec{\mathbf{R}}_i(s,t)}{\partial s}\,\delta(\vec{\mathbf{R}}-\vec{\mathbf{R}}_i(s,t))\right)}_{(4)}$$

$$\underbrace{-\frac{1}{2}\left[\int \mathrm{d}t\;\vec{\mathbf{P}}_4(\vec{\mathbf{r}},t)\cdot\left(-\sum_i\int_0^L \mathrm{d}s\;\frac{\partial\vec{\mathbf{R}}_i(s,t)}{\partial s}\,\delta(\vec{\mathbf{R}}-\vec{\mathbf{R}}_i(s,t))\right)\right]^2 \dots}_{(4^2)}\Big) \times$$

$$\exp\left\{i\int \mathrm{d}t\;\hat{\vec{\mathbf{r}}}_j(t)\cdot\left(\sum_j \mathcal{L}_{\perp,j}(t)\,\hat{\mathbf{\Phi}}_{\perp,j}(t)\;+\vec{\mathcal{L}}_{\text{int}}(t)\right)\right\}. \tag{4.3.1}$$

The numbering above the terms in the expansion is simply for convenience later when discussing the RPA calculation.

Following this, we evaluate each term that results from the expansion, including the quadratic order cross terms but neglecting any higher order terms. For example, the quadratic order cross term between $\vec{\mathbf{P}}_2(\vec{\mathbf{r}},t)$ and $P_3(\vec{\mathbf{R}},t)$ looks as follows:

$$\begin{aligned}
&(2)\times(3) = \\
&\prod_j\int[\mathrm{d}\vec{\mathbf{r}}_j(t)][\mathrm{d}\hat{\vec{\mathbf{r}}}_j(t)][\mathrm{d}\rho(\vec{\mathbf{r}},t)][\mathrm{d}P_1(\vec{\mathbf{r}},t)][\mathrm{d}\hat{\vec{\rho}}(\vec{\mathbf{r}},t)][\mathrm{d}\vec{\mathbf{P}}_2(\vec{\mathbf{r}},t)]\times \\
&\int[\mathrm{d}\vec{\mathbf{R}}_i(s,t)][\mathrm{d}\rho_R(\vec{\mathbf{R}},t)][\mathrm{d}P_3(\vec{\mathbf{R}},t)][\mathrm{d}\vec{\pi}(\vec{\mathbf{R}},t)][\mathrm{d}\vec{\mathbf{P}}_4(\vec{\mathbf{R}},t)]\times \\
&\int[\mathrm{d}\hat{\mathbf{r}}_j(t)][\mathrm{d}\Phi_{0,j}(t)][\mathrm{d}\phi_{1,j}(t)]\;\delta\left(\phi_{1,j}(t)-\tfrac{2\ell}{v\pi}\dot{\Phi}_{0,j}(t)\right)\times \\
&\delta\left(\vec{\mathbf{r}}_j(t)-\left[\ell\cos\Phi_{0,j}(t)-\tfrac{2\pi}{\ell}\,\phi_{1,j}(t)\sin\Phi_{0,j}(t)\right]\hat{\mathbf{i}}-\left[\ell\sin\Phi_{0,j}(t)-\tfrac{2\pi}{\ell}\,\phi_{1,j}(t)\cos\Phi_{0,j}(t)\right]\hat{\mathbf{j}}\right)\times \\
&\delta\left(\vec{\mathbf{R}}_i(t)-\vec{\mathbf{R}}_i(0,0)-v\int_0^t \mathrm{d}T\;\cos(\Phi_{0,i}(T))\hat{\mathbf{i}}+\sin(\Phi_{0,i}(T))\hat{\mathbf{j}}\right)\times \\
&(-1)\int \mathrm{d}t\;\vec{\mathbf{P}}_2(\vec{\mathbf{r}},t)\cdot\left(-\sum_j \hat{\vec{\mathbf{r}}}_j\;\delta\left(\vec{\mathbf{r}}-\vec{\mathbf{r}}_j(t)\right)\right)\int \mathrm{d}t\;P_3(\vec{\mathbf{R}},t)\left(-\sum_i\delta\left(\vec{\mathbf{R}}-\vec{\mathbf{R}}_i(t)\right)\right) \\
&\times\;\exp\left\{i\int \mathrm{d}t\;\hat{\vec{\mathbf{r}}}_j(t)\cdot\left(\sum_j \mathcal{L}_{\perp,j}(t)\,\hat{\mathbf{\Phi}}_{\perp,j}(t)+\vec{\mathcal{L}}_{\text{int}}(t)\right)\right\}.
\end{aligned} \tag{4.3.2}$$

Once all these terms have been calculated so that only the collective variables and their auxillary fields remain and the other variables have been integrated out, the result is re-exponentiated. This leaves us with a generating functional for the collective variables (after intgeration over the now Guassian auxillarys), as discussed in Section 4.1. The generating functional will be Gaussian since the non-interacting part will be quadratic in the collective fields, thanks to the RPA, and the interacting part is linear in the collective fields.

4.3.1 Relation between s and t

Because we have the relations in equations (2.1.3) and (2.1.4) that relates any angle on the filament body back to the angle at the join at an earlier time and equations (2.1.19) and (2.1.20) governing the continuity of this join, we can write the position of the body entirely in terms of the angle at the head-body join.

We have

$$\begin{aligned}
\vec{\mathbf{R}}_j(s,t) &= \vec{\mathbf{R}}_j(0, t - {}^{s}\!/_{v}) \\
&= \vec{\mathbf{R}}_j(0,0) + \int_0^{t-{}^{s}\!/_{v}} \mathrm{d}T \, \frac{\partial \vec{\mathbf{R}}_j(0,T)}{\partial T} \\
&= \vec{\mathbf{R}}_j(0,0) - v \int_0^{t-{}^{s}\!/_{v}} \mathrm{d}T \, \frac{\partial \vec{\mathbf{R}}_j(s,T)}{\partial s}\bigg|_{s=0} \\
&= \vec{\mathbf{R}}_j(0,0) - v \int_0^{t-{}^{s}\!/_{v}} \mathrm{d}T \, \Big(\cos(\theta_j(0,T))\hat{\mathbf{i}} + \sin(\theta_j(0,T))\hat{\mathbf{j}}\Big) \\
&= \vec{\mathbf{R}}_j(0,0) + v \int_0^{t-{}^{s}\!/_{v}} \mathrm{d}T \, \Big(\cos(\Phi_{0,\,j}(T))\hat{\mathbf{i}} + \sin(\Phi_i(0,t))\hat{\mathbf{j}}\Big) \\
&= \vec{\mathbf{R}}_j(0,0) + v \int_0^{t-{}^{s}\!/_{v}} \mathrm{d}T \, \hat{\mathbf{\Phi}}_{\parallel,\,j}(T)
\end{aligned} \tag{4.3.3}$$

Note that in the last line we have chosen to write $\vec{\mathbf{R}}_j(s,t)$ in terms of the parallel projection vector $\hat{\mathbf{\Phi}}_{\parallel,\,j}(t)$. We can also do this with other terms in equations (4.2.24) and (4.3.1). For example, we can replace $\vec{\mathbf{r}}_j(t)$ with

$$\vec{\mathbf{r}}_j(t) = \tfrac{2\ell}{\pi}\,\phi_{1,\,j}(t)\,\hat{\mathbf{\Phi}}_{\perp,\,j}(t) + \ell\,\hat{\mathbf{\Phi}}_{\parallel,\,j}(t) \tag{4.3.4}$$

and further we can now write $\vec{\pi}(\vec{\mathbf{R}},t)$ as

$$\begin{aligned}
\vec{\pi}(\vec{\mathbf{R}},t) &= \sum_i \int \mathrm{d}s \, \frac{\partial \vec{\mathbf{R}}_i(s,t)}{\partial s}\,\delta(\vec{\mathbf{R}} - \vec{\mathbf{R}}_i(s,t)) \\
&= \sum_i \left[\int \mathrm{d}s \, \hat{\mathbf{\Phi}}_{\parallel,\,i}(t - {}^{s}\!/_{v}) \;\; \delta\left(\vec{\mathbf{R}} - \vec{\mathbf{R}}_i(0,0) - v\int_0^{t-{}^{s}\!/_{v}} \mathrm{d}T \, \hat{\mathbf{\Phi}}_{\parallel,\,i}(T)\right)\right].
\end{aligned} \tag{4.3.5}$$

4.4 Proceeding with the RPA calculation

Several complications arise when proceeding with the calculation of the terms in equation (4.3.1). In this section, we shall elaborate on the various approaches and complications encountered. The lists A and B of Section 4.4.1, below, give a rough overview of the different avenues explored during the calculation.

Although dropping the contribution of the $\mathcal{L}_{\parallel,\,j}$ from the Langevin equation has already been motivated and stated from the beginning, we did not start out our calculation this way. We spent a long time exploring ways of integrating the terms of equation (4.3.1) with the

contribution of $\mathcal{L}_{\parallel,j}$ included. List A covers this period, whereas List B concerns the attempts after discarding the $\mathcal{L}_{\parallel,j}$ contribution.

Both calculations began with the same steps to start with, but then diverged at Step 4. At this step we were trying to integrate over $\phi_{1,j}(t)$ and $\Phi_{0,j}(t)$ to obtain the generating functional solely in terms of the collective variables. These attempts shall be discussed in greater detail below.

4.4.1 Schematic outline of calculation attempts

A: Including $\mathcal{L}_{\perp,j}$ and $\mathcal{L}_{\parallel,j}$

1. Integration over the initial position of the head-body join, $\vec{\mathbf{R}}_j(0,0)$
2. Integration over the stochastic force, $\vec{\mathbf{f}}_j$
3. Integration over the conjugate field in the projection directions, $\hat{\mathbf{r}}_{\perp,j}, \hat{\mathbf{r}}_{\parallel,j}$

↓

4.i. Fourier Transform (transform to frequency domain, ω)

   a. Fourier Transform of both $\phi_{1,j}(t)$ and $\Phi_{0,j}(t)$
      - Approximations required for $\Phi_{0,j}(t)$ terms
   b. Fourier Transform of $\phi_{1,j}(t)$ only
      - Integration over ω

4.ii. Remain in time domain

   a. Matrix approach

B: Including $\mathcal{L}_{\perp,j}$ only

1. Integration over the initial position of the head-body join, $\vec{\mathbf{R}}_j(0,0)$
2. Integration over the stochastic force, $\vec{\mathbf{f}}_j$
3. Integration over the conjugate field, $\hat{\mathbf{r}}_j$

↓

4.i. Fourier Transform (transform to frequency domain, ω)

   a. Fourier Transform of $\phi_{1,j}(t)$ only
      - Integration over ω

4.ii. Remain in time domain

a. Harmonic propagator in $\phi_{1,j}(t)$

b. Include $\dot{\phi}_{1,j}(t), \phi_{1,j}(t)$ relation explicitly

- Rewrite each of the terms in equation (4.3.1) in terms of the projection vectors $\hat{\mathbf{\Phi}}_{\perp,j}(t)$ and $\hat{\mathbf{\Phi}}_{\parallel,j}(t)$
- Investigate properties of projection vectors $\hat{\mathbf{\Phi}}_{\perp,j}(t)$ and $\hat{\mathbf{\Phi}}_{\parallel,j}(t)$
- Try transform the integral so that in terms of $\hat{\mathbf{\Phi}}_{\perp,j}(t)$ only, instead of $\Phi_{0,j}$ and both projection vectors $\hat{\mathbf{\Phi}}_{\perp,j}(t)$ and $\hat{\mathbf{\Phi}}_{\parallel,j}(t)$

c. Use results from Bhattacharjee *et al.* [72]

4.4.2 First steps in the RPA calculation

When we calculate the RPA terms of equation (4.3.1), we focus on a particular filament j. We can do this because we assume no particular filament is unique, rather we assume each filament is statistically identical to the other. This means that if we have N filaments, we simply have N copies of the same expression.

For simplicity, we concentrate on the terms without the $\mathcal{L}_{\parallel,j}$ contribution. In other words, we present the expressions as outlined in List B of Section 4.4.1. However, for these initial steps the results are exactly the same for both lists. Later, in Section 4.4.3 and beyond, specific reference will be made to either the version from List A or List B.

As a first step, we integrate each term in the RPA over the initial position $\vec{\mathbf{R}}_j(0,0)$. We assume that this initial position is homogenously distributed. The result of this integration then is a delta function, which drastically simplifies the expression. As an example, consider (3) or (3^2) of equation (4.3.1), for a particular filament j.

$$
\begin{aligned}
(3) = &\int \ldots [\mathrm{d}\vec{\mathbf{R}}_j(s,t)] \ldots \int \mathrm{d}t\; P_3(\vec{\mathbf{R}},t) \\
&\times \delta\left(\vec{\mathbf{R}} - \vec{\mathbf{R}}_j(0,0) + v\int_0^t \mathrm{d}T\; \cos(\Phi_{0,j}(T))\hat{\mathbf{i}} + \sin(\Phi_{0,j}(T))\hat{\mathbf{j}}\right) \\
&\times\; \exp\left\{ i \int \mathrm{d}t\; \hat{\vec{\mathbf{r}}}_j(t) \cdot \mathcal{L}_{\perp,j}(t)\, \hat{\mathbf{\Phi}}_{\perp,j}(t) \right\} \qquad (4.4.1) \\
= &\int \ldots [\mathrm{d}\vec{\mathbf{R}}_j(s,t)_{\text{not zero}}]\; \mathrm{d}\vec{\mathbf{R}}_i(0,0)\; \ldots \int \mathrm{d}t\; \mathrm{d}\vec{\boldsymbol{\mu}}\; P_3(\vec{\mathbf{R}},t) \\
&\times \exp\left\{ i\vec{\boldsymbol{\mu}} \cdot \left(\vec{\mathbf{R}} - \vec{\mathbf{R}}_j(0,0) + v\int_0^t \mathrm{d}T\; \cos(\Phi_{0,j}(T))\hat{\mathbf{i}} + \sin(\Phi_{0,j}(T))\hat{\mathbf{j}}\right)\right\} \\
&\times\; \exp\left\{ i \int \mathrm{d}t\; \hat{\vec{\mathbf{r}}}_j(t) \cdot \mathcal{L}_{\perp,j}(t)\, \hat{\mathbf{\Phi}}_{\perp,j}(t) \right\} \qquad (4.4.2) \\
= &\int \ldots [\mathrm{d}\vec{\mathbf{R}}_j(s,t)_{\text{not zero}}]\; \mathrm{d}\vec{\mathbf{R}}_i(0,0)\; \exp\left\{ -i\,\vec{\boldsymbol{\mu}} \cdot \vec{\mathbf{R}}_i(0,0)\right\} \ldots \\
&\times \int \mathrm{d}t\; \mathrm{d}\vec{\boldsymbol{\mu}}\; P_3(\vec{\mathbf{R}},t) \exp\left\{ i\vec{\boldsymbol{\mu}} \cdot \left(\vec{\mathbf{R}} + v\int_0^t \mathrm{d}T\; \cos(\Phi_{0,j}(T))\hat{\mathbf{i}} + \sin(\Phi_{0,j}(T))\hat{\mathbf{j}}\right)\right\} \\
&\times\; \exp\left\{ i \int \mathrm{d}t\; \hat{\vec{\mathbf{r}}}_j(t) \cdot \mathcal{L}_{\perp,j}(t)\, \hat{\mathbf{\Phi}}_{\perp,j}(t) \right\} \qquad (4.4.3)
\end{aligned}
$$

$$= \int \ldots [\mathrm{d}\vec{\mathbf{R}}_j(s,t)_{\text{not zero}}]\ \delta(\vec{\boldsymbol{\mu}}) \ldots$$
$$\times \int \mathrm{d}t\ \mathrm{d}\vec{\boldsymbol{\mu}}\ P_3(\vec{\mathbf{R}},t) \exp\left\{ i\vec{\boldsymbol{\mu}} \cdot \left(\vec{\mathbf{R}} + v \int_0^t \mathrm{d}T\ \cos(\Phi_{0,j}(T))\hat{\mathbf{i}} + \sin(\Phi_{0,j}(T))\hat{\mathbf{j}} \right) \right\}$$
$$\times \exp\left\{ i \int \mathrm{d}t\ \hat{\vec{\mathbf{r}}}_j(t) \cdot \mathcal{L}_{\perp,j}(t)\ \hat{\boldsymbol{\Phi}}_{\perp,j}(t) \right\} \tag{4.4.4}$$
$$= \int \ldots [\mathrm{d}\vec{\mathbf{R}}_j(s,t)_{\text{not zero}}] \ldots \int \mathrm{d}t\ P_3(\vec{\mathbf{R}},t)\ \exp\left\{ i \int \mathrm{d}t\ \hat{\vec{\mathbf{r}}}_j(t) \cdot \mathcal{L}_{\perp,j}(t)\ \hat{\boldsymbol{\Phi}}_{\perp,j}(t) \right\} \tag{4.4.5}$$

$$(3^2) = \int \ldots [\mathrm{d}\vec{\mathbf{R}}_j(s,t)] \ldots \left[\int \mathrm{d}t\ P_3(\vec{\mathbf{R}},t) \left(\rho_R(\vec{\mathbf{R}},t) - \sum_j \int_0^L \mathrm{d}s\ \delta\left(\vec{\mathbf{R}} - \vec{\mathbf{R}}_j(t) \right) \right) \right]^2$$
$$\times \exp\left\{ i \int \mathrm{d}t\ \hat{\vec{\mathbf{r}}}_j(t) \cdot \mathcal{L}_{\perp,j}(t)\ \hat{\boldsymbol{\Phi}}_{\perp,j}(t) \right\} \tag{4.4.6}$$
$$= \int \ldots [\mathrm{d}\vec{\mathbf{R}}_j(s,t)] \ldots \int \mathrm{d}t\ \mathrm{d}t'\ \mathrm{d}\vec{\boldsymbol{\mu}}\ \mathrm{d}\vec{\boldsymbol{\mu}}'\ P_3(\vec{\mathbf{R}},t)\ P_3(\vec{\mathbf{R}}',t')$$
$$\times \exp\left\{ i\vec{\boldsymbol{\mu}} \cdot \left(\vec{\mathbf{R}} - \vec{\mathbf{R}}_j(t) \right) \right\} \exp\left\{ i\vec{\boldsymbol{\mu}}' \cdot \left(\vec{\mathbf{R}}' - \vec{\mathbf{R}}'_j(t') \right) \right\}$$
$$\times \exp\left\{ i \int \mathrm{d}t\ \hat{\vec{\mathbf{r}}}_j(t) \cdot \mathcal{L}_{\perp,j}(t)\ \hat{\boldsymbol{\Phi}}_{\perp,j}(t) \right\} \tag{4.4.7}$$
$$= \int \ldots [\mathrm{d}\vec{\mathbf{R}}_j(s,t)_{\text{not zero}}][\mathrm{d}\vec{\mathbf{R}}_j(0,0)] \ldots \int \mathrm{d}t\ \mathrm{d}t'\ \mathrm{d}\vec{\boldsymbol{\mu}}\ \mathrm{d}\vec{\boldsymbol{\mu}}'\ P_3(\vec{\mathbf{R}},t)\ P_3(\vec{\mathbf{R}}',t')$$
$$\times \exp\left\{ i\vec{\boldsymbol{\mu}} \cdot \left(\vec{\mathbf{R}} - \vec{\mathbf{R}}_j(0,0) + v \int_0^t \mathrm{d}T\ \cos(\Phi_{0,j}(T))\hat{\mathbf{i}} + \sin(\Phi_{0,j}(T))\hat{\mathbf{j}} \right) \right\}$$
$$\times \exp\left\{ i\vec{\boldsymbol{\mu}}' \cdot \left(\vec{\mathbf{R}}' - \vec{\mathbf{R}}_j(0,0) + v \int_0^{t'} \mathrm{d}T\ \cos(\Phi_{0,j}(T))\hat{\mathbf{i}} + \sin(\Phi_{0,j}(T))\hat{\mathbf{j}} \right) \right\}$$
$$\times \exp\left\{ i \int \mathrm{d}t\ \hat{\vec{\mathbf{r}}}_j(t) \cdot \mathcal{L}_{\perp,j}(t)\ \hat{\boldsymbol{\Phi}}_{\perp,j}(t) \right\} \tag{4.4.8}$$
$$= \int \ldots [\mathrm{d}\vec{\mathbf{R}}_j(s,t)_{\text{not zero}}]\ \mathrm{d}\vec{\boldsymbol{\mu}}\ \mathrm{d}\vec{\boldsymbol{\mu}}'\ [\mathrm{d}\vec{\mathbf{R}}_j(0,0)] \exp\left\{ i\vec{\mathbf{R}}_j(0,0) \cdot (\vec{\boldsymbol{\mu}} + \vec{\boldsymbol{\mu}}') \right\} \ldots$$
$$\times \int \mathrm{d}t\ \mathrm{d}t'\ P_3(\vec{\mathbf{R}},t)\ P_3(\vec{\mathbf{R}}',t')$$
$$\times \exp\left\{ i\vec{\boldsymbol{\mu}} \cdot \left(\vec{\mathbf{R}} + v \int_0^t \mathrm{d}T\ \cos(\Phi_{0,j}(T))\hat{\mathbf{i}} + \sin(\Phi_{0,j}(T))\hat{\mathbf{j}} \right) \right\}$$
$$\times \exp\left\{ i\vec{\boldsymbol{\mu}}' \cdot \left(\vec{\mathbf{R}}' + v \int_0^{t'} \mathrm{d}T\ \cos(\Phi_{0,j}(T))\hat{\mathbf{i}} + \sin(\Phi_{0,j}(T))\hat{\mathbf{j}} \right) \right\}$$
$$\times \exp\left\{ i \int \mathrm{d}t\ \hat{\vec{\mathbf{r}}}_j(t) \cdot \mathcal{L}_{\perp,j}(t)\ \hat{\boldsymbol{\Phi}}_{\perp,j}(t) \right\} \tag{4.4.9}$$
$$= \int \ldots [\mathrm{d}\vec{\mathbf{R}}_j(s,t)_{\text{not zero}}]\ \mathrm{d}\vec{\boldsymbol{\mu}}\ \mathrm{d}\vec{\boldsymbol{\mu}}'\ \delta\left(\vec{\boldsymbol{\mu}} + \vec{\boldsymbol{\mu}}'\right) \ldots \int \mathrm{d}t\ \mathrm{d}t'\ P_3(\vec{\mathbf{R}},t)\ P_3(\vec{\mathbf{R}}',t')$$
$$\times \exp\left\{ i\vec{\boldsymbol{\mu}} \cdot \left(\vec{\mathbf{R}} + v \int_0^t \mathrm{d}T\ \cos(\Phi_{0,j}(T))\hat{\mathbf{i}} + \sin(\Phi_{0,j}(T))\hat{\mathbf{j}} \right) \right\}$$
$$\times \exp\left\{ i\vec{\boldsymbol{\mu}}' \cdot \left(\vec{\mathbf{R}}' + v \int_0^{t'} \mathrm{d}T\ \cos(\Phi_{0,j}(T))\hat{\mathbf{i}} + \sin(\Phi_{0,j}(T))\hat{\mathbf{j}} \right) \right\}$$

$$\times \exp\left\{ i \int \mathrm{d}t\, \hat{\vec{\mathbf{r}}}_j(t) \cdot \mathcal{L}_{\perp,j}(t)\, \hat{\mathbf{\Phi}}_{\perp,j}(t) \right\} \tag{4.4.10}$$

$$= \int \ldots [\mathrm{d}\vec{\mathbf{R}}_j(s,t)_{\text{not zero}}]\, \mathrm{d}\vec{\boldsymbol{\mu}}\ \ldots \int \mathrm{d}t\, \mathrm{d}t'\ P_3(\vec{\mathbf{R}},t)\, P_3(\vec{\mathbf{R}}',t')$$
$$\times \exp\left\{ i\vec{\boldsymbol{\mu}} \cdot \left(\vec{\mathbf{R}} - \vec{\mathbf{R}}' + v \int_{t'}^{t} \mathrm{d}T\ \cos(\Phi_{0,j}(T))\hat{\mathbf{i}} + \sin(\Phi_{0,j}(T))\hat{\mathbf{j}} \right) \right\}$$
$$\times \exp\left\{ i \int \mathrm{d}t\, \hat{\vec{\mathbf{r}}}_j(t) \cdot \mathcal{L}_{\perp,j}(t)\, \hat{\mathbf{\Phi}}_{\perp,j}(t) \right\} \tag{4.4.11}$$

Note that for equation (4.4.11), if $j \neq j'$ in the double sum, it simply reduces to equation (4.4.5) squared.

The next few steps are straightforward. For these steps List A and List B are again similar and we present the less cluttered List B version of equation (4.3.1). We integrate over the delta functionals detailed in equations (4.2.22) and (4.2.23), which amounts to substituting in the relations between the position vectors and the angles $\phi_{1,j}$ and $\Phi_{0,j}$. All the terms are then in terms of $\hat{\vec{\mathbf{r}}}_j$ and the angles. The projected stochastic force $\vec{\mathbf{f}}_{\mathrm{h}} \cdot \hat{\mathbf{\Phi}}_{\perp,j}$ – call it f_j – is still around, however, so before integrating over $\hat{\vec{\mathbf{r}}}_j$ we integrate over f_j. As before in Section 2.1.6, we assume the projected force is still Gaussian distributed. To illustrate the form of these terms, the calculations for term (2) of equation (4.3.1) are below. See also Appendix E for a more detailed treatment of the functional integration.

$$(2) = \int \ldots [\mathrm{d}f_j(t)][\mathrm{d}\hat{\mathbf{r}}_j(t)][\mathrm{d}\phi_{1,j}(t)][\mathrm{d}\Phi_{0,j}(t)]\, \mathrm{d}\vec{\mathbf{r}}\, \mathrm{d}t\, \frac{1}{\lambda}\, \vec{\mathbf{P}}_2(\vec{\mathbf{r}},t) \cdot \hat{\mathbf{r}}_j(t)$$
$$\times \exp\left\{ i \int \mathrm{d}t\, \hat{\vec{\mathbf{r}}}_j(t) \cdot\ \hat{\mathbf{\Phi}}_{\perp,j}(t) \left(-\xi \dot{\phi}_{1,j}(t) - k\phi_{1,j}(t) \right) + \hat{\vec{\mathbf{r}}}_j(t) \cdot\ \hat{\mathbf{\Phi}}_{\perp,j}(t)\, f_j \right\}$$
$$\times \exp\left\{ -\frac{1}{2\lambda} \int_0^\infty \mathrm{d}t\ f^{\,2}(t) \right\} \tag{4.4.12}$$

$$= \int \ldots [\mathrm{d}\hat{\mathbf{r}}_j(t)][\mathrm{d}\phi_{1,j}(t)][\mathrm{d}\Phi_{0,j}(t)]\, \mathrm{d}\vec{\mathbf{r}}\, \mathrm{d}t\, \frac{1}{\lambda}\, \vec{\mathbf{P}}_2(\vec{\mathbf{r}},t) \cdot \hat{\mathbf{r}}_j(t)$$
$$\times \exp\left\{ i \int \mathrm{d}t\, \hat{\vec{\mathbf{r}}}_j(t) \cdot\ \hat{\mathbf{\Phi}}_{\perp,j}(t) \left(-\xi \dot{\phi}_{1,j}(t) - k\phi_{1,j}(t) \right) + \frac{\lambda}{2i}\, \hat{\vec{\mathbf{r}}}_j(t)^2 \right\} \tag{4.4.13}$$

$$= \int \ldots [\mathrm{d}\phi_{1,j}(t)][\mathrm{d}\Phi_{0,j}(t)]\, \mathrm{d}\vec{\mathbf{r}}\, \mathrm{d}t\, \frac{1}{\lambda}\, \vec{\mathbf{P}}_2(\vec{\mathbf{r}},t) \cdot \hat{\mathbf{\Phi}}_{\perp,j}(t)$$
$$\times \left(-\,\xi\, \dot{\phi}_{1,j}(t)\ -\ k\, \phi_{1,j}(t) \right) \exp\left\{ \int \mathrm{d}t\, \frac{-1}{2\lambda} \left(-\xi \dot{\phi}_{1,j}(t) - k\phi_{1,j}(t) \right)^2 \right\} \tag{4.4.14}$$

Where the averaging over the stochastic force f_j was performed to go from equation (4.4.12) to equation (4.4.13) and to go from equation (4.4.13) to equation (4.4.14) the integration over $\hat{\mathbf{r}}_j$ was performed.

4.4.3 Integration over the angles (Step 4 in Section 4.4.1 outline)

After this, complications arise and the way forward is no longer clear. Our hope was to integrate over $\phi_{1,j}$, followed by $\Phi_{0,j}$ leaving only the collective variables.

4.4.3.1 Using the Fourier transform

It is common to use the Fourier transform to simplify expressions, particularly when dealing with time derivatives since these become much more straightforward in the Fourier transform. We try using this to simplify the integration over $\phi_{1,j}$. Once again we shall present the less cluttered List B version of equation (4.3.1). However, we shall also discuss the terms as we originally dealt with them as per List A, i.e. with both $\mathcal{L}_{\perp,j}$ and $\mathcal{L}_{\parallel,j}$ contributions.

Consider term (2) of equation (4.3.1) again.

$$
\begin{aligned}
(2) &= \int \ldots [\mathrm{d}\phi_{1,j}(t)][\mathrm{d}\Phi_{0,j}(t)]\,\mathrm{d}\vec{\mathbf{r}}\,\mathrm{d}t\;\frac{1}{\lambda}\,\vec{\mathbf{P}}_2(\vec{\mathbf{r}},t)\cdot\hat{\mathbf{\Phi}}_{\perp,j}(t)\left(-\,\xi\,\dot{\phi}_{1,j}(t)\;-\;k\,\phi_{1,j}(t)\right)\\
&\quad\times\exp\left\{\int \mathrm{d}t\;\frac{-1}{2\lambda}\left(-\xi\dot{\phi}_{1,j}(t)-k\phi_{1,j}(t)\right)^2\right\} \qquad (4.4.15)\\
&= \int \ldots [\mathrm{d}\phi_{1,j}(t)][\mathrm{d}\Phi_{0,j}(t)]\,\mathrm{d}\vec{\mathbf{r}}\,\mathrm{d}t\;\frac{1}{\lambda}\,\vec{\mathbf{P}}_2(\vec{\mathbf{r}},t)\cdot\hat{\mathbf{\Phi}}_{\perp,j}(t)\left(-\xi\dot{\phi}_{1,j}(t)-k\phi_{1,j}(t)\right)\\
&\quad\times\exp\left\{\int \mathrm{d}t\;\frac{-1}{2\lambda}\left(\xi^2\dot{\phi}^2_{1,j}(t)+k^2\phi^2_{1,j}(t)+\xi k\dot{\phi}_{1,j}(t)\phi_{1,j}(t)\right)\right\} \qquad (4.4.16)\\
&= \int \ldots [\mathrm{d}\phi_{1,j}(t)][\mathrm{d}\Phi_{0,j}(t)]\,\mathrm{d}\vec{\mathbf{r}}\,\mathrm{d}t\;\frac{1}{\lambda}\,\vec{\mathbf{P}}_2(\vec{\mathbf{r}},t)\cdot\hat{\mathbf{\Phi}}_{\perp,j}(t)\left(-\xi\dot{\phi}_{1,j}(t)-k\phi_{1,j}(t)\right)\\
&\quad\times\exp\left\{\int \mathrm{d}t\;\frac{-1}{2\lambda}\left(\xi^2\dot{\phi}^2_{1,j}(t)+k^2\phi^2_{1,j}(t)\right)\right\} \qquad (4.4.17)
\end{aligned}
$$

To go from equation (4.4.16) to equation (4.4.17), we note that the cross term can be rewritten as half the total time derivative of $\phi^2_{1,j}(t)$ and hence

$$
\int \mathrm{d}t\,\dot{\phi}_{1,j}(t)\phi_{1,j}(t) = \int \mathrm{d}t\;\frac{1}{2}\,\frac{\mathrm{d}\phi^2_{1,j}(t)}{\mathrm{d}t} = \frac{1}{2}\Big(\phi_{1,j}(t=\infty)-\phi_{1,j}(t=-\infty)\Big). \qquad (4.4.18)
$$

We assume $\phi_{1,j}$ at limiting values of t can be taken as vanishing. If this is not the case, then equation (4.4.18) will just be a finite constant which will have no effect on the average values or correlation functions of the collective variables.

Writing the argument of the exponential in equation (4.4.17) is straightforward:

$$
\int \mathrm{d}t\;\frac{-1}{2\lambda}\left(\xi^2\dot{\phi}^2_{1,j}(t)+k^2\phi^2_{1,j}(t)\right) = \frac{1}{2\pi}\int \mathrm{d}\omega\;\frac{-1}{2\lambda}\left(\omega^2\xi^2+k^2\right)\phi_{1,j}(\omega)\,\phi_{1,j}(-\omega). \qquad (4.4.19)
$$

However, the rest presents problems. We attempted the following, where we simply wrote the functions $\dot{\phi}_{1,j}$ and $\phi_{1,j}$ in their Fourier representations while leaving the other time-dependent functions alone:

$$
\begin{aligned}
&\int \ldots [\mathrm{d}\phi_{1,j}(t)][\mathrm{d}\Phi_{0,j}(t)]\,\mathrm{d}\vec{\mathbf{r}}\,\mathrm{d}t\;\frac{1}{\lambda}\,\vec{\mathbf{P}}_2(\vec{\mathbf{r}},t)\cdot\hat{\mathbf{\Phi}}_{\perp,j}(t)\left(-\xi\dot{\phi}_{1,j}(t)-k\phi_{1,j}(t)\right)\ldots\\
&= \int \ldots [\mathrm{d}\phi_{1,j}(\omega)][\mathrm{d}\Phi_{0,j}(t)]\,\mathrm{d}\vec{\mathbf{r}}\,\mathrm{d}t\;\frac{1}{2\pi\lambda}\,\vec{\mathbf{P}}_2(\vec{\mathbf{r}},t)\cdot\hat{\mathbf{\Phi}}_{\perp,j}(t)\int \mathrm{d}\omega\;(i\omega\xi-k)\,e^{-i\omega t}\phi_{1,j}(\omega)\ldots
\end{aligned} \qquad (4.4.20)
$$

The integration over $\phi_{1,j}(\omega)$ is now possible, because taken together equations (4.4.19) and (4.4.20) have the form of a Gaussian with a linear downstairs term. To take our example forward, when

we integrate (2) over $\phi_{1,j}(\omega)$ we obtain

$$(2) = \int \ldots [\mathrm{d}\phi_{1,j}(\omega)][\mathrm{d}\Phi_{0,j}(t)]\,\mathrm{d}\vec{\mathbf{r}}\,\mathrm{d}t\,\frac{1}{2\pi\lambda}\,\vec{\mathbf{P}}_2(\vec{\mathbf{r}},t)\cdot\hat{\mathbf{\Phi}}_{\perp,j}(t)\int \mathrm{d}\omega\;(i\omega\xi-k)\,e^{-i\omega t}\phi_{1,j}(\omega)$$
$$\times\exp\left\{\frac{1}{2\pi}\int \mathrm{d}\omega\,\frac{-1}{2\lambda}\left(\omega^2\xi^2+k^2\right)\phi_{1,j}(\omega)\,\phi_{1,j}(-\omega)\right\} \tag{4.4.21}$$
$$= 0. \tag{4.4.22}$$

In this case we get zero, because the integral in $\phi_{1,j}$ is odd overall, whereas our integration range is even.

To get a better idea of how complications arise in the $\phi_{1,j}$ integration, we turn our attention to the (2)×(4) term of equation (4.3.1).

$$(2)\times(4)$$
$$= \int \ldots [\mathrm{d}\phi_{1,j}(t)][\mathrm{d}\Phi_{0,j}(t)]\,\mathrm{d}\vec{\mathbf{r}}\,\mathrm{d}\vec{\mathbf{R}}\,\mathrm{d}t\,\mathrm{d}t'\,\mathrm{d}\vec{\boldsymbol{\mu}}\,\frac{1}{\lambda}\vec{\mathbf{P}}_2(\vec{\mathbf{r}},t)\cdot\hat{\mathbf{\Phi}}_{\parallel,j}(t)\left(-\xi\dot{\phi}_{1,j}(t)-k\phi_{1,j}(t)\right)$$
$$\times\int_0^L \mathrm{d}s\;\vec{\mathbf{P}}_4(\vec{\mathbf{R}},t')\cdot\hat{\mathbf{\Phi}}_{\parallel,j}(t'-{}^{s}\!/_{v})\,\exp\left\{\int \mathrm{d}t\,\frac{-1}{2\lambda}\left(\xi^2\dot{\phi}_{1,j}^2(t)+k^2\phi_{1,j}^2(t)\right)\right\}$$
$$\times\exp\left\{i\vec{\boldsymbol{\mu}}\cdot\left(\vec{\mathbf{r}}-\vec{\mathbf{R}}-v\int_{t'-{}^{s}\!/_{v}}^{t}\mathrm{d}T\;\hat{\mathbf{\Phi}}_{\parallel,j}(T)+\ell\hat{\mathbf{\Phi}}_{\parallel,j}(t)+\frac{2\pi}{\ell}\phi_{1,j}(t)\hat{\mathbf{\Phi}}_{\perp,j}(t)\right)\right\} \tag{4.4.23}$$

$$= \int \ldots [\mathrm{d}\phi_{1,j}(\omega)][\mathrm{d}\Phi_{0,j}(t)]\,\mathrm{d}\vec{\mathbf{r}}\,\mathrm{d}\vec{\mathbf{R}}\,\mathrm{d}t\,\mathrm{d}t'\,\mathrm{d}\vec{\boldsymbol{\mu}}$$
$$\times\frac{1}{2\pi\lambda}\vec{\mathbf{P}}_2(\vec{\mathbf{r}},t)\cdot\hat{\mathbf{\Phi}}_{\parallel,j}(t)\int \mathrm{d}\omega\;(i\omega\xi-k)\,e^{-i\omega t}\phi_{1,j}(\omega)\int_0^L \mathrm{d}s\;\vec{\mathbf{P}}_4(\vec{\mathbf{R}},t')\cdot\hat{\mathbf{\Phi}}_{\parallel,j}(t'-{}^{s}\!/_{v})$$
$$\times\exp\left\{\frac{1}{2\pi}\int \mathrm{d}\omega\,\frac{-1}{2\lambda}\left(\omega^2\xi^2+k^2\right)\phi_{1,j}(\omega)\,\phi_{1,j}(-\omega)+\frac{2\pi i}{\ell}\,e^{-i\omega t}\,\phi_{1,j}(\omega)\,\vec{\boldsymbol{\mu}}\cdot\hat{\mathbf{\Phi}}_{\perp,j}(t)\right\}$$
$$\times\exp\left\{i\vec{\boldsymbol{\mu}}\cdot\left(\vec{\mathbf{r}}-\vec{\mathbf{R}}-v\int_{t'-{}^{s}\!/_{v}}^{t}\mathrm{d}T\;\hat{\mathbf{\Phi}}_{\parallel,j}(T)+\ell\hat{\mathbf{\Phi}}_{\parallel,j}(t)\right)\right\} \tag{4.4.24}$$
$$= \int \ldots [\mathrm{d}\Phi_{0,j}(t)]\,\mathrm{d}\vec{\mathbf{r}}\,\mathrm{d}\vec{\mathbf{R}}\,\mathrm{d}t\,\mathrm{d}t'\,\mathrm{d}\vec{\boldsymbol{\mu}}\,\frac{1}{2\pi\lambda}\,\vec{\mathbf{P}}_2(\vec{\mathbf{r}},t)\cdot\hat{\mathbf{\Phi}}_{\parallel,j}(t)\int_0^L \mathrm{d}s\;\vec{\mathbf{P}}_4(\vec{\mathbf{R}},t')\cdot\hat{\mathbf{\Phi}}_{\parallel,j}(t'-{}^{s}\!/_{v})$$
$$\times\int \mathrm{d}\omega\,\frac{2\lambda\,(i\omega\xi-k)\,e^{-i\omega t}}{\omega^2\xi^2+k^2}\,\frac{i}{\ell}\,\vec{\boldsymbol{\mu}}\cdot\hat{\mathbf{\Phi}}_{\perp,j}(t)\,\exp\left\{\frac{-\lambda}{2\ell^2}\int \mathrm{d}\omega\,\frac{1}{\omega^2\xi^2+k^2}\left(\vec{\boldsymbol{\mu}}\cdot\hat{\mathbf{\Phi}}_{\perp,j}(t)\right)^2\right\}$$
$$\times\exp\left\{i\vec{\boldsymbol{\mu}}\cdot\left(\vec{\mathbf{r}}-\vec{\mathbf{R}}-v\int_{t'-{}^{s}\!/_{v}}^{t}\mathrm{d}T\;\hat{\mathbf{\Phi}}_{\parallel,j}(T)+\ell\hat{\mathbf{\Phi}}_{\parallel,j}(t)\right)\right\} \tag{4.4.25}$$

The ω integration can be performed. However, this leaves a very complicated expression with respect to $\Phi_{0,j}$.

Now we consider the terms of equation (4.3.1) with the contribution of $\mathcal{L}_{\parallel,j}$ included, as per List A. We spent a substantial amount time exploring ways of integrating these terms. To give an example of the complications we encountered, consider term (2) of equation (4.3.1) again, but with the $\mathcal{L}_{\parallel,j}$ contribution included:

$$(2) = \int \ldots [\mathrm{d}\phi_{1,j}(t)][\mathrm{d}\Phi_{0,j}(t)]\,\mathrm{d}\vec{\mathbf{r}}\,\mathrm{d}t\,\frac{1}{\lambda}$$

$$\times \vec{\mathbf{P}}_2(\vec{\mathbf{r}},t)\cdot\left[\left(-\xi\dot{\phi}_{1,j}(t)-k\phi_{1,j}(t)\right)\hat{\mathbf{\Phi}}_{\perp,j}(t)+\left(\frac{\kappa\pi^3}{8\ell^2}\,\phi_{1,j}(t)\cot\left(2\Phi_{0,j}(t)\right)-\gamma v\right)\hat{\mathbf{\Phi}}_{\parallel,j}(t)\right]$$
$$\times\ \exp\left\{\int \mathrm{d}t\,\frac{-1}{2\lambda}\left[\left(-\xi\dot{\phi}_{1,j}(t)-k\phi_{1,j}(t)\right)^2+\left(\frac{\kappa\pi^3}{8\ell^2}\,\phi_{1,j}(t)\cot\left(2\Phi_{0,j}(t)\right)-\gamma v\right)^2\right]\right\}. \tag{4.4.26}$$

The Fourier transform of the terms due to $\mathcal{L}_{\parallel,j}$ is not straightforward. To illustrate the difficulties of using the Fourier transform in equation (4.4.26), we focus the argument of the exponential – cf. equation (4.4.26):

$$\int \mathrm{d}t\,\frac{-1}{2\lambda}\left[\left(-\xi\dot{\phi}_{1,j}(t)-k\phi_{1,j}(t)\right)^2+\left(\frac{\kappa\pi^3}{8\ell^2}\,\phi_{1,j}(t)\cot\left(2\Phi_{0,j}(t)\right)-\gamma v\right)^2\right]. \tag{4.4.27}$$

We have already discussed how to deal with the $\mathcal{L}_{\perp,j}$ terms, so we look at how to transform the terms arising from $\mathcal{L}_{\parallel,j}$:

$$\int \mathrm{d}t\,\frac{-1}{2\lambda}\left(\frac{\kappa\pi^3}{8\ell^2}\,\phi_{1,j}(t)\cot\left(2\Phi_{0,j}(t)\right)-\gamma v\right)^2$$
$$=\int \mathrm{d}t\,\frac{-1}{2\lambda}\left[\frac{\kappa^2\pi^6}{64\ell^4}\,\phi_{1,j}^2(t)\cot^2\left(2\Phi_{0,j}(t)\right)-\frac{\gamma v\kappa\pi^3}{8\ell^2}\phi_{1,j}(t)\cot\left(2\Phi_{0,j}(t)\right)+\gamma^2v^2\right] \tag{4.4.28}$$

Unlike before in equation (4.4.19), there is more than a single time-dependent function. At first, we tried transforming both $\Phi_{0,j}$ and $\phi_{1,j}$. However, the Fourier transform of $\cot\left(2\Phi_{0,j}(t)\right)$ and $\cot^2\left(2\Phi_{0,j}(t)\right)$ do not simplify – even less so when multiplied by $\phi_{1,j}^2$ and $\phi_{1,j}$, respectively. We considered approximations like

$$\int \mathrm{d}\omega\,\mathrm{d}\omega'\,\phi_{1,j}(\omega)\,\phi_{1,j}(\omega-\omega')\,\chi_j(\omega')\approx\int \mathrm{d}\omega\,\phi_{1,j}(\omega)\,\phi_{1,j}(-\omega)\,\chi_j(0) \tag{4.4.29}$$

where $\chi_j(\omega)$ denotes the Fourier transform of $\cot^2\left(2\Phi_{0,j}(t)\right)$. We have assumed here that the integration will be dominated by the contributions where $\omega\approx\omega'$ and so have set ω' to zero. In other words, we assumed we could still approximate the integral as diagonal. However, our investigations were not promising.

4.4.3.2 Remaining in the time domain

Next, we considered whether integrating over $\phi_{1,j}$ with a matrix approach might have better results. The idea is to discretise the function into N intervals of Δt. The derivative $\dot{\phi}_{1,j}$ is then written as

$$\dot{\phi}_{1,j}(t)\mapsto\frac{\phi_{1,j,t}-\phi_{1,j,t-1}}{\Delta t}, \tag{4.4.30}$$

where the notation $\phi_{1,j,t}$ indicates the discretised function at the instant where time is equal to t. Substituting this into the terms into equation (4.3.1) means we once again simply have Gaussians to evaluate. However, the $\Phi_{0,j}$ integration is not simplified by this approach either.

The next idea we explored was to see if we could map the results of the harmonic oscillator propagator described in the book by Chaichian and Demichev [73] and the lecture notes of Müller-Nedebock [74]. Since equation (4.2.12) of $\mathcal{L}_{\perp,j}$ is essentially a harmonic oscillator, we hoped there could be a useful connection.

Following the notation of Müller-Nedebock [74], in one dimension a propagator $K(x,t;x_0,t_0)$ satisfies the following two equivalent conditions:

$$1.\quad K(x,t;x_0,t_0) = \begin{cases} \langle x|\,\hat{U}(t,t_0)\,|x_0\rangle & \text{if } t \geq t_0 \\ 0 & \text{if } t < t_0 \end{cases} \tag{4.4.31}$$

$$2.\quad \psi(x,t) = \int \mathrm{d}x\, K(x,t;x_0,t_0)\,\psi(x_0,t_0). \tag{4.4.32}$$

That is to say, the propagator takes us from the probability amplitude at a time t_0 and position x_0 to the probability amplitude at a time t and position x.

Using the Feynman-Kac theorem, we can obtain a path-integral representation of the propagator.

For a harmonic oscillator, the form of the propagator in the path-integral representation is known and the path integral can be explicitly calculated. The harmonic propagator $K(x,t;x_0,t_0)$ that goes from a point (x_0,t_0) to (x,t) is given by

$$K(x,t;x_0,t_0) = \mathcal{N}\int [\mathrm{d}x(\tau)]\,\exp\left\{\frac{im}{2\hbar}\int_{t_0}^{t}\mathrm{d}\tau\,\left(\dot{x}^2(\tau)-\omega^2x^2(\tau)\right)\right\} \tag{4.4.33}$$

$$= \sqrt{\frac{m\omega}{2\pi i\hbar\sin(\omega(t-t_0))}}\,\exp\left\{\frac{im\omega}{2\hbar}\frac{(x^2+x_0^2)\,\cos(\omega(t-t_0))-2xx_0}{\sin(\omega(t-t_0))}\right\}. \tag{4.4.34}$$

At this point, we also realised that we had not adequately included the relationship between $\phi_{1,j}$ and $\Phi_{0,j}$. This led us to include the delta functional $\delta[\phi_{1,j}(t) - \frac{2\ell}{v\pi}\dot{\Phi}_{0,j}(t)]$ of equation (4.2.21). This changed the form of the terms to a degree, but did not solve the problem of the $\Phi_{0,j}$ integration. Transforming $\Phi_{0,j}$ into the Fourier transform was not helpful, since the $\Phi_{0,j}$ angle was inside various $\sin$ and $\cos$ functions. Nor would a matrix approach help, for the same reasons. We turned to investigation of $\phi_{1,j}$ and $\Phi_{0,j}$ in light of this relationship, and in the company of the projection vectors $\hat{\mathbf{\Phi}}_{\perp,j}$ and $\hat{\mathbf{\Phi}}_{\parallel,j}$, to see whether we could rewrite our terms in a simpler way with fewer variables. This also tied in with what we noticed in Section 4.3.1 where we saw that the terms in equation (4.3.1) could be written more transparently when written in terms of the projection vectors.

We began by noting that products of $\phi_{1,j}$ (or equivalently $\dot{\Phi}_{0,j}$) and the projection vectors could be written as time derivatives of the projection vectors.

$$\frac{\mathrm{d}}{\mathrm{d}t}\,\hat{\mathbf{\Phi}}_{\perp,j}(t) = -\,\dot{\Phi}_{0,j}(t)\,\hat{\mathbf{\Phi}}_{\parallel,j}(t) = -\,\frac{\pi v}{2\ell}\,\phi_{1,j}(t)\,\hat{\mathbf{\Phi}}_{\parallel,j}(t) \tag{4.4.35}$$

$$\frac{\mathrm{d}}{\mathrm{d}t}\,\hat{\mathbf{\Phi}}_{\parallel,j}(t) = \dot{\Phi}_{0,j}(t)\,\hat{\mathbf{\Phi}}_{\perp,j}(t) = \frac{\pi v}{2\ell}\,\phi_{1,j}(t)\,\hat{\mathbf{\Phi}}_{\perp,j}(t) \tag{4.4.36}$$

We also noted that the projection vectors are not independent and one projection vector could be written in terms of another.

$$\hat{\mathbf{\Phi}}_{\parallel,j} = \left(\begin{smallmatrix} 0 & 1 \\ -1 & 0 \end{smallmatrix}\right) \hat{\mathbf{\Phi}}_{\perp,j} \tag{4.4.37}$$

$$\hat{\mathbf{\Phi}}_{\perp,j} = - \left(\begin{smallmatrix} 0 & 1 \\ -1 & 0 \end{smallmatrix}\right) \hat{\mathbf{\Phi}}_{\perp,j} \tag{4.4.38}$$

We hoped that by writing any products of $\phi_{1,j}$ and a projection vector as the derivative of a projection vector, and by replacing all instances of $\hat{\mathbf{\Phi}}_{\parallel,j}(t)$ with $\hat{\mathbf{\Phi}}_{\perp,j}(t)$, the integration would be sufficiently simplified to perform since the number of variables would be decreased.

Our last attempt at the calculation of equation (4.1.8) involved trying to perform a mapping between the results presented in Bhattacharjee *et al.* [72] and our equations. In the paper by Bhattacharjee *et al.* [72], functional integral formalism is used with an alternative treatment of the semi-flexible condition equation (1.4.16). The hard constraint of equation (1.4.16)

$$\left| \frac{\partial \vec{\mathbf{R}}(s,t)}{\partial s} \right| = 1, \quad \forall s \in [0, L] \tag{4.4.39}$$

is replaced by a global, mean-field constraint

$$\left\langle \left| \frac{\partial \vec{\mathbf{R}}(s,t)}{\partial s} \right| \right\rangle = 1, \quad \forall s \in [0, L] \tag{4.4.40}$$

and the end-to-end distance is calculated. The mean-field approach is also used in the papers of Ha and Thirumalai [75, 76].

4.5 A minimalist approach

Given all the complications and dead-ends encountered with the RPA, we decided to consider a stripped-down version of the calculation. We keep track of only a single position vector per filament, namely the position vector $\vec{\mathbf{R}}_j(0,t)$ that points from the origin to the head-body join. Since we now have only a single point to keep track of, we drop the position dependence in our notation and refer simply to $\vec{\mathbf{R}}_j(t)$. See Figure 4.2 (and compare this with Figure 4.1).

Since we have the constraint that the actin filament moves at a constant speed of v,

$$\left| \dot{\vec{\mathbf{R}}}_j(t) \right| = v \quad \text{for all } t, \tag{4.5.1}$$

and the relationship between the angles $\phi_{1,j}$ and $\Phi_{0,j}$ of equation (2.1.23)

$$\dot{\Phi}_{0,j}(t) = v \, \frac{\pi}{2\ell} \, \phi_{1,j}(t) \quad \text{for all } t, \tag{4.5.2}$$

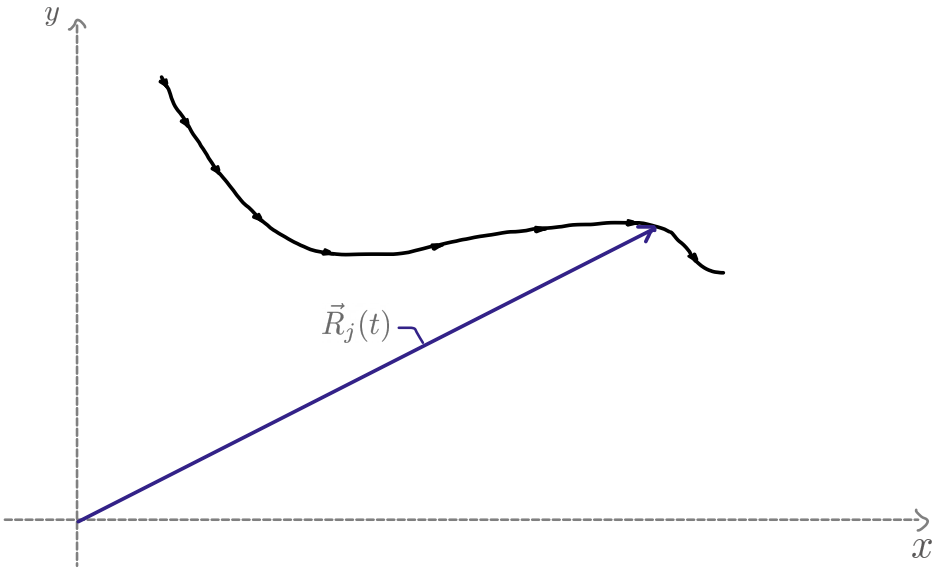

Figure 4.2: Diagram showing our minimalist approach. The vector $\vec{\mathbf{R}}_j(t)$ points from the origin to the head-body join. Instead of keeping track of the positions of the body, the head-body join and the head, we take the head-body join coordinate – renamed $\vec{\mathbf{R}}_j(t)$ – as a proxy for all the other coordinates.

we can write

$$\dot{\vec{\mathbf{R}}}_j(t) = v\left[\cos(\Phi_{0,j}(t))\,\hat{\mathbf{x}} + \sin(\Phi_{0,j}(t))\,\hat{\mathbf{y}}\right] \tag{4.5.3}$$

$$\ddot{\vec{\mathbf{R}}}_j(t) = v\,\dot{\Phi}_{0,j}(t)\left[-\sin(\Phi_{0,j}(t))\,\hat{\mathbf{x}} + \cos(\Phi_{0,j}(t))\,\hat{\mathbf{y}}\right] \tag{4.5.4}$$

$$= v^2\,\frac{\pi}{2\ell}\,\phi_{1,j}(t)\left[-\sin(\Phi_{0,j}(t))\,\hat{\mathbf{x}} + \cos(\Phi_{0,j}(t))\,\hat{\mathbf{y}}\right] \tag{4.5.5}$$

$$\begin{aligned}\dddot{\vec{\mathbf{R}}}_j(t) &= v\,\ddot{\Phi}_j(t)\left[-\sin(\Phi_{0,j}(t))\,\hat{\mathbf{x}} + \cos(\Phi_{0,j}(t))\,\hat{\mathbf{y}}\right] \\ &\quad + v\,\dot{\Phi}^2_{0,j}(t)\left[-\cos(\Phi_{0,j}(t))\,\hat{\mathbf{x}} - \sin(\Phi_{0,j}(t))\,\hat{\mathbf{y}}\right] \qquad (4.5.6)\\ &\approx v\,\ddot{\Phi}_j(t)\left[-\sin(\Phi_{0,j}(t))\,\hat{\mathbf{x}} + \cos(\Phi_{0,j}(t))\,\hat{\mathbf{y}}\right]. \qquad (4.5.7)\end{aligned}$$

In equation (4.5.7) we discarded the second term because, by equation (4.5.2), $\dot{\Phi}^2_{0,j}(t)$ is of the order $\phi^2_{1,j}$, which we have taken as being negligible.

This allows us to write the non-interacting part of the Langevin equation (cf. equations (2.1.24), (4.2.9), (4.2.12) and (4.2.13)) as

$$\vec{\mathbf{0}} = -\varsigma\,\dot{\vec{\mathbf{R}}}_j(t) - \frac{\varsigma\ell}{v}\,\ddot{\vec{\mathbf{R}}}_j(t) - \varsigma\left(\frac{2\ell}{v\pi}\right)^2\dddot{\vec{\mathbf{R}}}_j(t) - \frac{k}{v^2}\,\frac{2\ell}{\pi}\,\ddot{\vec{\mathbf{R}}}_j(t) + \vec{\mathbf{f}}, \tag{4.5.8}$$

remembering that this equation still needs to be constrained to ensure equation (4.5.1) holds.

The analogue of the overdamped situation would be if we neglect the $\dddot{\vec{\mathbf{R}}}_j(t)$ term so that

$$\vec{\mathbf{0}} = -\varsigma\,\dot{\vec{\mathbf{R}}}_j(t) - \left(\frac{\varsigma\ell}{v} + \frac{k}{v^2}\,\frac{2\ell}{\pi}\right)\ddot{\vec{\mathbf{R}}}_j(t) + \vec{\mathbf{f}}, \tag{4.5.9}$$

where we still require that $\left|\dot{\vec{\mathbf{R}}}_j(t)\right| = v$. Note that this equation resembles a harmonic oscillator in $\dot{\vec{\mathbf{R}}}_j(t)$. This is especially clear if we let

$$\alpha = \varsigma \quad \text{and} \quad \beta = \frac{\varsigma \ell}{v} + \frac{k}{v^2}\frac{2\ell}{\pi} \tag{4.5.10}$$

so that equation (4.5.9) is written as

$$\vec{\mathbf{0}} = -\alpha\, \dot{\vec{\mathbf{R}}}_j(t) - \beta\, \ddot{\vec{\mathbf{R}}}_j(t) + \vec{\mathbf{f}} \quad \text{with} \quad \left|\dot{\vec{\mathbf{R}}}_j(t)\right| = v \quad \text{for all } t. \tag{4.5.11}$$

Physically, the overdamped situation would necessarily require ℓ to be very small in comparison with the other parameters of the problem. Since ℓ is determined by the density of motors on the substrate, ℓ is effectively the free length until attachment and we can reasonably assume that the tethering of motors to subtrate is sufficiently dense.

4.5.1 Moving to a MSR equation

First we define some stripped-down collective fields. Since now we only focus on a single vector $\vec{\mathbf{R}}_j(t)$ of the head-body join, we define

$$\mathrm{p}(\vec{\mathbf{r}}, t) = \sum_{j=1}^{N} \delta\left(\vec{\mathbf{r}} - \vec{\mathbf{R}}_j(t)\right) \tag{4.5.12}$$

$$\hat{\vec{\mathbf{p}}}(\vec{\mathbf{r}}, t) = \sum_{j=1}^{N} \hat{\mathbf{r}}_j(t)\, \delta\left(\vec{\mathbf{r}} - \vec{\mathbf{R}}_j(t)\right) \tag{4.5.13}$$

$$\vec{\Theta}(\vec{\mathbf{r}}, t) = \sum_{j=1}^{N} \dot{\vec{\mathbf{R}}}_j(t)\, \delta\left(\vec{\mathbf{r}} - \vec{\mathbf{R}}_j(t)\right) \tag{4.5.14}$$

and their Fourier-space companions

$$\begin{aligned}\mathrm{p}(\vec{\boldsymbol{\mu}}, t) &= \int \mathrm{d}\vec{\mathbf{r}}\, \mathrm{p}(\vec{\mathbf{r}}, t)\, \exp\{i\vec{\boldsymbol{\mu}} \cdot \vec{\mathbf{r}}\} = \int \mathrm{d}\vec{\mathbf{r}} \sum_{j=1}^{N} \delta\left(\vec{\mathbf{r}} - \vec{\mathbf{R}}_j(t)\right) \exp\{i\vec{\boldsymbol{\mu}} \cdot \vec{\mathbf{r}}\} \\ &= \sum_{j=1}^{N} \exp\left\{i\, \vec{\boldsymbol{\mu}} \cdot \vec{\mathbf{R}}_j(t)\right\} \end{aligned} \tag{4.5.15}$$

$$\hat{\vec{\mathbf{p}}}(\vec{\boldsymbol{\mu}}, t) = \sum_{j=1}^{N} \hat{\mathbf{r}}_j(t)\, \exp\left\{i\, \vec{\boldsymbol{\mu}} \cdot \vec{\mathbf{R}}_j(t)\right\} \tag{4.5.16}$$

$$\vec{\Theta}(\vec{\boldsymbol{\mu}}, t) = \sum_{j=1}^{N} \dot{\vec{\mathbf{R}}}_j(t)\, \exp\left\{i\, \vec{\boldsymbol{\mu}} \cdot \vec{\mathbf{R}}_j(t)\right\}. \tag{4.5.17}$$

We wish to use these collective fields to rewrite our Langevin equation, as we did in Section 4.2.1.

We have not yet discussed the hydrodynamic interactions term for our minimalist calculation. The key feature of this interaction is that the tip of the filament experiences drag relative

to the underlying velocity of the surrounding fluid. We used the Oseen tensor to model this effect. Now, in terms of the head-body join $\vec{\mathbf{R}}_j(t)$, this relative drag – equation (4.2.8) – is

$$\vec{\mathbf{v}}_f(\vec{\mathbf{r}}_i(\ell,t)) = \frac{f_a}{v}\sum_j \int_0^L \mathrm{d}s\, \mathbf{H}\left(\vec{\mathbf{r}}_i(t) - \vec{\mathbf{R}}_j(t - s/v)\right)\cdot \dot{\vec{\mathbf{R}}}_j(t - s/v), \tag{4.5.18}$$

recalling that we can write any position s on the polymer at a time t in terms of the head-body join at an earlier time – see Section 4.3.1.

In the MSR integral formalism, the Langevin equation is multiplied by a auxillary field (see equation (4.1.3)) and hence the drag term enters via

$$\sum_i \hat{\mathbf{r}}_i(t)\cdot\vec{\mathbf{v}}_f(\vec{\mathbf{r}}_i(\ell,t)) = \sum_{i,j}\frac{f_a}{v}\int_0^L \mathrm{d}s\, \hat{\mathbf{r}}_i(t)\cdot\mathbf{H}\left(\vec{\mathbf{r}}_i(t) - \vec{\mathbf{R}}_j(t - s/v)\right)\cdot\dot{\vec{\mathbf{R}}}_j(t - s/v) \tag{4.5.19}$$

$$= \sum_{i,j}\frac{f_a}{v}\int_0^L \mathrm{d}s\, \hat{\mathbf{r}}_i(t)\cdot\mathbf{H}\left(\vec{\mathbf{R}}_j(t) + \ell\,\vec{\mathbf{\Delta}}(t) - \vec{\mathbf{R}}_j(t - s/v)\right)\cdot\dot{\vec{\mathbf{R}}}_j(t - s/v) \tag{4.5.20}$$

where $\left|\vec{\mathbf{r}}_j(\ell,t) - \vec{\mathbf{R}}_j(t)\right| \approx \ell$ and $\ell\,\vec{\mathbf{\Delta}}(t)$ gives the extension from the head-body join to the tip.

If we assume the hydrodynamic field only changes slowly over distances greater than ℓ, we can ignore the extension $\ell\,\vec{\mathbf{\Delta}}(t)$, allowing us to write

$$\vec{\mathcal{L}}_{\text{int}}(t) \approx \vec{\mathcal{L}}'_{\text{int}}(t) = \frac{\varsigma f_a}{v}\int \mathrm{d}\vec{\mathbf{r}}\,\mathrm{d}\vec{\mathbf{r}}'\int_0^L \mathrm{d}s\;\hat{\vec{\mathbf{p}}}(\vec{\mathbf{r}},t)\cdot\mathbf{H}(\vec{\mathbf{r}}-\vec{\mathbf{r}}')\cdot\vec{\Theta}(\vec{\mathbf{r}}',t - s/v) \tag{4.5.21}$$

as in equation (4.2.18). Although a rough approximation, we hope it captures the essentials.

The full Langevin equation can be written as

$$\vec{\mathcal{L}}(t) = \sum_j \vec{\mathcal{L}}_{\text{min},j}(t) + \vec{\mathcal{L}}'_{\text{int}}(t) \tag{4.5.22}$$

as we did in equation (4.2.19), where

$$\vec{\mathcal{L}}_{\text{min},j}(t) = -\alpha\,\dot{\vec{\mathbf{R}}}_j(t) - \beta\,\ddot{\vec{\mathbf{R}}}_j(t). \tag{4.5.23}$$

We note that the previously defined π field can be written in terms of the new Θ field as follows:

$$\vec{\pi}(\vec{\mathbf{R}},t) = \sum_i\int_0^L \mathrm{d}s\,\frac{\partial\vec{\mathbf{R}}_i(s,t)}{\partial s}\,\delta(\vec{\mathbf{R}} - \vec{\mathbf{R}}_i(s,t))$$

$$= \int_0^L \mathrm{d}s\,\vec{\Theta}(\vec{\mathbf{r}},t - s/v). \tag{4.5.24}$$

4.5.1.1 A minimalist generating functional

We continue as in Section 4.2.2 and write down the generating functional.

$$\mathcal{Z} = \prod_j \int [\mathrm{d}\vec{\mathbf{R}}_j(t)][\mathrm{d}\hat{\vec{\mathbf{r}}}_j(t)][\mathrm{dp}(\vec{\mathbf{r}},t)][\mathrm{d}\hat{\vec{\mathbf{p}}}(\vec{\mathbf{r}},t)][\mathrm{d}\vec{\Theta}(\vec{\mathbf{r}},t)]\times$$

$$\delta\left[\mathrm{p}(\vec{\mathbf{r}},t)-\sum_j \delta\left(\vec{\mathbf{r}}-\vec{\mathbf{R}}_j(t)\right)\right]\ \delta\left[\hat{\vec{\mathbf{p}}}(\vec{\mathbf{r}},t)-\sum_j \hat{\vec{\mathbf{r}}}_j\,\delta\left(\vec{\mathbf{r}}-\vec{\mathbf{R}}_j(t)\right)\right]\ \times$$
$$\delta\left[\vec{\Theta}(\vec{\mathbf{r}},t)-\sum_j \dot{\vec{\mathbf{R}}}_j(t)\,\delta\left(\vec{\mathbf{r}}-\vec{\mathbf{R}}_j(t)\right)\right]\ \delta\left[\dot{\vec{\mathbf{R}}}_j(t)^2-v^2\right]\ \times$$
$$\exp\left\{i\int \mathrm{d}t\,\hat{\vec{\mathbf{r}}}_j(t)\cdot\left(\sum_j \vec{\mathcal{L}}_{\mathrm{min},\,j}(t)+\vec{\mathcal{L}}'_{\mathrm{int}}(t)\right)\right\} \tag{4.5.25}$$

We have included the constraint in equation (4.5.1) via the delta functional $\delta\left[\dot{\vec{\mathbf{R}}}_j(t)^2-v^2\right]$. However, drawing from the papers of Ha and Thirumalai [75, 76], we approximate this constraint with the mean-field constraint

$$\int_0^\tau \mathrm{d}t\,\dot{\vec{\mathbf{R}}}_j(t)^2 = v^2\,\tau \tag{4.5.26}$$

where τ represents the total time interval under consideration. Hence an approximate generating functional is given by

$$\mathcal{Z}_{\text{approx}} = \prod_j \int [\mathrm{d}\vec{\mathbf{R}}_j(t)][\mathrm{d}\hat{\vec{\mathbf{r}}}_j(t)][\mathrm{d}\mathrm{p}(\vec{\mathbf{r}},t)][\mathrm{d}\hat{\vec{\mathbf{p}}}(\vec{\mathbf{r}},t)][\mathrm{d}\vec{\Theta}(\vec{\mathbf{r}},t)]\ \times$$
$$\delta\left[\mathrm{p}(\vec{\mathbf{r}},t)-\sum_j \delta\left(\vec{\mathbf{r}}-\vec{\mathbf{R}}_j(t)\right)\right]\ \delta\left[\hat{\vec{\mathbf{p}}}(\vec{\mathbf{r}},t)-\sum_j \hat{\vec{\mathbf{r}}}_j\,\delta\left(\vec{\mathbf{r}}-\vec{\mathbf{R}}_j(t)\right)\right]\ \times$$
$$\delta\left[\vec{\Theta}(\vec{\mathbf{r}},t)-\sum_j \dot{\vec{\mathbf{R}}}_j(t)\,\delta\left(\vec{\mathbf{r}}-\vec{\mathbf{R}}_j(t)\right)\right]\ \frac{1}{2\pi}\int \mathrm{d}\,\wr\,\exp\left\{i\,\wr\int_0^\tau \mathrm{d}t\,\dot{\vec{\mathbf{R}}}_j(t)^2 - i\,\wr\,v^2\,\tau\right\}\ \times$$
$$\exp\left\{i\int \mathrm{d}t\,\hat{\vec{\mathbf{r}}}_j(t)\cdot\left(\sum_j \vec{\mathcal{L}}_{\mathrm{min},\,j}(t)+\vec{\mathcal{L}}'_{\mathrm{int}}(t)\right)\right\}. \tag{4.5.27}$$

In the RPA, this gets expanded to

$$\mathcal{Z}_{\text{approx}} = \prod_j \int [\mathrm{d}\vec{\mathbf{R}}_j(t)][\mathrm{d}\hat{\vec{\mathbf{r}}}_j(t)][\mathrm{d}\mathrm{p}(\vec{\mathbf{r}},t)][\mathrm{dP}(\vec{\mathbf{r}},t)][\mathrm{d}\hat{\vec{\mathbf{p}}}(\vec{\mathbf{r}},t)][\mathrm{d}\hat{\vec{\mathbf{P}}}(\vec{\mathbf{r}},t)][\mathrm{d}\vec{\Theta}(\vec{\mathbf{r}},t)][\mathrm{d}\vec{\mathbf{\Omega}}(\vec{\mathbf{r}},t)]\ \times$$
$$\exp\left\{i\int \mathrm{d}t\,\mathrm{P}(\vec{\mathbf{r}},t)\mathrm{p}(\vec{\mathbf{r}},t)\right\}\Bigg(\underbrace{1-i\int \mathrm{d}t\,\mathrm{P}(\vec{\mathbf{r}},t)\left(-\sum_j \delta\left(\vec{\mathbf{r}}-\vec{\mathbf{R}}_j(t)\right)\right)}_{\text{(I)}}$$
$$\underbrace{-\frac{1}{2}\left[\int \mathrm{d}t\,\mathrm{P}(\vec{\mathbf{r}},t)\left(-\sum_j \delta\left(\vec{\mathbf{r}}-\vec{\mathbf{R}}_j(t)\right)\right)\right]^2\ldots}_{\text{(I}^2\text{)}}\Bigg)\ \times$$
$$\exp\left\{i\int \mathrm{d}t\,\hat{\vec{\mathbf{P}}}(\vec{\mathbf{r}},t)\cdot\hat{\vec{\mathbf{p}}}(\vec{\mathbf{r}},t)\right\}\Bigg(\underbrace{1-i\int \mathrm{d}t\,\hat{\vec{\mathbf{P}}}(\vec{\mathbf{r}},t)\cdot\left(-\sum_j \hat{\vec{\mathbf{r}}}_j\,\delta\left(\vec{\mathbf{r}}-\vec{\mathbf{R}}_j(t)\right)\right)}_{\text{(II)}}\Bigg)$$

$$\underbrace{-\frac{1}{2}\left[\int \mathrm{d}t\, \hat{\vec{\mathbf{P}}}(\vec{\mathbf{r}},t)\cdot\left(-\sum_j \hat{\vec{\mathbf{r}}}_j\,\delta\left(\vec{\mathbf{r}}-\vec{\mathbf{R}}_j(t)\right)\right)\right]^2 \ldots}_{\text{II}^2}\Big) \times$$

$$\exp\left\{i\int \mathrm{d}t\, \vec{\mathbf{\Omega}}(\vec{\mathbf{r}},t)\cdot\vec{\Theta}(\vec{\mathbf{r}},t)\right\}\Big(1-\underbrace{i\int \mathrm{d}t\, \vec{\mathbf{\Omega}}(\vec{\mathbf{r}},t)\cdot\left(-\sum_j \dot{\vec{\mathbf{R}}}_j(t)\,\delta\left(\vec{\mathbf{r}}-\vec{\mathbf{R}}_j(t)\right)\right)}_{\text{III}}$$

$$\underbrace{-\frac{1}{2}\left[\int \mathrm{d}t\, \vec{\mathbf{\Omega}}(\vec{\mathbf{r}},t)\cdot\left(-\sum_j \dot{\vec{\mathbf{R}}}_j(t)\,\delta\left(\vec{\mathbf{r}}-\vec{\mathbf{R}}_j(t)\right)\right)\right]^2 \ldots}_{\text{III}^2}\Big) \times$$

$$\frac{1}{2\pi}\int \mathrm{d}\zeta\, \exp\left\{i\zeta\int_0^\tau \mathrm{d}t\, \dot{\vec{\mathbf{R}}}_j(t)^2 - i\zeta\, v^2\,\tau\right\}\, \exp\left\{i\int \mathrm{d}t\, \hat{\vec{\mathbf{r}}}_j(t)\cdot\left(\sum_j \vec{\mathcal{L}}_{\mathrm{min},\,j}(t)+\vec{\mathcal{L}}'_{\mathrm{int}}(t)\right)\right\}. \tag{4.5.28}$$

4.5.2 Calculating the RPA

Similarly to before, we begin by averaging over the stochastic force $\vec{\mathbf{f}}$. For the non-interacting part of the Langevin equation in equation (4.5.28), we have terms with

$$\left\langle\int[\mathrm{d}\hat{\mathbf{r}}_j(t)]\exp\left\{i\int \mathrm{d}t\, \hat{\mathbf{r}}_j(t)\cdot\left(-\alpha\,\dot{\vec{\mathbf{R}}}_j(t)-\beta\,\ddot{\vec{\mathbf{R}}}_j(t)+\vec{\mathbf{f}}\right)\right\}\right\rangle_{\vec{\mathbf{f}}} \tag{4.5.29}$$

$$=\mathcal{N}\int[\mathrm{d}\hat{\mathbf{r}}_j(t)]\exp\left\{i\int \mathrm{d}t\, \hat{\mathbf{r}}_j(t)\cdot\left(-\alpha\,\dot{\vec{\mathbf{R}}}_j(t)-\beta\,\ddot{\vec{\mathbf{R}}}_j(t)\right)\right\}\exp\left\{-\frac{1}{2\lambda}\int \mathrm{d}t\, \hat{\mathbf{r}}_j^2(t)\right\} \tag{4.5.30}$$

as in detailed in Appendix E and shown in equation (4.4.13) for (2).

Including the cross terms, in total we have nine terms to calculate for the RPA from the expanded generating functional in equation (4.5.28). Some of these terms will be zero, however.

In the spacial Fourier transform, we have

$$\text{(I)} = \ldots\int[\mathrm{d}\vec{\mathbf{R}}_j(t)]\,\mathrm{d}\vec{\boldsymbol{\mu}}\,\mathrm{P}(\vec{\boldsymbol{\mu}},t)\exp\left\{i\,\vec{\boldsymbol{\mu}}\cdot\vec{\mathbf{R}}_j(t)\right\}\ldots \tag{4.5.31}$$

$$=\ldots\int \mathrm{d}\vec{\boldsymbol{\mu}}\,\mathrm{P}(\vec{\boldsymbol{\mu}},t)\,\delta(\vec{\boldsymbol{\mu}})\ldots=\ldots\mathrm{P}(0,t)\ldots \tag{4.5.32}$$

$$\text{(I}^2\text{)} = \ldots\int[\mathrm{d}\vec{\mathbf{R}}_j(t)]\,\mathrm{d}\vec{\boldsymbol{\mu}}\,\mathrm{P}(\vec{\boldsymbol{\mu}},t)\mathrm{P}(-\vec{\boldsymbol{\mu}},0)\exp\left\{i\,\vec{\boldsymbol{\mu}}\cdot\left(\vec{\mathbf{R}}_j(t)-\vec{\mathbf{R}}_j(t')\right)\right\}\ldots \tag{4.5.33}$$

$$\text{(II)} = \ldots\int[\mathrm{d}\vec{\mathbf{R}}_j(t)]\,\mathrm{d}\vec{\boldsymbol{\mu}}\,\hat{\vec{\mathbf{P}}}(\vec{\boldsymbol{\mu}},t)\cdot\hat{\mathbf{r}}_j(t)\exp\left\{i\,\vec{\boldsymbol{\mu}}\cdot\vec{\mathbf{R}}_j(t)\right\}\ldots \tag{4.5.34}$$

$$=0\quad\text{because the system is isotropically distributed} \tag{4.5.35}$$

$$\text{II}^2 = \ldots \int [\mathrm{d}\vec{\mathbf{R}}_j(t)]\, \mathrm{d}\vec{\boldsymbol{\mu}}\, \hat{\vec{\mathbf{P}}}(\vec{\boldsymbol{\mu}}, t) \cdot \hat{\mathbf{r}}_j(t)\, \hat{\vec{\mathbf{P}}}(-\vec{\boldsymbol{\mu}}, t') \cdot \hat{\mathbf{r}}_j(t') \times \exp\Big\{ i\, \vec{\boldsymbol{\mu}} \cdot \vec{\mathbf{R}}_j(t) \Big\} \ldots \tag{4.5.36}$$

$$= 0 \quad \text{by Jensen's causality rules [67]} \tag{4.5.37}$$

$$\text{III} = \ldots \int [\mathrm{d}\vec{\mathbf{R}}_j(t)]\, \mathrm{d}\vec{\boldsymbol{\mu}}\, \vec{\boldsymbol{\Omega}}(\vec{\boldsymbol{\mu}}, t) \cdot \dot{\vec{\mathbf{R}}}_j(t) \exp\Big\{ i\, \vec{\boldsymbol{\mu}} \cdot \vec{\mathbf{R}}_j(t) \Big\} \ldots \tag{4.5.38}$$

$$= 0 \quad \text{because the system is isotropically distributed} \tag{4.5.39}$$

$$\text{III}^2 = \ldots \int [\mathrm{d}\vec{\mathbf{R}}_j(t)]\, \mathrm{d}\vec{\boldsymbol{\mu}}\, \vec{\boldsymbol{\Omega}}(\vec{\boldsymbol{\mu}}, t)\, \cdot \dot{\vec{\mathbf{R}}}_j(t)\, \vec{\boldsymbol{\Omega}}(-\vec{\boldsymbol{\mu}}, t') \cdot \dot{\vec{\mathbf{R}}}_j(t') \times \exp\Big\{ i\, \vec{\boldsymbol{\mu}} \cdot \Big(\vec{\mathbf{R}}_j(t) - \vec{\mathbf{R}}_j(t') \Big) \Big\} \ldots \tag{4.5.40}$$

$$\text{I} \times \text{II} = \ldots \int [\mathrm{d}\vec{\mathbf{R}}_j(t)]\, \mathrm{d}\vec{\boldsymbol{\mu}}\, \mathrm{P}(\vec{\boldsymbol{\mu}}, t)\, \hat{\vec{\mathbf{P}}}(-\vec{\boldsymbol{\mu}}, t) \cdot \Big(\lambda\alpha \dot{\vec{\mathbf{R}}}_j(t') + \lambda\beta \ddot{\vec{\mathbf{R}}}_j(t') \Big) \times \exp\Big\{ i\, \vec{\boldsymbol{\mu}} \cdot \Big(\vec{\mathbf{R}}_j(t) - \vec{\mathbf{R}}_j(t') \Big) \Big\} \ldots \tag{4.5.41}$$

$$\text{I} \times \text{III} = \ldots \int [\mathrm{d}\vec{\mathbf{R}}_j(t)]\, \mathrm{d}\vec{\boldsymbol{\mu}}\, \mathrm{P}(\vec{\boldsymbol{\mu}}, t)\, \vec{\boldsymbol{\Omega}}(-\vec{\boldsymbol{\mu}}, t) \cdot \dot{\vec{\mathbf{R}}}_j(t') \exp\Big\{ i\, \vec{\boldsymbol{\mu}} \cdot \Big(\vec{\mathbf{R}}_j(t) - \vec{\mathbf{R}}_j(t') \Big) \Big\} \ldots \tag{4.5.42}$$

$$\text{II} \times \text{III} = \ldots \int [\mathrm{d}\vec{\mathbf{R}}_j(t)]\, \mathrm{d}\vec{\boldsymbol{\mu}}\, \vec{\boldsymbol{\Omega}}(-\vec{\boldsymbol{\mu}}, t) \cdot \dot{\vec{\mathbf{R}}}_j(t')\, \hat{\vec{\mathbf{P}}}(\vec{\boldsymbol{\mu}}, t) \cdot \Big(\lambda\alpha \dot{\vec{\mathbf{R}}}_j(t) + \lambda\beta \ddot{\vec{\mathbf{R}}}_j(t) \Big) \times \exp\Big\{ i\, \vec{\boldsymbol{\mu}} \cdot \Big(\vec{\mathbf{R}}_j(t) - \vec{\mathbf{R}}_j(t') \Big) \Big\} \ldots \tag{4.5.43}$$

In equation (4.5.32), the $\delta(\vec{\boldsymbol{\mu}})$ arises from averaging over the initial position of the head-body join $\vec{\mathbf{R}}_j(0)$, as was the case in Section 4.4.2.

Equations (4.5.35) and (4.5.39) are zero for two reasons. Mathematically, these terms will be zero because of an even integration region with odd integrands. Physically, it is because we are taking the average of an isotropic system and so there is no preferred direction of either $\hat{\mathbf{r}}_j$ or $\dot{\vec{\mathbf{R}}}_j$. This means that when taking the average they cancel out to zero.

Of the nine terms above, only the five picked out in colour still need to be calculated. We further simplify our calculations by looking at two limiting scenarios, since at this stage we wish to gain insights into the system with the simplest calculations possible. We shall in fact be replacing the mean-field *semiflexible* constraint, explained above, with the appropriate constraints for these limiting scenarios.

Recalling the effective persistence length ℓ_p of equation (2.2.7), we define *persistence time*

by dividing the persistence length by the active velocity, v.

$$\tau_{\mathrm{p}} = \frac{\ell_{\mathrm{p}}}{v} = \frac{\left(\kappa\pi^3 + 4\pi v\ell^3\varsigma\right)^2}{8\pi^2 v\ell^4\lambda}\,\frac{1}{v} \tag{4.5.44}$$

For all times $t \ll \tau_{\mathrm{p}}$, we take take our semiflexible polymer as being stiff and for all times $t \gg \tau_{\mathrm{p}}$, we take take our semiflexible polymer as being completely flexible. This is same approach we followed to derive the average end-to-end distances of a single actin filament in equations (2.2.8)–(2.2.10).

4.5.2.1 Times less than the persistence time ($0 < t \ll \tau_{\mathrm{p}}$)

We take the averages over $\vec{\mathbf{R}}_j$ and, without loss of generality, we take $t' = 0$. Essentially, we are looking at a semiflexible walk in time. However, since we are considering the actin in the short-time limit, we say the walk is "stiff" and so simply a *straight walk* of distance vt in the direction $\hat{\mathbf{n}}$. Here v is the active velocity, t the elapsed time and $\hat{\mathbf{n}}$ a random, isotropically distributed unit vector. Put mathematically, we have

$$\vec{\mathbf{R}}_j(t) - \vec{\mathbf{R}}_j(0) = vt\,\hat{\mathbf{n}} \tag{4.5.45}$$

$$\dot{\vec{\mathbf{R}}}_j(t) = v\,\hat{\mathbf{n}} \tag{4.5.46}$$

$$\ddot{\vec{\mathbf{R}}}_j(t) = \vec{\mathbf{0}}. \tag{4.5.47}$$

This set of equations then replaces the semiflexible constraint by encoding "stiffness" at short times $0 < t \ll \tau_{\mathrm{p}}$. Now we return to the five remaining integrals.

$$\text{(I}^2\text{)} = \left\langle \exp\left\{ i\,\vec{\boldsymbol{\mu}} \cdot \left(\vec{\mathbf{R}}_j(t) - \vec{\mathbf{R}}_j(0)\right)\right\}\right\rangle \tag{4.5.48}$$

$$= \frac{1}{2\pi}\int \mathrm{d}\hat{\mathbf{n}}\,\exp\{i\,\vec{\boldsymbol{\mu}} \cdot vt\,\hat{\mathbf{n}}\} \tag{4.5.49}$$

$$= \frac{1}{2\pi}\int_0^{2\pi} \mathrm{d}\theta\,\exp\{ivt\mu\cos\theta\} \tag{4.5.50}$$

$$= J_0(tv|\mu|) \tag{4.5.51}$$

In equation (4.5.49), we are integrating over all possible orientations of the unit vector. In equation (4.5.50), we reparameterise by letting the angle θ between $\vec{\boldsymbol{\mu}}$ and $\hat{\mathbf{n}}$ vary between 0 and 2π. The result of this integration is a Bessel function of the first kind with argument $tv|\mu|$.

$$\text{(III}^2\text{)} = \left\langle \dot{\vec{\mathbf{R}}}_j(t)\,\dot{\vec{\mathbf{R}}}_j(0)\exp\left\{ i\,\vec{\boldsymbol{\mu}} \cdot \left(\vec{\mathbf{R}}_j(t) - \vec{\mathbf{R}}_j(0)\right)\right\}\right\rangle \tag{4.5.52}$$

$$= v^2\,\frac{1}{2\pi}\int \mathrm{d}\hat{\mathbf{n}}\,\exp\{i\,\vec{\boldsymbol{\mu}} \cdot vt\,\hat{\mathbf{n}}\} \tag{4.5.53}$$

$$= v^2\,J_0(tv|\mu|) \tag{4.5.54}$$

$$\text{(I)} \times \text{(II)} = \left\langle \left(\lambda\alpha\dot{\vec{\mathbf{R}}}_j(0) + \lambda\beta\ddot{\vec{\mathbf{R}}}_j(0)\right)\exp\left\{ i\,\vec{\boldsymbol{\mu}} \cdot \left(\vec{\mathbf{R}}_j(t) - \vec{\mathbf{R}}_j(0)\right)\right\}\right\rangle \tag{4.5.55}$$

$$= \lambda\alpha \left\langle \dot{\vec{\mathbf{R}}}_j(0) \exp\Big\{ i\,\vec{\boldsymbol{\mu}} \cdot \Big(\vec{\mathbf{R}}_j(t) - \vec{\mathbf{R}}_j(0) \Big) \Big\} \right\rangle$$
$$+ \lambda\beta \left\langle \ddot{\vec{\mathbf{R}}}_j(0) \exp\Big\{ i\,\vec{\boldsymbol{\mu}} \cdot \Big(\vec{\mathbf{R}}_j(t) - \vec{\mathbf{R}}_j(0) \Big) \Big\} \right\rangle \tag{4.5.56}$$
$$= \lambda\alpha \left\langle \dot{\vec{\mathbf{R}}}_j(0) \exp\Big\{ i\,\vec{\boldsymbol{\mu}} \cdot \Big(\vec{\mathbf{R}}_j(t) - \vec{\mathbf{R}}_j(0) \Big) \Big\} \right\rangle + 0 \tag{4.5.57}$$
$$= \frac{\lambda\alpha}{2\pi} \int \mathrm{d}\hat{\mathbf{n}}\; v\,\hat{\mathbf{n}} \exp\{ i\,\vec{\boldsymbol{\mu}} \cdot vt\,\hat{\mathbf{n}} \} \tag{4.5.58}$$
$$= \frac{\lambda\alpha}{2\pi} \left[\int \mathrm{d}\hat{\mathbf{n}}\; v\,(\hat{\boldsymbol{\mu}} \cdot \hat{\mathbf{n}})\,\hat{\boldsymbol{\mu}} \exp\{ i\,\vec{\boldsymbol{\mu}} \cdot vt\,\hat{\mathbf{n}} \} + \int \mathrm{d}\hat{\mathbf{n}}\; v\,(\hat{\boldsymbol{\mu}}_\perp \cdot \hat{\mathbf{n}})\,\hat{\boldsymbol{\mu}}_\perp \exp\{ i\,\vec{\boldsymbol{\mu}} \cdot vt\,\hat{\mathbf{n}} \} \right] \tag{4.5.59}$$
$$= \frac{\lambda\alpha}{2\pi}\, v \left[\int_0^{2\pi} \mathrm{d}\theta\;\; \cos\theta\,\hat{\boldsymbol{\mu}} \exp\{ ivt\mu\cos\theta \} + \int_0^{2\pi} \mathrm{d}\theta\;\; \sin\theta\,\hat{\boldsymbol{\mu}}_\perp \exp\{ ivt\mu\cos\theta \} \right] \tag{4.5.60}$$
$$= i\,\lambda\alpha v\, J_1(tv\mu)\,\hat{\boldsymbol{\mu}} \;\; + \;\; 0 \tag{4.5.61}$$

In equation (4.5.61), $J_1(tv\mu)$ is the Bessel function of the first kind with argument $tv\mu$.

$$\text{(I)} \times \text{(III)} = \left\langle \dot{\vec{\mathbf{R}}}_j(0) \exp\Big\{ i\,\vec{\boldsymbol{\mu}} \cdot \Big(\vec{\mathbf{R}}_j(t) - \vec{\mathbf{R}}_j(0) \Big) \Big\} \right\rangle \tag{4.5.62}$$
$$= \frac{1}{2\pi} \int \mathrm{d}\hat{\mathbf{n}}\; v\,\hat{\mathbf{n}} \exp\{ i\,\vec{\boldsymbol{\mu}} \cdot vt\,\hat{\mathbf{n}} \} \tag{4.5.63}$$
$$= i\,v\,J_1(tv\mu)\,\hat{\boldsymbol{\mu}} \tag{4.5.64}$$

$$\text{(II)} \times \text{(III)} = \left\langle \dot{\vec{\mathbf{R}}}_j(0) \Big(\lambda\alpha \dot{\vec{\mathbf{R}}}_j(t) + \lambda\beta \ddot{\vec{\mathbf{R}}}_j(t) \Big) \exp\Big\{ i\,\vec{\boldsymbol{\mu}} \cdot \Big(\vec{\mathbf{R}}_j(t) - \vec{\mathbf{R}}_j(0) \Big) \Big\} \right\rangle \tag{4.5.65}$$
$$= \lambda\alpha \,\text{(III}^2\text{)} + \lambda\beta \left\langle \dot{\vec{\mathbf{R}}}_j(0) \ddot{\vec{\mathbf{R}}}_j(t) \exp\Big\{ i\,\vec{\boldsymbol{\mu}} \cdot \Big(\vec{\mathbf{R}}_j(t) - \vec{\mathbf{R}}_j(0) \Big) \Big\} \right\rangle \tag{4.5.66}$$
$$= \lambda\alpha v^2\, J_0(tv|\mu|) \;\; + \;\; 0 \tag{4.5.67}$$

4.5.2.2 Times greater than the persistence time ($t \gg \tau_\mathrm{p}$)

In the long-time limit, we take the walk as being the normal random walk of a flexible polymer. To approach the calculations of the five remaining integrals, we use a discrete *bond-vector* model [52] illustrated in Figure 4.3.

Again we take $t' = 0$. We discretise the time interval into N steps where

$$N = {}^{t}/_{\tau_\mathrm{p}}. \tag{4.5.68}$$

At each time step t_n, we say the polymer travels a distance $\vec{\mathbf{b}}_n$ and that these steps are Gaussian distributed as

$$\mathrm{P}[\vec{\mathbf{b}}_n] = \mathcal{N} \exp\left\{ -\frac{1}{2\,\ell_\mathrm{p}^2}\, \vec{\mathbf{b}}_n^{\,2} \right\}, \tag{4.5.69}$$

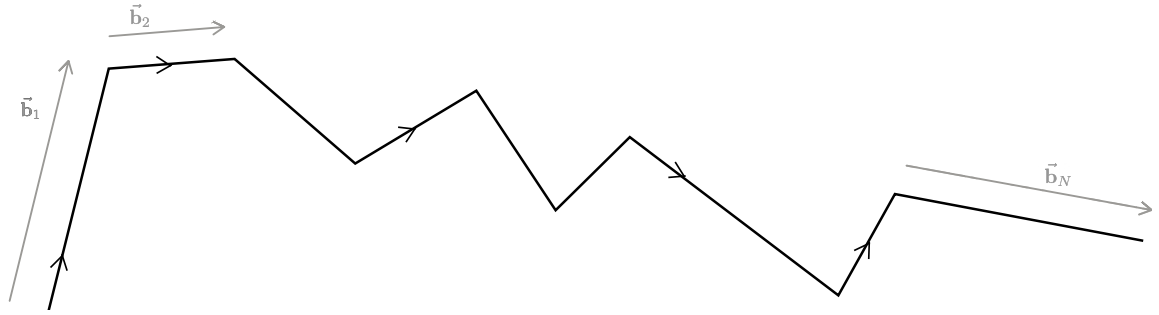

Figure 4.3: In the long-time, flexible limit, the movement of the polymer is broken into a series of bond vectors.

which corresponds with the assumption that during the persistence time τ_p, the actin will have moved a distance ℓ_p on average. Recall that the persistence length and time are related to each other via the active velocity as given in equation (4.5.44).

Then we have that

$$\vec{\mathbf{R}}_j(t) - \vec{\mathbf{R}}_j(0) = \vec{\mathbf{b}}_1 + \vec{\mathbf{b}}_2 + \ldots + \vec{\mathbf{b}}_N = \sum_{n=1}^{N} \vec{\mathbf{b}}_n \tag{4.5.70}$$

$$\dot{\vec{\mathbf{R}}}_j(t_n) = \vec{\mathbf{b}}_n \tag{4.5.71}$$

$$\ddot{\vec{\mathbf{R}}}_j(t_n) = \frac{\vec{\mathbf{b}}_{n+1} - \vec{\mathbf{b}}_n}{2}. \tag{4.5.72}$$

The remaining five integrals can then be evaluated.

$$\text{(I}^2\text{)} = \left\langle \exp\left\{ i\,\vec{\boldsymbol{\mu}} \cdot \left(\vec{\mathbf{R}}_j(t) - \vec{\mathbf{R}}_j(0) \right) \right\} \right\rangle \tag{4.5.73}$$

$$= \lim_{t_n \to 0} \mathcal{N}' \prod_{n=1}^{N} \int \mathrm{d}\vec{\mathbf{b}}_n \exp\left\{ \sum_{n=1}^{N} -\frac{1}{2\,\ell_p^2}\, \vec{\mathbf{b}}_n^2 + i\vec{\boldsymbol{\mu}} \cdot \vec{\mathbf{b}}_n \right\} \tag{4.5.74}$$

$$= \lim_{t_n \to 0} \exp\left\{ -\tfrac{1}{2}\, \ell_p^2\, \mu^2\, N \right\} \tag{4.5.75}$$

$$= \exp\left\{ -\tfrac{1}{2}\, \ell_p\, \mu^2\, vt \right\} \tag{4.5.76}$$

We replace N with t in equation (4.5.76), by using equations (4.5.44) and (4.5.68). We use $\lim_{t_n \to 0}$ as a shorthand to indicate that we are working in the discretised picture, but that we still need to return to the continuous picture terms of time, t, as we did in equation (4.5.76).

$$\text{(III}^2\text{)} = \left\langle \dot{\vec{\mathbf{R}}}_j(t)\, \dot{\vec{\mathbf{R}}}_j(0) \exp\left\{ i\,\vec{\boldsymbol{\mu}} \cdot \left(\vec{\mathbf{R}}_j(t) - \vec{\mathbf{R}}_j(0) \right) \right\} \right\rangle \tag{4.5.77}$$

$$= \lim_{t_n \to 0} \mathcal{N}' \prod_{n=1}^{N} \int \mathrm{d}\vec{\mathbf{b}}_n\, \vec{\mathbf{b}}_N\, \vec{\mathbf{b}}_1 \exp\left\{ \sum_{n=1}^{N} -\frac{1}{2\,\ell_p^2}\, \vec{\mathbf{b}}_n^2 + i\vec{\boldsymbol{\mu}} \cdot \vec{\mathbf{b}}_n \right\} \tag{4.5.78}$$

$$= -\,\ell_p^4\, \mu^2\, \vec{\boldsymbol{\mu}}\vec{\boldsymbol{\mu}} \exp\left\{ -\tfrac{1}{2}\, \ell_p\, \mu^2\, vt \right\} \tag{4.5.79}$$

$$\text{(I)} \times \text{(II)} = \left\langle \left(\lambda\alpha \dot{\vec{\mathbf{R}}}_j(0) + \lambda\beta \ddot{\vec{\mathbf{R}}}_j(0) \right) \exp\left\{ i\,\vec{\boldsymbol{\mu}} \cdot \left(\vec{\mathbf{R}}_j(t) - \vec{\mathbf{R}}_j(0) \right) \right\} \right\rangle \tag{4.5.80}$$

$$= -i\,\lambda\alpha\ell_{\mathrm{p}}^4\,\vec{\boldsymbol{\mu}}\exp\{-\tfrac{1}{2}\,\ell_{\mathrm{p}}\,\mu^2\,vt\}\;+\;0 \tag{4.5.81}$$

$$\textcircled{\mathrm{I}}\times\textcircled{\mathrm{III}} = \left\langle \dot{\vec{\mathbf{R}}}_j(0)\exp\left\{i\,\vec{\boldsymbol{\mu}}\cdot\left(\vec{\mathbf{R}}_j(t)-\vec{\mathbf{R}}_j(0)\right)\right\}\right\rangle \tag{4.5.82}$$

$$= -i\,\ell_{\mathrm{p}}^4\,\vec{\boldsymbol{\mu}}\exp\{-\tfrac{1}{2}\,\ell_{\mathrm{p}}\,\mu^2\,vt\} \tag{4.5.83}$$

$$\textcircled{\mathrm{II}}\times\textcircled{\mathrm{III}} = \left\langle \dot{\vec{\mathbf{R}}}_j(0)\left(\lambda\alpha\dot{\vec{\mathbf{R}}}_j(t)+\lambda\beta\ddot{\vec{\mathbf{R}}}_j(t)\right)\exp\left\{i\,\vec{\boldsymbol{\mu}}\cdot\left(\vec{\mathbf{R}}_j(t)-\vec{\mathbf{R}}_j(0)\right)\right\}\right\rangle \tag{4.5.84}$$

$$= -\lambda\alpha\ell_{\mathrm{p}}^4\,\mu^2\vec{\boldsymbol{\mu}}\vec{\boldsymbol{\mu}}\exp\{-\tfrac{1}{2}\,\ell_{\mathrm{p}}\,\mu^2\,vt\}\;+\;0 \tag{4.5.85}$$

4.5.3 Calculating the density-density correlation function

Now we can complete the RPA for the both time regimes. For the non-interacting part, re-exponentiating then means we have the following matrix to deal with in the exponential of equation (4.5.27):

$$\begin{bmatrix}\mathrm{P}(\vec{\mathbf{r}},t) & \hat{\vec{\mathbf{P}}}(\vec{\mathbf{r}},t) & \vec{\boldsymbol{\Omega}}(\vec{\mathbf{r}},t)\end{bmatrix}\begin{bmatrix}\textcircled{\mathrm{I}^2} & \frac{1}{2}\left(\textcircled{\mathrm{I}}\times\textcircled{\mathrm{II}}\right) & \frac{1}{2}\left(\textcircled{\mathrm{I}}\times\textcircled{\mathrm{III}}\right)\\ \frac{1}{2}\left(\textcircled{\mathrm{I}}\times\textcircled{\mathrm{II}}\right) & \textcircled{\mathrm{II}^2} & \frac{1}{2}\left(\textcircled{\mathrm{II}}\times\textcircled{\mathrm{III}}\right)\\ \frac{1}{2}\left(\textcircled{\mathrm{I}}\times\textcircled{\mathrm{III}}\right) & \frac{1}{2}\left(\textcircled{\mathrm{II}}\times\textcircled{\mathrm{III}}\right) & \textcircled{\mathrm{III}^2}\end{bmatrix}\begin{bmatrix}\mathrm{P}(\vec{\mathbf{r}},0)\\ \hat{\vec{\mathbf{P}}}(\vec{\mathbf{r}},0)\\ \vec{\boldsymbol{\Omega}}(\vec{\mathbf{r}},0)\end{bmatrix}. \tag{4.5.86}$$

The interacting part can also be written in matrix form as

$$\begin{bmatrix}\mathrm{p}(\vec{\mathbf{r}},t) & \hat{\vec{\mathbf{p}}}(\vec{\mathbf{r}},t) & \vec{\Theta}(\vec{\mathbf{r}},t)\end{bmatrix}\begin{bmatrix}0 & \frac{1}{2}\mathbf{H} & 0\\ \frac{1}{2}\mathbf{H} & 0 & 0\\ 0 & 0 & 0\end{bmatrix}\begin{bmatrix}\mathrm{p}(\vec{\mathbf{r}},t-{}^{s}\!/_{v})\\ \hat{\vec{\mathbf{p}}}(\vec{\mathbf{r}},t-{}^{s}\!/_{v})\\ \vec{\Theta}(\vec{\mathbf{r}},t-{}^{s}\!/_{v})\end{bmatrix}. \tag{4.5.87}$$

There are also linear terms remaining:

$$\ldots\exp\left\{i\int \mathrm{d}t\,\mathrm{P}(\vec{\mathbf{r}},t)\mathrm{p}(\vec{\mathbf{r}},t)+\hat{\vec{\mathbf{P}}}(\vec{\mathbf{r}},t)\cdot\hat{\vec{\mathbf{p}}}(\vec{\mathbf{r}},t)+\vec{\boldsymbol{\Omega}}(\vec{\mathbf{r}},t)\cdot\vec{\Theta}(\vec{\mathbf{r}},t)\right\}\ldots \tag{4.5.88}$$

Notice that the interacting part is quadratic in the collective fields $\mathrm{p}, \hat{\vec{\mathbf{p}}}$ and $\vec{\Theta}$, whereas the non-interacting part is quadratic in the auxillary fields $\mathrm{P}, \hat{\vec{\mathbf{P}}}$ and $\vec{\boldsymbol{\Omega}}$. This is not a problem, however, and can be dealt with. Once integration over the auxillary fields $\mathrm{P}, \hat{\vec{\mathbf{P}}}$ and $\vec{\boldsymbol{\Omega}}$ has taken place, the result will be a Gaussian in the collective fields $\mathrm{p}, \hat{\vec{\mathbf{p}}}$ and $\vec{\Theta}$. Note, this process is the same regardless of exact details of the expressions in RPA. The result will be of the following form:

$$\ldots\exp\left\{-\mathbf{p}^T\left[\mathbf{A}^{-1}+\mathbf{B}\right]^{-1}\mathbf{p}\right\} \tag{4.5.89}$$

where

$$\mathbf{p} = \begin{bmatrix}\mathrm{p}(\vec{\mathbf{r}},t-{}^{s}\!/_{v})\\ \hat{\vec{\mathbf{p}}}(\vec{\mathbf{r}},t-{}^{s}\!/_{v})\\ \vec{\Theta}(\vec{\mathbf{r}},t-{}^{s}\!/_{v})\end{bmatrix}, \tag{4.5.90}$$

$$\mathbf{A} = \begin{bmatrix} \textcircled{\text{I}^2} & \frac{1}{2}\left(\textcircled{\text{I}} \times \textcircled{\text{II}}\right) & \frac{1}{2}\left(\textcircled{\text{I}} \times \textcircled{\text{III}}\right) \\ \frac{1}{2}\left(\textcircled{\text{I}} \times \textcircled{\text{II}}\right) & \textcircled{\text{II}^2} & \frac{1}{2}\left(\textcircled{\text{II}} \times \textcircled{\text{III}}\right) \\ \frac{1}{2}\left(\textcircled{\text{I}} \times \textcircled{\text{III}}\right) & \frac{1}{2}\left(\textcircled{\text{II}} \times \textcircled{\text{III}}\right) & \textcircled{\text{III}^2} \end{bmatrix} \tag{4.5.91}$$

and

$$\mathbf{B} = \begin{bmatrix} 0 & \frac{1}{2}\mathbf{H} & 0 \\ \frac{1}{2}\mathbf{H} & 0 & 0 \\ 0 & 0 & 0 \end{bmatrix} \tag{4.5.92}$$

and the correlation functions are the diagonal elements of $\left[\mathbf{A}^{-1} + \mathbf{B}\right]^{-1}$. The off-diagonal elements correspond to response functions [65]. Since we have expressions for all the terms in this matrix, we can in principle get expressions for any correlation or response function. We shall concentrate on the density-density correlation function $\langle \mathrm{p}(\vec{\mathbf{r}}, t)\, \mathrm{p}(\vec{\mathbf{r}}, 0)\rangle$ that is directly observed in experiments. We shall also employ one last approximation: if the hydrodynamics are weak, we can manipulate equation (4.5.89) and show that the *non-interacting* matrix $\mathbf{A}$ alone will sufficiently describe the correlation and response functions. This is shown below.

$$\begin{aligned} &\left[\mathbf{A}^{-1} + \mathbf{B}\right]^{-1} = \left[\left(\mathbf{1} + \mathbf{BA}\right)\mathbf{A}^{-1}\right]^{-1} = \mathbf{A}\left[\mathbf{1} + \mathbf{BA}\right]^{-1} \\ &\approx \mathbf{A}\left(\mathbf{1} - \mathbf{BA} + \ldots\right) \approx \mathbf{A} \end{aligned} \tag{4.5.93}$$

Therefore the density-density correlation function will be given by the {1,1} element of $\mathbf{A}$. The first correction to this will be given by $\mathbf{ABA}$. For the {1,1} element, we can represent this correction symbolically as

$$\frac{1}{2}\textcircled{\text{I}^2}\,\mathbf{H}\left(\textcircled{\text{I}} \times \textcircled{\text{II}}\right). \tag{4.5.94}$$

The hydrodynamic interactions create a mixing of length scales, since $\mathbf{H}$ also introduces a length scale.

4.5.3.1 Short times ($t \ll \tau_{\mathbf{p}}$)

For short times, the expression for the density-density correlation function is given by $J_0(tv|\mu|)$. A plot of this as a function of μ for two different t values, one smaller than the other, is shown in Figure 4.4. It is sensible to remain in the Fourier space domain, since this links more directly to what is measured in experiments: the density-density correlation function in Fourier space is the structure factor, as a function of momentum transfer, obtained from dynamical light scattering measurements.

It is interesting to observe that there are points at which the density of the filaments is uncorrelated (the zero points $j_{0,n}$), followed by regions where the density is *anti*-correlated (at negative values for the correlation function). These cross-over points can easily be evaluated, since the zeros of the Bessel functions are known and from there we can find the relevant length or time scales. Using the first zero, we can estimate the scale of the largest such structure (perhaps in the form of swirling shapes).

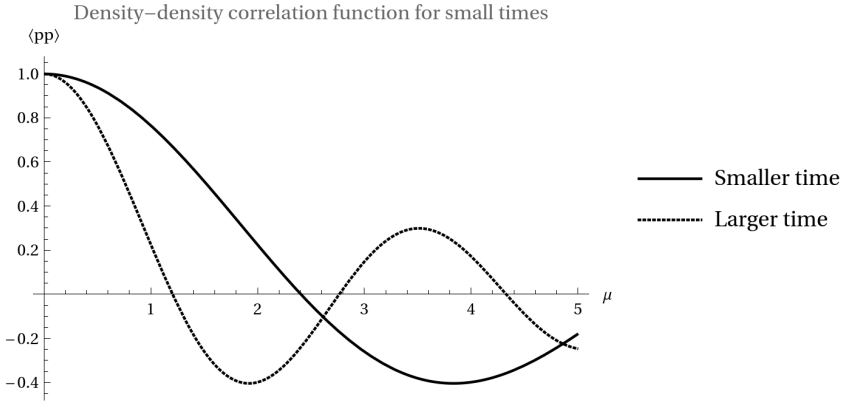

Figure 4.4: A plot showing the form of the density-density correlation function for two different $t \ll \tau_{\mathrm{p}}$ values, plotted as a function of the Fourier space variable μ.

4.5.3.2 Long times ($t \gg \tau_{\mathrm{p}}$)

For long times, the expression for the density-density correlation function is given by $\exp\{-\frac{1}{2}\,\ell_{\mathrm{p}}\,\mu^2\,vt\}$. We plot this as a function of μ in Figure 4.5. Here it can be seen that the density becomes rapidly more and more uncorrelated.

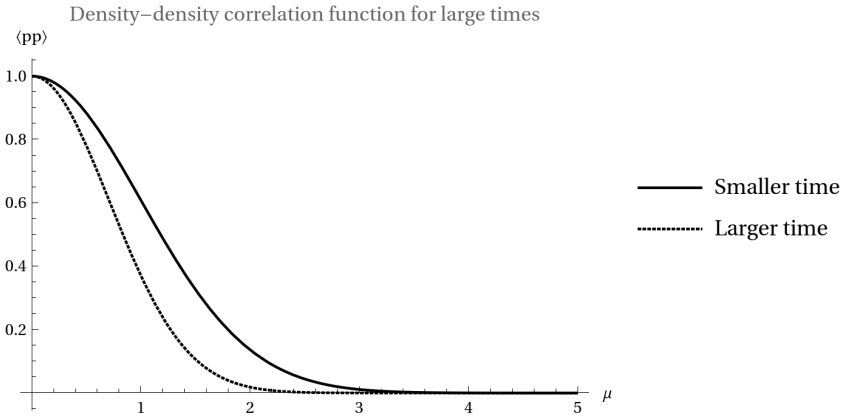

Figure 4.5: A plot showing the form of the density-density correlation function for two different $t \gg \tau_{\mathrm{p}}$ values, plotted as a function of the Fourier space variable μ.

Chapter 5

Conclusions

5.1 Discussion and summary

The actin-myosin motility assay is an interesting subject to study from a physics point of view. For one, it is interesting because from relatively simple and autonomous mechanisms, complex collected behaviours emerge. It is also a meaningful object of study for other disciplines. Studying cell components "from the bottom up" [2] gives physiologists and chemical biologists and related researchers fundamental insights about the working of a cell.

In this work, our goal was to create a microscopic model for the actin-myosin motility assay to complement the coarse-grained approach of hydrodynamic equations. (A good example of this latter approach would be the paper by Giomi and Marchetti [63].) From our model, we hoped to see a prediction of the actual behaviour seen. This would indicate that our way of modelling the problem was sensible. Following this, we hoped to analyse the correlation functions in order to unearth intrinsic time and length scales.

We began with an approach based off the likes of Doi and Edwards [52] and Liverpool [31], where we determined the Langevin equation that described the motility assay and determined consistency relations between the parameters. From there our initial approach was to analyse the system directly via the Langevin equation. Here we saw emergent time and length scales for the special case of a uniform flow field.

To take things further we reformulated our equations in terms of path integrals via the MSR formalism and used the RPA. Here we tried a few different ways of going about the problem. We gradually pared down our equations until we were left with the simplified expressions for the two regimes of short and long times. We ended by looking at the density-density correlation function for these scenarios.

5.2 Outlook

While we have already achieved some results, this work could still be taken further. Some of these avenues have already been touched on in previous chapters. For example, we mentioned

that the hydrodynamics of the fluid could be dealt with in different ways. In the paper by Fredrickson and Helfand [65], an additional, coupled equation was introduced for the hydrodynamic flow field rather than utilising the Oseen tensor. This approach also links to the work of Giomi and Marchetti [63], for example, as mentioned in the introduction to Chapter 4.

Furthermore, we could take the mean-field approach for the semiflexibility constraint of Ha and Thirumalai [75, 76] that we introduced in equation (4.5.26) further. This was beyond the scope of the thesis, but in Appendix F a possible calculation using the mean-field constraint is sketched. We employed a rough approximation, which we hope still captures the essential elements, by looking at two extreme cases for times much less or far greater than the persistence time. The mean-field approach entails dealing with much more mathematical complexity.

Lastly, one could investigate the effects of a boundary on the actin-myosin motility assay, which may link to the work on patterns in active fluids by Elgeti *et al.* [5]; Giomi and Marchetti [63] or the work on hydrodynamics of confined active systems by Brotto *et al.* [77]. These papers address slightly different systems to the actin-myosin motility assay, but it is possible that there would be analogous findings.

Appendices

Appendix A

Deriving the modes of the head of the filament[1]

The Langevin equation for the head is

$$\zeta \frac{\partial \phi(\mathfrak{z},t)}{\partial t} = \kappa \frac{\partial^2 \phi(\mathfrak{z},t)}{\partial \mathfrak{z}^2} + f_\phi(\mathfrak{z},t) \tag{A.0.1}$$

with boundary conditions

$$\left.\frac{\partial \phi(\mathfrak{z},t)}{\partial \mathfrak{z}}\right|_{\mathfrak{z}=\ell} = 0 \qquad \text{and} \qquad \phi(0,t) = 0 \qquad \text{for all } t. \tag{A.0.2}$$

The first boundary condition ensures that the exploring end of the head is free of any forces acting on it, while second boundary condition is the requirement that the angle at the head-body join is zero. There is no special significance to choosing the angle at the start of the head to be zero, it was simply chosen for convenience. Later on, this condition is generalised.

Following the procedure in Appendix 4.II of [52], we first determine what basis functions are appropriate for the modes and then determine properties of the modes.

We define

$$\tilde{\phi}_m = \int_0^\ell \mathrm{d}\mathfrak{z}\ \eta_m(\mathfrak{z})\ \phi(\mathfrak{z},t) \tag{A.0.3}$$

where η_m are the basis functions for the mode expansion and $\tilde{\phi}_m$ are the modes. We shall choose η_m such that the equation of motion for the modes has the same form as before:

$$\zeta_m \frac{\partial \tilde{\phi}_m(t)}{\partial t} = -\kappa_m\ \tilde{\phi}_m(t) + \tilde{f}_m(t). \tag{A.0.4}$$

Using (A.0.3) and (A.0.1) we have

$$\zeta_m \frac{\partial \tilde{\phi}_m}{\partial t} = \frac{\zeta_m}{\zeta} \int_0^\ell \mathrm{d}\mathfrak{z}\ \eta_m \left(\kappa \frac{\partial^2 \phi}{\partial \mathfrak{z}^2} + f\right) \tag{A.0.5}$$

$$= \frac{\zeta_m}{\zeta} \left(\left[\eta_m\ \kappa \frac{\partial \phi}{\partial \mathfrak{z}}\right|_0^\ell - \left[\kappa \frac{\partial \eta_m}{\partial \mathfrak{z}} \phi\right|_0^\ell + \int_0^\ell \mathrm{d}\mathfrak{z}\ \left(\kappa \frac{\partial^2 \eta_m}{\partial \mathfrak{z}^2} \phi + \eta_m f\right) \right) \tag{A.0.6}$$

[1] This is taken directly from [62].

$$= \frac{\zeta_m}{\zeta}\left(\left[\eta_m\,\kappa\frac{\partial\phi}{\partial\mathfrak{z}}\right|_{\mathfrak{z}=0} - \left[\kappa\frac{\partial\eta_m}{\partial\mathfrak{z}}\phi\right|_{\mathfrak{z}=\ell} + \int_0^\ell \mathrm{d}\mathfrak{z}\,\left(\kappa\frac{\partial^2\eta_m}{\partial\mathfrak{z}^2}\phi + \eta_m f\right)\right). \tag{A.0.7}$$

From (A.0.4), we have that (A.0.7) must equal

$$-\kappa_m\int_0^\ell \mathrm{d}\mathfrak{z}\;\eta_m\phi \;+\; \tilde{f}_m.$$

This requires:

1. $$-\kappa_m\eta_m = \kappa\frac{\zeta_m}{\zeta}\,\frac{\partial^2\eta_m}{\partial\mathfrak{z}^2};$$

2. $$\eta_0 = 0;$$

3. $$\left.\frac{\partial\eta_m}{\partial\mathfrak{z}}\right|_{\mathfrak{z}=\ell} = 0;\ \text{and}$$

4. $$\tilde{f}_m = \frac{\zeta_m}{\zeta}\int_0^\ell \mathrm{d}\mathfrak{z}\;\eta_m f.$$

The first three conditions form a standard boundary value problem. Defining

$$\alpha_m^2 = {}^{\zeta\kappa_m}\!/_{\zeta_m\kappa},$$

we can rewrite (1) as

$$\frac{\partial^2\eta_m}{\partial\mathfrak{z}^2} = -\alpha_m^2\eta_m \tag{A.0.8}$$

which has the known solution

$$\eta_m = A\cos(\alpha_m\mathfrak{z}) + B\sin(\alpha_m\mathfrak{z}). \tag{A.0.9}$$

Using the boundary conditions (2) and (3) we see that $A = 0$ and hence $B\alpha\cos(\alpha\ell) = 0$. This implies that

$$\alpha_m = \frac{m\pi}{2\ell},\quad m = 1, 3, 5, \ldots \tag{A.0.10}$$

We now have that $\eta_m = B\sin(\alpha_m s)$ and normalisation requires that $B^2 = \frac{2}{\ell}$. Therefore

$$\eta_m = \sqrt{\tfrac{2}{\ell}}\;\sin(\alpha_m\mathfrak{z}). \tag{A.0.11}$$

Now we wish to determine the properties of the transformed stochastic force $\tilde{f}_m$. Again following from Appendix 4.II in [52], we choose ζ_m such that $\tilde{f}_m$ satisfies

$$\left\langle \tilde{f}_m(t)\tilde{f}_m(0)\right\rangle = 2\zeta_m k_B T\delta(t). \tag{A.0.12}$$

In equation (A.0.12) above, T gives the temperature and k_B is the Boltzmann constant.

From

$$\tilde{f}_m(t) = \frac{\zeta_m}{\zeta}\int_0^\ell \mathrm{d}\mathfrak{z}\ \eta_m f(\mathfrak{z},t) \tag{A.0.13}$$

$$= \frac{\zeta_m}{\zeta}\int_0^\ell \mathrm{d}\mathfrak{z}\ \sqrt{\tfrac{2}{\ell}}\ \sin(\alpha_m\mathfrak{z}) f(\mathfrak{z},t), \tag{A.0.14}$$

we have that

$$\left\langle \tilde{f}_m(t)\tilde{f}_n(0)\right\rangle = \left(\frac{2\zeta_m\zeta_n}{\zeta^2\ell}\right)\int_0^\ell\int_0^\ell \mathrm{d}\mathfrak{z}\ \mathrm{d}\mathfrak{z}'\ \sin(\alpha_m\mathfrak{z})\sin(\alpha_n\mathfrak{z}')\left\langle\ f(\mathfrak{z},t)f(\mathfrak{z}',0)\right\rangle \tag{A.0.15}$$

$$= \left(\frac{2\zeta_m\zeta_n}{\zeta^2\ell}\right)\int_0^\ell\int_0^\ell \mathrm{d}\mathfrak{z}\ \mathrm{d}\mathfrak{z}'\ \sin(\alpha_m\mathfrak{z})\sin(\alpha_n\mathfrak{z}')2\ \zeta k_B T\delta(t)\delta(\mathfrak{z}-\mathfrak{z}') \tag{A.0.16}$$

$$= \left(\frac{2\zeta_m\zeta_n}{\zeta^2\ell}\right)\int_0^\ell \mathrm{d}\mathfrak{z}\ \sin(\alpha_m\mathfrak{z})\sin(\alpha_n\mathfrak{z})2\zeta k_B T\delta(t) \tag{A.0.17}$$

$$= 4\frac{\zeta_m^2}{\zeta}\frac{k_B T}{\ell}\delta(t)\delta_{mn} \tag{A.0.18}$$

and from this we can conclude that

$$\zeta_m = \frac{1}{2}\zeta\ell \qquad m = 1,3,5,... \tag{A.0.19}$$

and

$$\kappa_m = \frac{\kappa m^2\pi^2}{8\ell} \qquad m = 1,3,5,... \tag{A.0.20}$$

In summary,

$$\text{Modes:} \qquad \tilde{\phi}_m(t) = \int_0^\ell \mathrm{d}\mathfrak{z}\ \sqrt{\tfrac{2}{\ell}}\ \sin(\alpha_m\mathfrak{z})\phi(\mathfrak{z},t) \tag{A.0.21}$$

$$\text{Reverse:} \qquad \phi(\mathfrak{z},t) = \sum_{m\ \text{odd}} \tilde{\phi}_m(t)\sin(\alpha_m\mathfrak{z}) \tag{A.0.22}$$

Appendix B

Filling in the details of the calculation in equation (2.1.33)[1]

First we calculate the bending energy term in equation (2.1.24). Using equation (2.1.2) with equation (2.1.25), we have

$$x(\ell,t) = x(0,t) + \int_0^\ell \mathrm{d}\mathfrak{z}\ \cos\Big(\Phi_0 + \tilde{\phi}_1 \sin\left({}^{\pi\mathfrak{z}}/_{2\ell}\right)\Big) \tag{B.0.1}$$

$$x(\ell,t) = x(0,t) + \ell\cos\Phi_0(t) - \left({}^{2\ell}/_{\pi}\sin\Phi_0(t)\right)\tilde{\phi}_1(t) - \left({}^{\ell}/_{4}\cos\Phi_0(t)\right)\tilde{\phi}_1^2(t) \tag{B.0.2}$$

and

$$y(\ell,t) = y(0,t) + \int_0^\ell \mathrm{d}\mathfrak{z}\ \sin\Big(\Phi_0 + \tilde{\phi}_1 \sin\left({}^{\pi\mathfrak{z}}/_{2\ell}\right)\Big) \tag{B.0.3}$$

$$y(\ell,t) = y(0,t) + \ell\sin\Phi_0(t) + \left({}^{2\ell}/_{\pi}\cos\Phi_0(t)\right)\tilde{\phi}_1(t) - \left({}^{\ell}/_{4}\sin\Phi_0(t)\right)\tilde{\phi}_1^2(t), \tag{B.0.4}$$

where $\cos\phi$ and $\sin\phi$ have been expanded to second order in $\tilde{\phi}_1$ when evaluating the integral.

Differentiating (B.0.2) with respect to x and (B.0.4) with respect to y gives

$$\frac{\partial\tilde{\phi}_1}{\partial x} = \left[-{}^{2\ell}/_{\pi}\sin\Phi_0 - \left({}^{\ell}/_{2}\cos\Phi_0\right)\tilde{\phi}_1\right]^{-1} \tag{B.0.5}$$

$$\frac{\partial\tilde{\phi}_1}{\partial y} = \left[{}^{2\ell}/_{\pi}\cos\Phi_0 - \left({}^{\ell}/_{2}\sin\Phi_0\right)\tilde{\phi}_1\right]^{-1}. \tag{B.0.6}$$

The initial angle function Φ_0 was assumed to have zero derivatives with respect to x and y. We can assume this because the instantaneous value of Φ_0 is fixed by earlier fluctuations of the head, which has already been taken into account via equation (2.1.20) and (2.1.23). (See also equation (B.0.12) below.) This assumption still leads to a consistent set of equations.

With this in place, we return to equation (2.1.31). For consistency with the small $\tilde{\phi}_1$ approximation, we express (2.1.31) up to linear order in $\tilde{\phi}_1$. The bending energy force term becomes

$$\vec{\mathbf{f}}_{\text{approx}} = -\frac{\kappa\pi^2}{8\ell}\tilde{\phi}_1(t)\left\{-\frac{1}{{}^{2\ell}/_{\pi}\sin(\Phi_0(t))}\hat{\mathbf{i}} + \frac{1}{{}^{2\ell}/_{\pi}\cos(\Phi_0(t))}\hat{\mathbf{j}}\right\}. \tag{B.0.7}$$

[1] This is taken directly from [62].

The force is an approximation inasmuch as we only take the conformation of the head to the lowest mode.

Next we turn our attention to the drag force term in equation (2.1.24). Using equation (2.1.2) which relates the tangent vector to the tangent angle, we can write the drag force as

$$-\varsigma\frac{\partial\vec{\mathbf{R}}(\ell,t)}{\partial t}=-\varsigma\frac{\partial\vec{\mathbf{R}}(0,t)}{\partial t}-\varsigma\int_0^\ell \mathrm{d}\mathfrak{z}\;\frac{\partial\phi(\mathfrak{z},t)}{\partial t}\left(-\sin\phi(\mathfrak{z},t)\hat{\mathbf{i}}+\cos\phi(\mathfrak{z},t)\hat{\mathbf{j}}\right). \tag{B.0.8}$$

We can rewrite $\frac{\partial\vec{\mathbf{R}}(0,t)}{\partial t}$ using the chain rule as

$$\left.\frac{\partial\vec{\mathbf{R}}}{\partial\mathfrak{z}}\frac{\partial\mathfrak{z}}{\partial t}\right|_{\mathfrak{z}=0}=v\left.\frac{\partial\vec{\mathbf{R}}}{\partial\mathfrak{z}}\right|_{\mathfrak{z}=0} \tag{B.0.9}$$

$$=v\left[\cos\left(\Phi_0(t)\right)\hat{\mathbf{i}}+\sin\left(\Phi_0(t)\right)\hat{\mathbf{j}}\right]. \tag{B.0.10}$$

Up to first order in $\tilde{\phi}_1$ and $\frac{\partial\tilde{\phi}_1}{\partial t}=\tilde{\phi}_1'$ the expression for the drag force in equation (B.0.8) becomes

$$\begin{aligned}-\varsigma\frac{\partial\vec{\mathbf{R}}(\ell,t)}{\partial t}=&-\varsigma v(\cos(\Phi_0(t))\hat{\mathbf{i}}+\sin(\Phi_0(t))\hat{\mathbf{j}})\\&+\frac{\varsigma\ell}{\pi}\left[\pi\sin(\Phi_0(t))\;\Phi_0'(t)+2\cos(\Phi_0(t))\;\tilde{\phi}_1(t)\;\Phi_0'(t)+2\sin(\Phi_0(t))\;\tilde{\phi}_1'(t)\right]\hat{\mathbf{i}}\\&-\frac{\varsigma\ell}{\pi}\left[\pi\cos(\Phi_0(t))\;\Phi_0'(t)-2\sin(\Phi_0(t))\;\tilde{\phi}_1(t)\;\Phi_0'(t)+2\cos(\Phi_0(t))\;\tilde{\phi}_1'(t)\right]\hat{\mathbf{j}}.\end{aligned} \tag{B.0.11}$$

We recall equation (2.1.23) that relates the time derivative of Φ_0 to the remaining modes. With equation (2.1.25), this reduces to

$$\frac{\partial\Phi_0}{\partial t}=\frac{v\pi}{2\ell}\;\tilde{\phi}_1(t) \tag{B.0.12}$$

and inserting this into (B.0.11) results in further terms being discarded to keep the drag term to linear order in $\tilde{\phi}_1$.

$$\begin{aligned}-\varsigma\frac{\partial\vec{\mathbf{R}}(\ell,t)}{\partial t}=&-\varsigma\left(v\cos(\Phi_0(t))-\frac{\ell}{\pi}\left[\frac{v\pi^2}{2\ell}\sin(\Phi_0(t))\;\tilde{\phi}_1(t)+2\sin(\Phi_0(t))\;\tilde{\phi}_1'(t)\right]\right)\hat{\mathbf{i}}\\&-\varsigma\left(v\sin(\Phi_0(t))+\frac{\ell}{\pi}\left[\frac{v\pi^2}{2\ell}\cos(\Phi_0(t))\;\tilde{\phi}_1(t)+2\cos(\Phi_0(t))\;\tilde{\phi}_1'(t)\right]\right)\hat{\mathbf{j}}\end{aligned} \tag{B.0.13}$$

Appendix C

Determining the dimensions of a[1]

To determine the dimensions of a, we first determine the dimensions of ξ and k defined in equation (2.1.38).

For ξ we have

$$\left[\ \xi\ \right] = \left[\ \varsigma\ \ell\ \right] = \left[\ \frac{M\ L}{t}\ \right]. \tag{C.0.1}$$

The dimensions of ς were determined from equation (2.1.24), since the drag force must indeed have dimensions of force:

$$\left[\ \varsigma\frac{\partial\vec{\mathbf{R}}(\ell,t)}{\partial t}\ \right] = \left[\ \frac{M\ L}{t^2}\ \right] \implies \left[\ \frac{\varsigma\ L}{t}\ \right] = \left[\ \frac{M\ L}{t^2}\ \right] \implies \left[\ \varsigma\ \right] = \left[\ \frac{M}{t}\ \right]. \tag{C.0.2}$$

For k, we first determine the dimensions of κ. For this we refer to equation (1.4.15) and require that the bending energy has the dimensions of energy:

$$\left[\ \kappa\int_0^L \mathrm{d}s\ \left(\frac{\partial^2\vec{\mathbf{R}}(s,t)}{\partial s^2}\right)^2\ \right] = \left[\ \frac{M\ L^2}{t^2}\ \right] \implies \left[\ \frac{\kappa}{L}\ \right] = \left[\ \frac{M\ L^2}{t^2}\ \right] \implies \left[\ \kappa\ \right] = \left[\ \frac{M\ L}{t^2}\ \right]. \tag{C.0.3}$$

Therefore

$$\left[\ k\ \right] = \left[\ \frac{\kappa}{\ell} + \varsigma\ v\ \right] = \left[\ \frac{M\ L}{t^2} + \frac{M\ L}{t^2}\ \right] = \left[\ \frac{M\ L}{t^2}\ \right] \tag{C.0.4}$$

and hence we have the the dimension of a:

$$\left[\ a\ \right] = \left[\ t\ \right]. \tag{C.0.5}$$

[1] This is taken directly from [62].

Appendix D

Showing $\langle \Phi_0 \rangle$ is zero

Here we show that $\langle \Phi_0 \rangle$ is zero in just a few lines, using the definitions in equations (3.1.12), (3.1.14) and (3.1.16).

$$\langle \Phi_0 \rangle = \left\langle \tfrac{1}{2\pi} \int_{-\infty}^{\infty} \mathrm{d}\omega \; \overline{\Phi}_0(\omega) \; e^{i\omega t} \right\rangle \tag{D.0.1}$$

$$= \left\langle \tfrac{1}{2\pi} \int_{-\infty}^{\infty} \mathrm{d}\omega \; \jmath(\omega) \, \overline{f}_{\mathrm{proj}}(\omega) \; e^{i\omega t} \right\rangle \tag{D.0.2}$$

$$= \tfrac{1}{2\pi} \int_{-\infty}^{\infty} \mathrm{d}\omega \; \jmath(\omega) \; \left\langle \, \overline{f}_{\mathrm{proj}}(\omega) \, \right\rangle \; e^{i\omega t} \tag{D.0.3}$$

$$= 0 \tag{D.0.4}$$

Appendix E

Functional integration of a Langevin equation

In this appendix we go through the functional integration calculation for a simple one-dimensional Langevin equation

$$\mathcal{L} = -\gamma\,\dot{x}(t) + f(t), \tag{E.0.1}$$

where $f(t)$ is the stochastic force with Gaussian probability distribution

$$\mathrm{P}[f] = \mathcal{N}\ \exp\left\{-\frac{1}{2\lambda}\int_0^\infty \mathrm{d}t\ f^{\,2}(t)\right\}. \tag{E.0.2}$$

Hence we wish to calculate the following:

$$\int [\mathrm{d}f(t)][\mathrm{d}x(t)][\mathrm{d}\hat{x}(t)]\ \exp\left\{i\int \mathrm{d}t\ \hat{x}(t)\,(-\gamma\,\dot{x}(t) + f(t))\right\}\mathcal{N}\exp\left\{-\frac{1}{2\lambda}\int_0^\infty \mathrm{d}t\ f^{\,2}(t)\right\}. \tag{E.0.3}$$

To compute this, we discretise the time into N intervals of size Δt and then take the limit. This allows us to work with a product of regular integrals rather than the functional integrals. The notation f_t indicates the function at the t^{th} time interval.

$$\int [\mathrm{d}f(t)][\mathrm{d}x(t)][\mathrm{d}\hat{x}(t)]\ \exp\left\{i\int \mathrm{d}t\ \hat{x}(t)\,(-\gamma\,\dot{x}(t) + f(t))\right\}\mathcal{N}\exp\left\{-\frac{1}{2\lambda}\int_0^\infty \mathrm{d}t\ f^{\,2}(t)\right\} \tag{E.0.4}$$

$$= \lim_{\substack{\Delta t\to 0\\ N\to\infty}} \int \prod_{t=0}^{N} \mathrm{d}f_t\ \mathrm{d}x_t\ \mathrm{d}\hat{x}_t\ \mathcal{N}\ \exp\left\{i\sum_t \Delta t\ \left[\hat{x}_t\left(-\gamma\,\frac{x_t - x_{t-1}}{\Delta t} + f_t\right) - \frac{1}{2\lambda}f_t^2\right]\right\} \tag{E.0.5}$$

$$= \lim_{\substack{\Delta t\to 0\\ N\to\infty}} \left(\int \mathrm{d}f_t\ \mathrm{d}x_t\ \mathrm{d}\hat{x}_t\ \mathcal{N}\ \exp\left\{i\Delta t\ \left[\hat{x}_t\left(-\gamma\,\frac{x_t - x_{t-1}}{\Delta t} + f_t\right) - \frac{1}{2\lambda}f_t^2\right]\right\}\right)^N \tag{E.0.6}$$

$$= \lim_{\substack{\Delta t\to 0\\ N\to\infty}} \left(\int \mathrm{d}x_t\ \mathrm{d}\hat{x}_t\ \mathrm{d}f_t\ \mathcal{N}\ \exp\left\{-\frac{\Delta t}{2\lambda}f_t^2 + i\Delta t\ \hat{x}_t\ f_t\right\}\exp\{-i\,\gamma\,\hat{x}_t\,(x_t - x_{t-1})\}\right)^N \tag{E.0.7}$$

$$= \lim_{\substack{\Delta t \to 0 \\ N \to \infty}} \left(\int \mathrm{d}x_t \, \mathrm{d}\hat{x}_t \, \mathcal{N} \sqrt{\frac{2\pi\lambda}{\Delta t}} \, \exp\left\{ -\frac{\lambda}{2} \Delta t \, \hat{x}_t^2 \right\} \exp\{ -i\,\gamma\, \hat{x}_t \, (x_t - x_{t-1}) \} \right)^N \tag{E.0.8}$$

$$= \lim_{\substack{\Delta t \to 0 \\ N \to \infty}} \left(\int \mathrm{d}x_t \, \mathrm{d}\hat{x}_t \, \mathcal{N} \sqrt{\frac{2\pi\lambda}{\Delta t}} \, \exp\left\{ -\frac{\lambda}{2} \Delta t \, \hat{x}_t^2 - i\,\gamma\, \hat{x}_t \, (x_t - x_{t-1}) \right\} \right)^N \tag{E.0.9}$$

$$= \lim_{\substack{\Delta t \to 0 \\ N \to \infty}} \left(\int \mathrm{d}x_t \, \mathcal{N} \sqrt{\frac{2\pi\lambda}{\Delta t}} \sqrt{\frac{2\pi}{\Delta t \, \lambda}} \, \exp\left\{ -\frac{\gamma^2 \, (x_t - x_{t-1})^2}{2\,\lambda\,\Delta t} \right\} \right)^N \tag{E.0.10}$$

$$= \lim_{\substack{\Delta t \to 0 \\ N \to \infty}} \left(\int \mathrm{d}x_t \, \mathcal{N} \left(\frac{2\pi}{\Delta t} \right) \exp\left\{ -\frac{\gamma^2}{2\,\lambda} \Delta t \left(\frac{x_t - x_{t-1}}{2\,\lambda\,\Delta t} \right)^2 \right\} \right)^N \tag{E.0.11}$$

$$= \lim_{\substack{\Delta t \to 0 \\ N \to \infty}} \int \prod_{t=0}^{N} \mathrm{d}x_t \, \mathcal{N} \left(\frac{2\pi}{\Delta t} \right) \exp\left\{ -\frac{\gamma^2}{2\,\lambda} \sum_t \Delta t \left(\frac{x_t - x_{t-1}}{2\,\lambda\,\Delta t} \right)^2 \right\} \tag{E.0.12}$$

$$= \mathcal{N}' \int [\mathrm{d}x(t)] \exp\left\{ -\frac{\gamma^2}{2\lambda} \int \mathrm{d}t \, \dot{x}^2(t) \right\} \qquad \text{with} \quad \mathcal{N}' = \mathcal{N} \lim_{\substack{\Delta t \to 0 \\ N \to \infty}} \left(\frac{2\pi}{\Delta t} \right)^N \tag{E.0.13}$$

To go from equation (E.0.7) to equation (E.0.8), one simply recognises a one-dimensional Guassian integral. Similarly for equation (E.0.9) to equation (E.0.10).

While the prefactor $\mathcal{N}'$ may seem alarming, in reality it is not so since these factors will cancel when calculating averages and correlation functions.

Appendix F

Mean-field constraint approach

When calculating terms of the minimalist RPA in Section 4.5.2, we focused on two extreme time regimes in Sections 4.5.2.1 and 4.5.2.2. However, there is still a possible way to look at the intermediate time regime where the actin is truly semiflexible rather than rigid or flexible. We take the vector for the head-body join $\vec{\mathbf{R}}_j$ and break it up into modes using a Fourier series:

$$\vec{\mathbf{R}}_j(t) = \sum_{\omega=-\infty}^{\infty} \vec{\mathbf{R}}_{j,\omega}\, e^{i\pi\omega t/\tau} \tag{F.0.1}$$

where τ is the total time interval.

Recalling equations (4.5.27) and (4.5.30), we have the approximate generating functional

$$\begin{aligned}\mathcal{Z}_{\text{approx}} = \ldots \int [\mathrm{d}\vec{\mathbf{R}}_j(t)]\, \frac{1}{2\pi} \int_{-\infty}^{\infty} \mathrm{d}\wr\, \exp\left\{ -\frac{1}{2\lambda} \int_0^{\tau} \mathrm{d}t\, \left(\overbrace{\alpha^2\, \dot{\vec{\mathbf{R}}}_j(t)^2}^{=v^2} + \beta^2\, \ddot{\vec{\mathbf{R}}}_j(t)^2 \right) \right\} \\ \times \exp\left\{ i\wr \int_0^{\tau} \mathrm{d}t\, \dot{\vec{\mathbf{R}}}_j(t)^2 - i\wr\, v^2\, \tau \right\}\end{aligned} \tag{F.0.2}$$

and hence averages will look as follows:

$$\begin{aligned}\langle \mathcal{V} \rangle = \frac{1}{\mathcal{Z}_{\text{approx}}} \ldots \int [\mathrm{d}\vec{\mathbf{R}}_j(t)]\, \frac{1}{2\pi} \int_{-\infty}^{\infty} \mathrm{d}\wr\ \mathcal{V}\ \exp\left\{ -\frac{1}{2\lambda} \int_0^{\tau} \mathrm{d}t\ \left(\cancel{v^2} + \beta^2\, \ddot{\vec{\mathbf{R}}}_j(t)^2 \right) \right\} \\ \times \exp\left\{ i\wr \int_0^{\tau} \mathrm{d}t\, \dot{\vec{\mathbf{R}}}_j(t)^2 - i\wr\, v^2\, \tau \right\}\end{aligned} \tag{F.0.3}$$

where we have first replaced $\alpha^2\, \dot{\vec{\mathbf{R}}}_j(t)^2$ by v^2, since this is taken care of by the constraint term, and then taken this constant term out entirely because it will not contribute to the averages.

If we replace $\vec{\mathbf{R}}_j$ with the modes $\vec{\mathbf{R}}_{j,\omega}$, we get

$$\begin{aligned}\langle \mathcal{V} \rangle = \frac{1}{\mathcal{Z}_{\text{approx}}} \ldots \prod_{\omega} \int [\mathrm{d}\vec{\mathbf{R}}_{j,\omega}]\, \frac{1}{2\pi} \int_{-\infty}^{\infty} \mathrm{d}\wr\ \mathcal{V}\ \exp\{ -i\wr v^2 \tau \} \\ \times \exp\left\{ \sum_{\omega \neq 0} \left(-\frac{1}{2\lambda} \frac{\beta^2 \pi^2 \omega^2}{\tau} + i\wr \frac{\pi^4 \omega^4}{\tau^3} \right) \vec{\mathbf{R}}_{j,\omega} \cdot \vec{\mathbf{R}}_{j,-\omega} \right\}\end{aligned} \tag{F.0.4}$$

and expressions for the five coloured terms of Section 4.5.2 can be found in terms of these modes and the variable ω. For example, consider $\textcircled{\text{III}^2}$. To simplify the expressions, let

$$-\frac{1}{2}\mathrm{A}_\omega = -\frac{1}{2\lambda}\frac{\beta^2\pi^2\omega^2}{\tau} + i\wr\frac{\pi^4\omega^4}{\tau^3}. \tag{F.0.5}$$

$$\begin{aligned}\textcircled{\text{III}^2} &= \frac{1}{\mathcal{Z}_{\text{approx}}}\cdots\prod_{\omega\neq 0}\frac{1}{2\pi}\int_{-\infty}^{\infty}\mathrm{d}\wr\sum_{\omega',\omega''}\frac{i\pi\omega'}{\tau}(-1)^{\omega'}\frac{i\pi\omega''}{\tau}(-1)^{\omega''}\vec{\mathbf{R}}_{j,\omega'}\cdot\vec{\mathbf{R}}_{j,\omega''}\\ &\quad\times\exp\left\{-\frac{1}{2}\sum_{\omega\neq 0}\mathrm{A}_\omega\,\vec{\mathbf{R}}_{j,\omega}\cdot\vec{\mathbf{R}}_{j,-\omega}+2i\vec{\boldsymbol{\mu}}\cdot\sum_{\omega\,\text{odd}}\vec{\mathbf{R}}_{j,\omega}-i\wr v^2\tau\right\} \qquad \text{(F.0.6)}\\ &= \frac{1}{\mathcal{Z}_{\text{approx}}}\cdots\prod_{\omega\neq 0}\frac{1}{\mathrm{A}_\omega}\int_{-\infty}^{\infty}\mathrm{d}\wr\sum_{\omega'}\left(\frac{i\pi\omega'}{\tau}\right)^2\left[\frac{1}{\mathrm{A}_\omega}-\frac{4\mu^2}{\mathrm{A}_\omega^2}\,\delta_{\omega\,\text{odd}}\right]\\ &\quad\times\exp\left\{-4\sum_{\omega\neq 0}\frac{\mu^2}{\mathrm{A}_\omega}\,\vec{\mathbf{R}}_{j,\omega}\cdot\vec{\mathbf{R}}_{j,-\omega}-i\wr v^2\tau\right\} \qquad \text{(F.0.7)}\end{aligned}$$

Bibliography

[1] Ramaswamy, S.: The mechanics and statistics of active matter. *Annual Review of Condensed Matter Physics*, vol. 1, no. 1, pp. 323–345, 2010.

[2] Marchetti, M.C., Joanny, J.F., Ramaswamy, S., Liverpool, T.B., Prost, J., Rao, M. and Simha, R.A.: Hydrodynamics of soft active matter. *Reviews of Modern Physics*, vol. 85, no. 3, pp. 1143–1189, 2013.

[3] Peterson, M.S.E., Hagan, M.F. and Baskaran, A.: Statistical properties of a tangentially driven active filament. *Journal of Statistical Mechanics: Theory and Experiment*, vol. 2020, no. 1, p. 013216, 2020.

[4] Vicsek, T. and Zafeiris, A.: Collective motion. *Physics Reports*, vol. 517, no. 3-4, pp. 71–140, 2012.

[5] Elgeti, J., Cates, M.E. and Marenduzzo, D.: Defect hydrodynamics in 2D polar active fluids. *Soft Matter*, vol. 7, p. 3177, 2011.

[6] Ghosh, A. and Gov, N.: Dynamics of active semiflexible polymers. *Biophysical Journal*, vol. 107, no. 5, pp. 1065–1073, 2014.

[7] Eisenstecken, T., Gompper, G. and Winkler, R.: Conformational properties of active semiflexible polymers. *Polymers*, vol. 8, no. 8, p. 304, 2016.

[8] Sanchez, T., Chen, D.T.N., DeCamp, S.J., Heymann, M. and Dogic, Z.: Spontaneous motion in hierarchically assembled active matter. *Nature*, vol. 491, no. 7424, pp. 431–434, 2012.

[9] Redner, G.S., Hagan, M.F. and Baskaran, A.: Structure and dynamics of a phase-separating active colloidal fluid. *Physical Review Letters*, vol. 110, p. 055701, 2013.

[10] DeCamp, S.J., Redner, G.S., Baskaran, A., Hagan, M.F. and Dogic, Z.: Orientational order of motile defects in active nematics. *Nature Materials*, vol. 14, no. 11, pp. 1110–1115, 2015.

[11] Surrey, T., Nédélec, F., Leibler, S. and Karsenti, E.: Physical properties determining self-organization of motors and microtubules. *Science*, vol. 292, no. 5519, pp. 1167–1171, 2001.

[12] Deseigne, J., Dauchot, O. and Chaté, H.: Collective motion of vibrated polar disks. *Physical Review Letters*, vol. 105, no. 9, p. 098001, 2010.

[13] Palacci, J., Sacanna, S., Steinberg, A.P., Pine, D.J. and Chaikin, P.M.: Living crystals of light-activated colloidal surfers. *Science*, vol. 339, no. 6122, pp. 936–940, 2013.

[14] Copeland, M.F. and Weibel, D.B.: Bacterial swarming: a model system for studying dynamic self-assembly. *Soft Matter*, vol. 5, no. 6, p. 1174, 2009.

[15] Scharf, B.: Real-time imaging of fluorescent flagellar filaments of Rhizobium lupini H13-3: Flagellar rotation and pH-induced polymorphic transitions. *Journal of Bacteriology*, vol. 184, no. 21, pp. 5979–5986, 2002.

[16] Kearns, D.B.: A field guide to bacterial swarming motility. *Nature Reviews Microbiology*, vol. 8, no. 9, pp. 634–644, 2010.

[17] Elgeti, J., Winkler, R.G. and Gompper, G.: Physics of microswimmers — single particle motion and collective behavior: a review. *Reports on Progress in Physics*, vol. 78, no. 5, p. 056601, 2015.

[18] Talwar, S., Kumar, A., Rao, M., Menon, G.I. and Shivashankar, G.: Correlated spatio-temporal fluctuations in chromatin compaction states characterize stem cells. *Biophysical Journal*, vol. 104, no. 3, pp. 553–564, 2013.

[19] Hameed, F.M., Rao, M. and Shivashankar, G.V.: Dynamics of passive and active particles in the cell nucleus. *PLoS ONE*, vol. 7, no. 10, p. e45843, 2012.

[20] Weber, S.C., Spakowitz, A.J. and Theriot, J.A.: Nonthermal ATP-dependent fluctuations contribute to the in vivo motion of chromosomal loci. *Proceedings of the National Academy of Sciences*, vol. 109, no. 19, pp. 7338–7343, 2012.

[21] Hochrein, M.B., Leierseder, J.A., Golubović, L. and Rädler, J.O.: DNA localization and stretching on periodically microstructured lipid membranes. *Physical Review Letters*, vol. 96, no. 3, p. 038103, 2006.

[22] Bustamante, C., Bryant, Z. and Smith, S.B.: Ten years of tension: single-molecule DNA mechanics: The double helix: 50 years. *Nature (London)*, vol. 421, no. 6921, pp. 423–427, 2003.

[23] Winkler, R.G.: Semiflexible polymers in shear flow. *Physical Review Letters*, vol. 97, no. 12, p. 128301, 2006.

[24] Bianco, V., Locatelli, E. and Malgaretti, P.: Globulelike conformation and enhanced diffusion of active polymers. *Physical Review Letters*, vol. 121, no. 21, p. 217802, 2018.

[25] Winkler, R.G.: Deformation of semiflexible chains. *The Journal of Chemical Physics*, vol. 118, no. 6, p. 2919, 2003.

[26] Kierfeld, J., Frentzel, K., Kraikivski, P. and Lipowsky, R.: Active dynamics of filaments in motility assays. *The European Physical Journal Special Topics*, vol. 157, no. 1, pp. 123–133, 2008.

[27] Möller, K.: *Dynamics of an active crosslinker on a chain and aspects of the dynamics of polymer networks.* Masters thesis, Stellenbosch University, 2011.

[28] Schaller, V., Weber, C., Semmrich, C., Frey, E. and Bausch, A.R.: Polar patterns of driven filaments. *Nature*, vol. 467, no. 7311, pp. 73–77, 2010.

[29] Banerjee, S., Marchetti, M.C. and Müller-Nedebock, K.: Motor-driven dynamics of cytoskeletal filaments in motility assays. *Physical Review E*, vol. 84, no. 1, p. 011914, 2011.

[30] Munk, T., Hallatschek, O., Wiggins, C.H. and Frey, E.: Dynamics of semiflexible polymers in a flow field. *Physical Review E*, vol. 74, no. 4, p. 41911, 2006.

[31] Liverpool, T.B.: Anomalous fluctuations of active polar filaments. *Physical Review E*, vol. 67, no. 3, p. 031909, 2003.

[32] Nagai, K.H., Sumino, Y., Montagne, R., Aranson, I.S. and Chaté, H.: Collective motion of self-propelled particles with memory. *Physical Review Letters*, vol. 114, no. 16, p. 168001, 2015.

[33] Martin, S.E., Brunner, M.E. and Deutsch, J.M.: Spontaneous circulation of active microtubules confined by optical traps. *Journal of Biological Physics*, vol. 47, no. 3, pp. 237–251, 2021.

[34] Sumino, Y., Nagai, K.H., Shitaka, Y., Tanaka, D., Yoshikawa, K., Chaté, H. and Oiwa, K.: Large-scale vortex lattice emerging from collectively moving microtubules. *Nature*, vol. 483, no. 7390, pp. 448–452, 2012.

[35] Oza, A.U. and Dunkel, J.: Antipolar ordering of topological defects in active liquid crystals. *New Journal of Physics*, vol. 18, no. 9, p. 093006, 2016.

[36] Vicsek, T., Czirók, A., Ben-Jacob, E., Cohen, I. and Shochet, O.: Novel type of phase transition in a system of self-driven particles. *Physical Review Letters*, vol. 75, pp. 1226–1229, 1995.

[37] Schaller, V., Weber, C., Frey, E. and Bausch, A.R.: Polar pattern formation: hydrodynamic coupling of driven filaments. *Soft Matter*, vol. 7, no. 7, p. 3213, 2011.

[38] Kron, S.J. and Spudich, J.A.: Fluorescent actin filaments move on myosin fixed to a glass surface. *Proceedings of the National Academy of Sciences*, vol. 83, pp. 6272–6276, 1986.

[39] Butt, T., Mufti, T., Humayun, A., Rosenthal, P.B., Khan, S., Khan, S. and Molloy, J.E.: Myosin motors drive long range alignment of actin filaments. *The Journal of biological chemistry*, vol. 285, no. 7, pp. 4964–74, 2010.

[40] Batters, C., Veigel, C., Homsher, E. and Sellers, J.R.: To understand muscle you must take it apart. *Frontiers in Physiology*, vol. 5, 2014.

[41] Cooper, G.M.: *The cell: a molecular approach.* 6th edn. Sinauer Associates, Sunderland, Mass, 2013.

[42] Warshaw, D.: The in vitro motility assay: A window into the myosin molecular motor. *Physiology*, vol. 11, no. 1, pp. 1–7, 1996.

[43] Bopp, N., Scheid, L.-M., Fink, R.H.A. and Rohr, K.: Determination of the maximum velocity of filaments in the in vitro motility assay. *Frontiers in Physiology*, vol. 10, no. MAR, p. 289, 2019.

[44] Sheetz, M.P., Chasan, R. and Spudich, J.A.: ATP-dependent movement of myosin in vitro: characterization of a quantitative assay. *Journal of Cell Biology*, vol. 99, no. 5, pp. 1867–1871, 1984.

[45] Howard, J.: *Mechanics of motor proteins and the cytoskeleton.* Sinauer Associates, Sunderland, Mass, 2001.

[46] Schuh, M.: An actin-dependent mechanism for long-range vesicle transport. *Nature Cell Biology*, vol. 13, no. 12, pp. 1431–1436, 2011.

[47] Lodish, H., Berk, A., Kaiser, C., Amon, A., Ploegh, H., Bretscher, A., Krieger, M. and Martin, K.: *Molecular Cell Biology*. Macmillan Learning, 2016. ISBN 9781319101572.

[48] Winkler, R.G. and Gompper, G.: The physics of active polymers and filaments. *The Journal of Chemical Physics*, vol. 153, no. 4, p. 040901, 2020.

[49] Jung, W., Fillenwarth, L.A., Matsuda, A., Li, J., Inoue, Y. and Kim, T.: Collective and contractile filament motions in the myosin motility assay. *Soft Matter*, vol. 16, no. 6, pp. 1548–1559, 2020.

[50] Eisenstecken, T. and Winkler, R.G.: Path integral description of semiflexible active Brownian polymers. *The Journal of Chemical Physics*, vol. 156, p. 064105, 2022.

[51] Waigh, T.A.: *Applied biophysics: a molecular approach for physical scientists*. J. Wiley & Sons, Chichester, England, 2007.

[52] Doi, M. and Edwards, S.F.: *The theory of polymer dynamics*. International series of monographs on physics ; 73. Clarendon Press, Oxford [Oxfordshire], 1999.

[53] Happel, J. and Brenner, H.: *Low Reynolds number hydrodynamics*, vol. 1 of *Mechanics of fluids and transport processes*. Springer Netherlands, Dordrecht, 1981.

[54] Purcell, E.M.: Life at low Reynolds number. *American Journal of Physics*, vol. 45, no. 1, pp. 3–11, 1977.

[55] Schiessel, H.: *Biophysics for beginners: a journey through the cell nucleus*. Pan Stanford Pub., Singapore, 2014.

[56] Tibbitt, M.W.: Lecture 3: Ideal polymer chains. ETH Zürich 2021 Accessed: 16-12-2021. Available at: `https://macro.ethz.ch/education/macromolecular-engineering--networks-and-gels.html`

[57] Rubinstein, M.: *Polymer physics*. Oxford University Press Incorporated, Oxford, 2003.

[58] Aragon, S.R. and Pecora, R.: Dynamics of wormlike chains. *Macromolecules*, vol. 18, no. 10, pp. 1868–1875, 1985.

[59] Broedersz, C.P. and MacKintosh, F.C.: Modeling semiflexible polymer networks. *Reviews of Modern Physics*, vol. 86, no. 3, pp. 995–1036, 2014.

[60] Prasad, A., Hori, Y. and Kondev, J.: Elasticity of semiflexible polymers in two dimensions. *Physics Review E*, vol. 72, p. 041918, 2005.

[61] Stepanow, S.: Statistical mechanics of semiflexible polymers. *The European Physical Journal B*, vol. 39, no. 4, pp. 499–512, 2004.

[62] Saffer, Z.O.: *Self-propelling worm-like molecules considered singly and in two dimensions.* Bachelor (Honours) thesis, Stellenbosch University, Stellenbosch, South Africa, 2019.

[63] Giomi, L. and Marchetti, M.C.: Polar patterns in active fluids. *Soft Matter*, vol. 8, pp. 129–139, 2012.

[64] Harnau, L., Winkler, R.G. and Reineker, P.: Dynamic properties of molecular chains with variable stiffness. *The Journal of Chemical Physics*, vol. 102, no. 19, pp. 7750–7757, 1995.

[65] Fredrickson, G.H. and Helfand, E.: Collective dynamics of polymer solutions. *The Journal of Chemical Physics*, vol. 93, no. 3, pp. 2048–2061, 1990.

[66] Martin, P.C., Siggia, E.D. and Rose, H.A.: Statistical dynamics of classical systems. *Physical Review A*, vol. 8, pp. 423–437, 7 1973.

[67] Jensen, R.V.: Functional integral approach to classical statistical dynamics. *Journal of Statistical Physics*, vol. 25, pp. 183–210, 6 1981.

[68] Jouvet, B. and Phythian, R.: Quantum aspects of classical and statistical fields. *Physical Review A*, vol. 19, no. 3, pp. 1350–1355, 1979.

[69] Bohm, D. and Pines, D.: A collective description of electron interactions. I. Magnetic interactions. *Physical Review*, vol. 82, pp. 625–634, 1951.

[70] Müller-Nedebock, K.K. and Vilgis, T.A.: Dynamics of dense polyelectrolyte solutions. *Macromolecules*, vol. 31, pp. 5898–5903, 1998.

[71] Akcasu, A.Z., Benmouna, M. and Benoit, H.: Application of random phase approximation to the dynamics of polymer blends and copolymers. *Polymer*, vol. 27, pp. 1935–1942, 1986.

[72] Bhattacharjee, J.K., Thirumalai, D. and Bryngelson, J.D.: Distribution function of the end-to-end distance of semiflexible polymers. *arXiv*, 1997.

[73] Chaichian, M. and Demichev, A.: *Path Integrals in Physics*, vol. 1. IOP Publishing Ltd, Bristol, 2001.

[74] Müller-Nedebock, K.K.: Quantum mechanics C: Path integration. University lecture notes, 2008.

[75] Ha, B.-Y. and Thirumalai, D.: A mean-field model for semiflexible chains. *The Journal of Chemical Physics*, vol. 103, pp. 9408–9412, 1995.

[76] Ha, B.-Y. and Thirumalai, D.: Semiflexible chains under tension. *The Journal of Chemical Physics*, vol. 106, pp. 4243–4247, 1997.

[77] Brotto, T., Caussin, J.-B., Lauga, E. and Bartolo, D.: Hydrodynamics of confined active fluids. *Physical Review Letters*, vol. 110, p. 038101, 2013.